

IMPROVED STRAPDOWN INERTIAL SYSTEM CALIBRATION PROCEDURES

PART 1 - PROCEDURES AND ACCURACY ANALYSIS

Paul G. Savage

Strapdown Associates, Inc.
Maple Plain, MN 55359 USA

WBN-14020-1

www.strapdownassociates.com

October 20, 2017 (Updated November 10, 2017)

ABSTRACT

This article is Part 1 of a three part series describing an improved strapdown rotation test (SRT) for calibrating the compensation coefficients in a strapdown inertial measurement unit (IMU). The SRT consists of a set of IMU rotations and processing routines that enable precision measurements of IMU gyro/accelerometer misalignment, gyro/accelerometer scale factor, and accelerometer bias calibration errors, all without requiring precision rotation fixtures and IMU mounting setup. The improved SRT is compatible with a broad range of IMU types from aircraft accuracy inertial navigation systems (INSs) to low cost micro-machined electronic module system (MEMS) varieties. This Part 1 article describes the general theory for the improved rotation tests, rotation test operations, data collection during test, post-test data processing, rotation test fixture requirements, rotation design for sensor error determination, and SRT accuracy analysis of sensor error determination accuracy.

FOREWORD

This article is the first in a three part series describing improved strapdown rotation test (SRT) procedures for calibrating a strapdown inertial measurement unit (IMU) containing an orthogonal triad of inertial sensors (gyros and accelerometers), digital processor, associated sensor calibration software, and other computational elements. The improved rotation tests consist of a series of rotation sequences, each designed to measure one of the following errors in the sensor calibration coefficients: gyro-to-gyro misalignment, accelerometer-to-gyro misalignment, gyro/accelerometer scale-factor, and accelerometer bias. The second and third articles in the three-part series cover the following topics:

Part 2: Analytical Derivations - Derives the Part 1 equations for 1) IMU sensor output data processing, 2) Determining sensor calibration errors from the processed IMU data, and 3) SRT inaccuracies caused by rotation fixture error, IMU mounting misalignment on the rotation fixture, approximations in SRT data analysis equations, and residual gyro biases during the SRT.

Part 3 - Numerical Examples - Provides numerical examples showing how collected SRT rotation test data translates sensor errors into data collection measurements, and the impact of neglecting gyro bias in the SRT sensor error determination process. The results numerically confirm that rotation sequences designed in Part 1 measure the particular sensor error for which they were designed.

1.0 INTRODUCTION

One of the lesser known but important developments in the history of strapdown inertial navigation system (INS) development, was solving the problem of precision calibrating alignments between the strapdown sensors without requiring precision rotation test fixtures. Under rotation environments, misalignment between inertial sensors (and gyro scale factor error) can generate significant INS error buildup. Thus, it had been believed that calibrating a strapdown INS to the required sensor-to-sensor arc-sec alignment accuracy would require rotation test fixtures capable of generating precision arc-sec test rotations, a significant cost penalty for projected strapdown systems in production. The calibration problem was exacerbated by the fact that for most arc-sec alignment accuracy applications, the sensor cluster is attached to/within the INS chassis by elastomeric isolators of marginal angular stability, particularly under thermal changes induced during testing operations.

The solution to the problem was first disclosed in 1975 [1] based on the fundamental concept that a perfectly calibrated and initially self-aligned strapdown INS will have no velocity rate output (acceleration) when stationary, even under rotations between stationary test measurement orientations. Thus, non-zero stationary acceleration outputs would provide a direct measure of INS sensor calibration error without the need to execute precision INS rotations during the test. The result was a significant reduction in rotation test fixture accuracy requirements (and cost). Based on this principle, the strapdown rotation test (SRT or “S-Cal”) was conceived consisting of a set of rotation sequences with test measurements taken when the INS was stationary at the end of each sequence. The ensemble of sequences was designed to excite particular sensor error sources, thereby generating distinctive signatures on the stationary acceleration measurements. Processing the measurements at test completion (an analytic inversion process) allowed individual sensor errors to be determined. Results were then used to correct sensor calibration coefficients in the INS computer software.

In the original 1975 paper [1], each rotation test sequence was preceded by a standard INS inertial self-alignment (for attitude initialization in the INS computer), followed by entry into the free-inertial navigation mode. Each SRT rotation sequence was then executed in the free-inertial mode. At completion of each rotation sequence, the stationary test measurement was taken as the INS output average acceleration. Following the measurement, the INS was rotated to the starting orientation of the next rotation sequence where self-alignment/navigation-mode-entry was again performed. (The purpose for the repeated self-alignment was to eliminate attitude error build-up caused by gyro error during the previous rotation sequence.)

In 1977, the [1] concept was refined, changing the horizontal measurement to be the difference between average accelerations taken before and after rotation sequence execution [2,

Sect. 18.4]. The acceleration difference measurement eliminated initial attitude error generated by gyro error during the previous rotation sequence, thus, eliminating the need for INS self-alignment between rotation sequences, and allowing operation in the free inertial mode from rotation test initiation (following INS self-alignment at the start of the SRT). (The before/after measurement approach was introduced by Downs [2, Ref. 5] for compatibility with an existing Kalman filter used to extract the acceleration measurements.)

An additional refinement in the 1977 SRT concept was to generate the acceleration measurements from the output of a strapdown “analytical platform” rather than as INS computed velocity rate. An analytic platform is a fundamental computational element in a strapdown inertial system that transforms strapdown accelerometer signals through a direction cosine matrix (DCM) into a non-rotating reference coordinate frame (analogous to a mechanically gimbaled gyro-stabilized platform on which the accelerometers and gyros are mounted). For SRT application, the analytic platform would reside in the inertial system under test, or as software in the SRT test computer. The latter concept is depicted in Fig. 1, the DCM being calculated in the “Attitude Computation” block. In the Fig. 1 approach, SRT software would also include the ability to execute initial self-alignment of the DCM using the identical method employed in an INS. (Note: In Fig. 1 and in this article, Inertial Measurement Unit (IMU) designates a strapdown inertial system in general; INS designates a particular type of IMU in which the computer software is configured to calculate attitude, velocity, and position.)

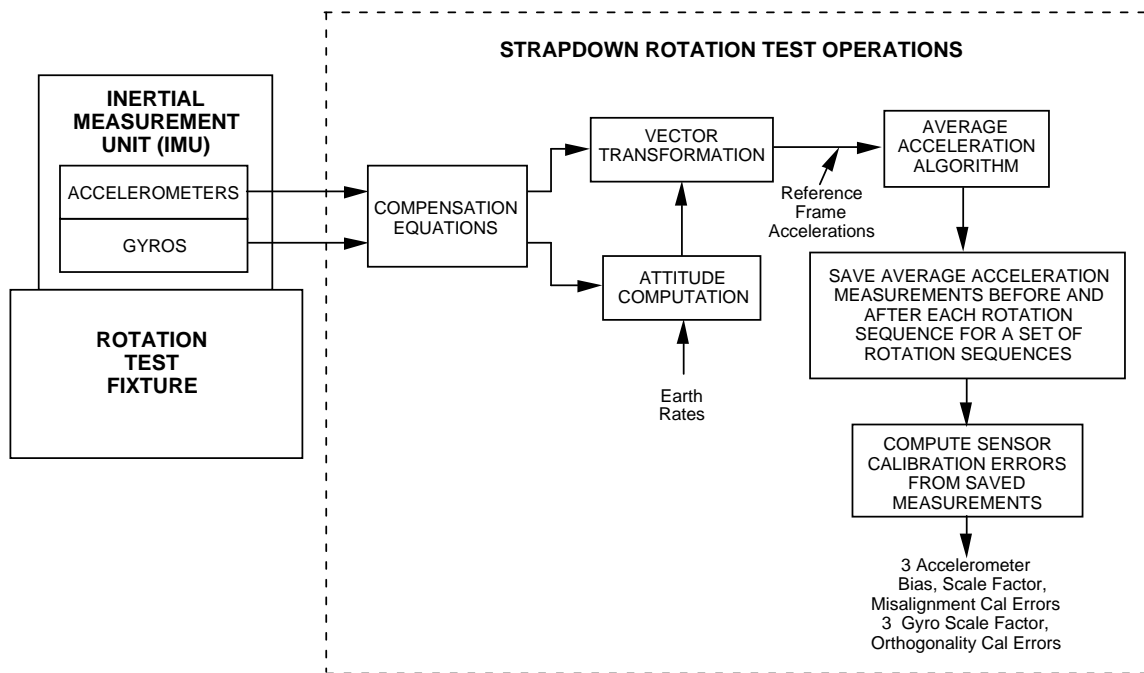


Fig. 1 - Strapdown Rotation Test (SRT) Setup

This article describes an improved version of the 1977 SRT that eliminates the need for attitude reference self-alignment at the start of the test, and revises the measurement concept to enable design of each SRT rotation sequence for determination of a particular sensor calibration error. This contrasts with the 1977 SRT which generated measurements containing groupings of

several sensor error effects, requiring an intuitive “cut-and-try” approach to find a set of rotation sequences that were analytically sufficient to determine all sensor calibration errors. The result [2, Sect. 8.4] was a set of 16 rotation sequences to determine the Fig. 1 sensor calibration errors. The improved SRT determines the same errors with 14 rotation sequences.

As with the 1977 SRT, acceleration measurements for the improved SRT are taken in a locally level coordinate frame (“Reference Frame Accelerations” indicated in Fig. 1). In the 1977 version, the DCM was initialized (and locally level frame thereby analytically “erected”) at the start of the rotation test using traditional INS self-alignment attitude initialization software routines. The DCM was then maintained throughout the rotation test. A consequence of this method was that during the rotation test, the DCM accumulated error buildup from gyro calibration error, making it difficult to apply the SRT concept to IMUs having gyros of lower accuracy than used in a typical aircraft INS.

The self-alignment process executed with the 1977 SRT at test start for DCM initialization also determined earth rate components used for DCM updating during the test. With the new SRT approach, the initial self-alignment process is eliminated, the DCM is initialized to the nominal IMU attitude at the start of each rotation sequence, and known earth rate components at the nominal starting attitude are used for DCM updating during the rotation sequence (see Fig. 1). This approach induces a small angular tilt-from-vertical error in the initial DCM that is subsequently eliminated from the SRT measurement by the Fig. 1 before/after difference method. Similarly, the small earth rate error incurred using nominal rather than measured earth rate for DCM updating has negligible impact on SRT accuracy. More importantly, however, is that the time since DCM initialization for gyro and residual earth rate error buildup becomes the time to complete each rotation sequence (e.g., 30 seconds). In contrast, the time for DCM error buildup using the 1977 SRT was the total time from DCM initialization at test start until test completion. Thus, residual gyro and earth rate error effects with the new approach have much less time to propagate into DCM error. The result is that accurate sensor calibration can be accomplished with the new approach for a broader range of IMU accuracy configurations, not only those using aircraft INS accuracy sensors.

This article provides a detailed description of the improved SRT showing how it would be implemented using a standard modest accuracy (e.g., 0.1 deg) two-axis rotation test fixture. Sections 2.0 and 3.0 define the notation and coordinate frames used in the article analytics. Section 4.0 describes a two-axis rotation fixture used to execute SRT rotations, a set of recommended rotation sequences for the new SRT, IMU sensor “Compensation Equations” depicted in Fig. 1 for generating SRT gyro/accelerometer inputs, data processing to generate the SRT acceleration measurements, and computational routines for calculating sensor calibration errors from the measurements. Included in Section 4.0 are descriptions of a digital processing iteration approach for enhanced SRT accuracy and methods to mitigate the impact of gyro bias residual errors on test results. Section 5.0 presents an error analysis for the new SRT showing how sensor error determination accuracy is impacted by IMU mounting error on the rotation test fixture, rotation fixture error in executing SRT rotations, uncertainty in rotation fixture orientation relative to local north, east, down coordinates, approximations in the SRT processing equations, and IMU sensor calibration errors prior to SRT execution. Section 6.0 provides a

detailed description of the logic used in constructing rotation sequences for the new SRT that enable determination of a particular sensor error from each sequence.

2.0 NOTATION

The following general notation is used throughout this article.

\underline{V} = Vector without specific coordinate frame designation. A vector is a parameter that has length and direction. Vectors used in the paper are classified as “free vectors”, hence, have no preferred location in coordinate frames in which they are analytically described.

\underline{V}^A = Column matrix with elements equal to the projection of \underline{V} on coordinate frame A axes. The projection of \underline{V} on each frame A axis equals the dot product of \underline{V} with a unit vector parallel to that coordinate axis.

$(\underline{V}^A \times)$ = Skew symmetric (or cross-product) form of \underline{V}^A represented by the square matrix $\begin{bmatrix} 0 & -V_{ZA} & V_{YA} \\ V_{ZA} & 0 & -V_{XA} \\ -V_{YA} & V_{XA} & 0 \end{bmatrix}$ in which V_{XA} , V_{YA} , V_{ZA} are the components of \underline{V}^A . The matrix product of $(\underline{V}^A \times)$ with another A frame vector equals the cross-product of \underline{V}^A with the vector in the A frame, i.e.: $(\underline{V}^A \times) \underline{W}^A = \underline{V}^A \times \underline{W}^A$.

$C_{A_2}^{A_1}$ = Direction cosine matrix that transforms a vector from its coordinate frame A_2 projection form to its coordinate frame A_1 projection form, i.e., $\underline{V}^{A_1} = C_{A_2}^{A_1} \underline{V}^{A_2}$. The columns of $C_{A_2}^{A_1}$ are projections on A_1 axes of unit vectors parallel to A_2 axes. Conversely, the rows of $C_{A_2}^{A_1}$ are projections on A_2 axes of unit vectors parallel to A_1 axes. An important property of $C_{A_2}^{A_1}$ is that its inverse equals its transpose.

$\underline{\omega}_{I:A}$ = Angular rotation rate of generalized coordinate frame A relative to inertially non-rotating space ($I:A$ subscript).

$\underline{\omega}_{I:E}$ = Angular rotation rate of the earth relative to inertially non-rotating space ($I:E$ subscript).

$\underline{\omega}_{E:A}$ = Angular rotation rate of generalized coordinate frame A relative to the rotating earth ($E : A$ subscript). Note that $\underline{\omega}_{I:A} = \underline{\omega}_{I:E} + \underline{\omega}_{E:A}$ and equivalently, $\underline{\omega}_{E:A} = \underline{\omega}_{I:A} - \underline{\omega}_{I:E}$.

$\dot{()}$ = $\frac{d()}{dt}$ = Derivative of parameter $()$ with respect to time t .

$\widehat{()}$ = Computed or measured value of parameter $()$ that, in contrast with the idealized error free value $()$, contain errors.

3.0 COORDINATE FRAMES

The primary coordinate frame used in this article is the IMU fixed B frame that is rotated relative to the earth (and inertial space) during each SRT rotation sequence. Other coordinate frames related to B are fixed (non-rotating) relative to the earth, most aligned with the B frame at the start and end of a rotation sequence, one defined to be aligned with north, east, down coordinates at the test site. Specific definitions for the coordinate frame are as follows:

B = IMU sensor frame that is fixed relative to strapdown inertial sensor input axes, but that rotates relative to the earth during each rotation sequence of the SRT. The angular orientation of the B frame relative to sensor axes is arbitrary based on user or traditional preferences.

$MARS$ = Designation for a “mean-angular-rate-sensor” B frame selection, the orthogonal frame that best fits around the actual strapdown gyro input axes.

NED = Earth fixed coordinate frame with axes aligned to local north, east, down directions.

B_{Start} = Coordinate frame that is fixed (non-rotating) relative to the earth and aligned with the B frame at the start of the rotation sequence. Nominally, one of the B_{Start} frame axes would be aligned with the local vertical if the IMU being tested is perfectly mounted on an idealized rotation fixture.

B_{End} = Coordinate frame that is fixed (non-rotating) relative to the earth and aligned with the B frame at the end of the rotation sequence.

$B_{i, Start}$ = Coordinate frame that is fixed (non-rotating) relative to the earth and aligned with the B frame at the start of rotation i in a rotation sequence.

$B_{i, End}$ = Coordinate frame that is fixed (non-rotating) relative to the earth and aligned with the B frame at the end of rotation i in a rotation sequence.

4.0 STRAPDOWN IMU ROTATION TESTING

4.1 ROTATION TEST FIXTURE DESCRIPTION

The SRT process described in this article is designed for compatibility with IMU testing using a moderate accuracy (e.g., 0.1 deg) two-axis rotation fixture with outer axis rotation axis horizontal, inner rotation axis perpendicular to the outer axis, and the test article mounting platform plane perpendicular to the inner rotation axis. (The horizontal outer axis is sometimes denoted as the “trunion” axis.) For a computer controlled rotation fixture, electric torque motors are commanded to drive the inner and outer rotation angles at prescribed angular rates (or angular settings) specified by the test computer. For this article, we will assume that the IMU being tested is installed on the fixture test mount with one of its axes aligned with the rotation fixture inner rotation axis.

Fig. 2 illustrates the arrangement of a manual two-axis rotation fixture used at Honeywell during the 1975 - 1977 time period to calibrate engineering developmental INS configurations. The fixture had 90 deg spaced detents for each rotation axis, simplifying manual generation of 90 deg multiple rotations.



Fig. 2 - Manual Two-Axis Rotation Test Fixture
(1976 Photo - Minneapolis RLG INS Team, Yours Truly On The Right)

4.2 IMPROVED SRT ROTATION SEQUENCES

The SRT consists of a set of rotation sequences during which IMU data is processed and recorded for post-test determination of IMU calibration errors. Table 1 provides a set of 14 recommended rotation sequences based on the new SRT formulation using traditional mutually orthogonal x, y, z nomenclature to identify particular IMU axes during the test.

Sequence Number	Initial IMU Axis Directions		Initial Rotation Fixture Angles		Sequential IMU Axis Rotations
	Down	Along Outer Rotation Axis	Inner	Outer	
1	Z	Y	0	0	+360 Y
2	Z	Y	0	0	+360 X
3	X	Y	0	-90	+360 Z
1a	Z	Y	0	0	-360 Y
2a	Z	Y	0	0	-360 X
3a	X	Y	0	-90	-360 Z
4	Z	Y	0	0	+180 Y, +180 Z, +180 Y, +180 Z
5	Z	X	+90	0	+180 X, +180 Z, +180 X, +180 Z
6	X	Y	0	-90	+180 Y, +90 Z, +180 X, +90 Z, +180 Y, +90 Z, +180 X, +90 Z
7	Y	X	+90	90	+180 X
8	Z	X	+90	0	+180 X
9	X	Y	0	-90	+180 Z
10	Y	X	+90	90	+180 Z
11	Z	Y	0	0	+180 Y
12	X	Y	0	-90	+180 Y
13	Z	Y	0	0	+180 Z, +180 Y
14	Z	X	+90	0	+180 Z, +180 X

*Note - rotation sequences 1a - 3a are not needed when gyros have no scale factor asymmetry.

Table 1 - Improved Strapdown Rotation Test Sequences

Table 1 is based on the IMU mounted on the rotation fixture with z axis (of a mutually orthogonal x, y, z set) aligned with the inner rotation axis and downward when the outer axis rotation angle is zero. The IMU x, y axes mounting are defined as having the y axis aligned with

the outer rotation fixture axis when the inner axis rotation angle is zero. A detailed discussion on Table 1 rotation sequence selection is presented in Section 6.0.

4.3 SENSOR COMPENSATION

Compensation equations are contained in IMU (or SRT) software to correct modelable errors in the strapdown gyros and accelerometer outputs. Prior to SRT engagement, the compensation coefficients would be pre-calibrated for previously measured, approximated, or known error characteristics. The SRT operates on the compensated IMU sensor signals to determine error residuals remaining in the pre-calibrated coefficients. The coefficient error residuals are then used to update the compensation coefficients. In general, compensation coefficient pre-calibration only includes sensor alignment corrections measured on an individual sensor basis (if at all), prior to sensor installation in the IMU. The primary purpose for the SRT is to accurately measure and correct the sensor-to-sensor alignment coefficient errors, effects that can only be accurately measured after sensor installation in the IMU. The SRT also updates the calibration coefficients for gyro scale factor and accelerometer bias error residuals that may not have been accurately set in the pre-calibrated coefficients (or may not be representative of sensor changes since original calibration).

4.3.1 Sensor Compensation Equations

A two-stage approach is commonly used for sensor compensation operations. The first stage corrects errors due to IMU/sensor design configuration and individual sensor errors measured prior to installation in the IMU. The second stage corrects errors remaining in the first routine outputs. Calibration is the process of setting the error coefficients in the sensor compensation routines. The sensor compensation equations described in this article are based on the inverse of the sensor output models in Part 2 [3, Appendices A & B] with random noise terms deleted; Part 2 [3, Eqs. (A-4) & (B-4)] for the first stage compensation routines, Part 2 [3, Eqs. (A-7) with (A-17) & (B-7) with (B-17)] for the second stage compensation correction routines. The purpose for the SRT is to determine error residuals remaining in the second stage compensation routine coefficients. The first and second stage compensation routines are as follows:

$$\begin{aligned} \underline{\omega}' &= (I + K_{Scal})^{-1} \underline{\omega}_{Raw} & \underline{\tilde{\omega}} &= K_{Algn}^{-1} \left(\underline{\omega}' - \underline{\omega}_{Bias} - \underline{\omega}_{Quant} \right) \\ \underline{a}'_{SF} &= (I + L_{Scal})^{-1} \underline{a}_{SF Raw} \end{aligned} \quad (1)$$

$$\underline{\tilde{a}}_{SF} = L_{Algn}^{-1} \left(\underline{a}'_{SF} - \underline{a}_{Bias} - \underline{a}_{Size} - \underline{a}_{Aniso} - \underline{a}_{Quant} \right)$$

$$\begin{aligned} \underline{\hat{\omega}} &= \left(I + \hat{\kappa}_{Mis} + \hat{\kappa}_{LinScal} + \hat{\kappa}_{Asym} \Omega_{Sign}^B \right)^{-1} \left(\underline{\tilde{\omega}} - \hat{\kappa}_{Bias} \right) \\ \underline{\hat{a}}_{SF} &= \left(I + \hat{\lambda}_{Mis} + \hat{\lambda}_{LinScal} + \hat{\lambda}_{Asym} \tilde{A}_{SF Sign} \right)^{-1} \left(\underline{\tilde{a}}_{SF} - \hat{\lambda}_{Bias} \right) \end{aligned} \quad (2)$$

where

$\underline{\omega}_{Raw}$ = Gyro triad uncompensated (raw) output vector.

$\underline{\omega}'$ = Gyro triad output vector compensated for scale factor error.

$\underline{\tilde{\omega}}$ = First stage compensated gyro triad output vector.

$\underline{\hat{\omega}}$ = Second stage compensated gyro triad output vector. Shown with a $\hat{\quad}$ to indicate that the compensated angular rate may still contain residual errors to be measured and corrected by the SRT process.

I = Identity matrix.

K_{Scal} = Gyro triad scale factor correction matrix, a diagonal matrix in which each element adjusts the output scaling to correspond to the actual scaling for the particular sensor output. Nominally, the K_{Scal} matrix is zero. The K_{Scal} matrix may include non-linear scale factor effects and temperature dependency.

K_{Algn} = Gyro triad alignment correction matrix. Nominally, the K_{Algn} matrix is identity. The F_{Algn} matrix may include temperature dependency.

$\underline{\omega}_{Bias}$ = Gyro triad bias correction vector. Each element corrects the output from a particular gyro to zero under zero input inertial angular rate conditions. In some gyros, $\underline{\omega}_{Bias}$ may have temperature and specific force acceleration sensitivities.

$\underline{\omega}_{Quant}$ = Gyro triad pulse quantization correction vector for gyro outputs only being provided when the cumulative input equals the pulse weight per axis. Includes pulse output logic dead-band effect under turn-around conditions (See [2, Sect. 8.1.3.2]).

$\hat{\kappa}_{Mis}$ = Gyro triad misalignment compensation residual matrix having zero diagonal elements.

$\hat{\kappa}_{LinScal}$ = Gyro triad linear scale factor compensation residual diagonal matrix.

$\hat{\kappa}_{Asym}$ = Gyro triad asymmetric scale factor compensation residual diagonal matrix.

$\tilde{\Omega}_{Sign}^B$ = Diagonal matrix with elements equal to unity magnitude with the sign (plus or minus) of the $\underline{\tilde{\omega}}$ elements.

$\hat{\underline{\kappa}}_{Bias}$ = Gyro triad bias compensation residual vector.

$\underline{a}_{SF_{Raw}}$ = Accelerometer triad uncompensated (raw) specific force acceleration output vector.

\underline{a}'_{SF} = Accelerometer triad output vector compensated for scale factor error.

$\tilde{\underline{a}}_{SF}$ = First stage compensated accelerometer triad output vector.

$\hat{\underline{a}}_{SF}$ = Second stage compensated accelerometer triad output vector. Shown with a $\hat{\quad}$ to indicate that the compensated specific force acceleration may still contain residual errors to be measured and corrected by the SRT process.

L_{Scal} = Accelerometer triad scale factor correction matrix, a diagonal matrix in which each element adjusts the output scaling to correspond to the actual scaling for the particular sensor output. Nominally, the L_{Scal} matrix is zero. The L_{Scal} matrix may include non-linear scale factor effects and temperature dependency.

L_{Algn} = Accelerometer triad alignment correction matrix. Nominally, the L_{Algn} matrix is identity. The L_{Algn} matrix may include temperature dependency.

\underline{a}_{Bias} = Accelerometer triad bias correction vector. Each element corrects the output from a particular accelerometer to zero under zero input specific force acceleration conditions. In some accelerometers, \underline{a}_{Bias} may have temperature and angular rate sensitivities.

\underline{a}_{Size} = Accelerometer triad size effect correction vector that compensates the error created by accelerometers in the triad not being collocated, hence, not measuring components of identically the same acceleration vector (See [2, Sect. 8.1.4.1]).

\underline{a}_{Aniso} = Accelerometer triad anisoinertia correction vector that compensates for an error effect (in pendulous accelerometers) from mismatch in the moments of inertia around the input and pendulum axes (See [2, Sect. 8.1.4.2]).

\underline{a}_{Quant} = Accelerometer triad pulse quantization correction vector for accelerometer outputs only being provided when the cumulative input equals the pulse weight per axis. Includes pulse output logic dead-band effect under turn-around conditions (See [2, Sect. 8.1.3.2]).

$\hat{\lambda}_{Mis}$ = Accelerometer triad misalignment compensation residual matrix having zero diagonal elements.

$\hat{\lambda}_{LinScal}$ = Accelerometer triad linear scale factor compensation residual diagonal matrix.

$\hat{\lambda}_{Asym}$ = Accelerometer triad asymmetric scale factor compensation residual diagonal matrix.

\tilde{A}_{SFSign} = Diagonal matrix with elements equal to unity magnitude with the sign (plus or minus) of the \tilde{a}_{SF} elements.

$\hat{\lambda}_{Bias}$ = Accelerometer triad bias compensation residual vector.

Note 1: The $\hat{\kappa}$ and $\hat{\lambda}$ coefficient terms in (2) are shown with a $\hat{}$ to indicate that they may still contain residual errors to be measured and corrected by the SRT process.

Note 2: The \underline{a}_{Size} and \underline{a}_{Aniso} accelerometer compensation terms in (1) are functions of angular rate. Since SRT acceleration measurements are taken under stationary conditions, they will have no impact on SRT results and are only shown in (1) for completeness.

4.3.2 Compensation Coefficient Initialization For The SRT

The purpose for the SRT is to measure residual errors in the $\hat{\lambda}_{LinScal}$, $\hat{\lambda}_{Mis}$, $\hat{\lambda}_{Asym}$, $\hat{\lambda}_{Bias}$, $\hat{\kappa}_{LinScal}$, $\hat{\kappa}_{Mis}$, and $\hat{\kappa}_{Asym}$ elements (coefficients) of second stage compensation Eqs. (2). Prior to SRT execution, the IMU error coefficients imbedded in first stage compensation Eqs. (1) (i.e., K_{Scal} , K_{Align} , $\underline{\omega}_{Bias}$, L_{Scal} , L_{Align} , \underline{a}_{Bias}) would have been calibrated for previously measured sensor error effects (e.g., individual sensor temperature sensitivities, scale factor nonlinearities). The coefficients imbedded within the Eqs. (1) $\underline{\omega}_{Quant}$, \underline{a}_{Size} , \underline{a}_{Aniso} , and \underline{a}_{Quant} terms would be set to known sensor type and IMU configuration design characteristics (e.g., [2, Sects. 8.1.1.1 & 8.1.1.2]). The $\hat{\lambda}_{LinScal}$, $\hat{\lambda}_{Mis}$, $\hat{\lambda}_{Asym}$, $\hat{\lambda}_{Bias}$, $\hat{\kappa}_{LinScal}$, $\hat{\kappa}_{Mis}$, and $\hat{\kappa}_{Asym}$ coefficients in second stage compensation Eqs. (2) would be set to zero (unless the rotation test is to be an update following a previous SRT in which case the (1) coefficients would be set to their calibrated value following the previous test - To be discussed subsequently). The $\hat{\kappa}_{Bias}$ error vector in (2) would be set to zero or to a value measured separately since determination of the first stage compensation Eqs. (1) coefficients.

4.4 STRAPDOWN ROTATION TEST DATA COLLECTION

For each SRT rotation sequence, the following operations from Part 2 [3, Eqs. (15)] would be performed prior to and after completion of sequence rotations to obtain the “Reference Frame Accelerations” in Fig. 1:

$$\begin{aligned}
\hat{\underline{a}}_{SF}^{BStrt} &= \hat{C}_B^{BStrt} \hat{\underline{a}}_{SF}^B \\
\hat{\underline{a}}_{SF Strt}^{BStrt} &\equiv \left(\hat{\underline{a}}_{SF}^{BStrt} \right)_{StrtAvg} & \hat{\underline{a}}_{SF End}^{BStrt} &\equiv \left(\hat{\underline{a}}_{SF}^{BStrt} \right)_{EndAvg} \\
\Delta \hat{\underline{a}}_H^{BStrt} &= \left(\hat{\underline{a}}_{SF End}^{BStrt} - \hat{\underline{a}}_{SF Strt}^{BStrt} \right)_H \\
\hat{\underline{u}}_{Dwn}^{BStrt} &= \hat{C}_{NED}^{BStrt} \underline{u}_{Dwn}^{NED} & \underline{u}_{Dwn}^{NED} &= [0 \ 0 \ 1]^T \\
\hat{\underline{a}}_{Strt Down}^{BStrt} &= \hat{\underline{u}}_{Dwn}^{BStrt} \cdot \hat{\underline{a}}_{SF Strt}^{BStrt} + g & \hat{\underline{a}}_{End Down}^{BStrt} &= \hat{\underline{u}}_{Dwn}^{BStrt} \cdot \left(\hat{\underline{a}}_{SF End}^{BStrt} \right) + g
\end{aligned} \tag{3}$$

where

\hat{C}_B^{BStrt} = Direction cosine matrix that transforms vectors from the B frame to the B_{Strt} frame.

\hat{C}_{NED}^{BStrt} = Direction cosine matrix that transforms vectors from the NED frame to the B_{Strt} frame.

$\hat{\underline{a}}_{SF}^B$ = Specific force acceleration vector relative to the earth (in B frame coordinates), from the IMU accelerometer triad output.

$\hat{\underline{u}}_{Dwn}^{BStrt}$ = Unit vector downward (along plumb-bob gravity) in B_{Strt} frame coordinates.

$\underline{u}_{Dwn}^{NED}$ = Unit vector downward (along plumb-bob gravity) in NED frame coordinates, e.g., for local down along the NED third (e.g., z) axis, $\underline{u}_{Dwn}^{NED} = [0 \ 0 \ 1]^T$.

$\hat{\underline{a}}_{SF Strt}^{BStrt}, \left(\hat{\underline{a}}_{SF}^{BStrt} \right)_{StrtAvg}, \hat{\underline{a}}_{SF End}^{BStrt}, \left(\hat{\underline{a}}_{SF}^{BStrt} \right)_{EndAvg}$ = Average values of $\hat{\underline{a}}_{SF}^{BStrt}$ at the start and end of the SRT rotation sequence (when the IMU is stationary).

H = Subscript indicating the horizontal component of a vector.

$\Delta \hat{\underline{a}}_H^{BStrt}$ = Horizontal component of the difference between stationary acceleration measurements at the end and start of the rotation sequence.

g = Plumb-bob gravity magnitude at the test site.

$\hat{\underline{a}}_{Strt Down}^{BStrt}, \hat{\underline{a}}_{End Down}^{BStrt}$ = Downward components of stationary acceleration measurements at the start and end of the rotation sequence.

The components of $\hat{\underline{a}}_{SF}^{BStrt}$ in (3) represent the “Reference Frame Accelerations” in Fig. 1, the reference frame being the B frame at the start of the sequence (i.e., B_{Strt}). The $\left(\hat{\underline{a}}_{SF}^{BStrt}\right)_{StrtAvg}$, $\left(\hat{\underline{a}}_{SF}^{BStrt}\right)_{EndAvg}$ components in (3) represent outputs from the “Average Acceleration Algorithm” block in Fig. 1 calculated from the average value of $\hat{\underline{a}}_{SF}^{BStrt}$ over a designated time period at the start and end of the rotation sequence. The average acceleration measurements typically last for 10 seconds each using a simple averaging or average-of-averages type algorithm. The \hat{C}_{NED}^{BStrt} matrix in (3) is the orientation of the IMU B frame relative to local NED (north, east, down) coordinates at the start of the rotation sequence, approximately known from the rotation fixture north orientation in the test facility and the IMU mounting orientation on the test fixture. The \hat{C}_B^{BStrt} matrix in (3) is the output of the Fig. 1 “Attitude Computation” block, calculated from Part 2, [3, Eqs. (16)], as an integration process from the start of each rotation sequence:

$$\begin{aligned}\dot{\hat{C}}_B^{BStrt} &= \hat{C}_B^{BStrt} \left(\hat{\underline{\omega}}_{I:B}^B \times \right) - \left(\hat{\underline{\omega}}_{I:E}^{BStrt} \times \right) \hat{C}_B^{BStrt} \\ \hat{\underline{\omega}}_{I:E}^{BStrt} &= \hat{C}_{NED}^{BStrt} \underline{\omega}_{I:E}^{NED} \quad \underline{\omega}_{I:E}^{NED} = [\omega_e \cos l \quad 0 \quad -\omega_e \sin l]^T \\ \hat{C}_B^{BStrt} &= I + \int_{t_{SeqStrt}}^t \dot{\hat{C}}_B^{BStrt} dt\end{aligned}\quad (4)$$

where coordinate frames are defined in Section 3.0 and

I = Identity matrix.

$\hat{\underline{\omega}}_{I:B}^B$ = Angular rate vector of the B frame relative to non-rotating inertial space ($I:B$ subscript) measured in B frame coordinates (B superscript), i.e., the angular rate vector measured by the IMU strapdown gyro triad.

$\hat{\underline{\omega}}_{I:E}^{BStrt}$ = Angular rate vector of the earth relative to non-rotating inertial space ($I:E$ subscript) in B_{Strt} frame coordinates (superscript).

$\underline{\omega}_{I:E}^{NED}$ = Angular rate vector of the earth relative to non-rotating inertial space ($I:E$ subscript) in NED frame coordinates (superscript).

ω_e = Magnitude of earth’s rotation rate relative to non-rotating inertial space.

l = Latitude of the test site.

$t_{SeqStrt}$ = Time at the start of the first stationary acceleration measurement averaging process for the rotation sequence.

Note in (4) that the \hat{C}_B^{BStrt} matrix is initialized at identity, thus designating the B fame at the start of the sequence as the reference frame in Fig. 1 for making rotation sequence “Reference Frame Acceleration” measurements.

4.5 DETERMINING IMU SENSOR COMPENSATION COEFFICIENT ERRORS

Approximate error models are derived in Part 2 [3, Sect. 7.2] defining the $\Delta \hat{\underline{a}}_H^{BStrt}$, $\hat{\underline{a}}_{Down}^{BStrt}$, and $\hat{\underline{a}}_{Down}^{BEnd}$ measurements in (3) as a function of individual gyro and accelerometer compensation coefficient errors for each rotation sequence in the SRT. Equating the (3) measurements to the equivalent error model for each rotation sequence provides a simultaneous set of linear equations that can be inverted to determine the (2) compensation coefficient errors. Assuming the $\hat{\lambda}$ and $\hat{\kappa}$ compensation terms in (2) are unknown for the SRT (i.e., set to zero), Part 2 [3, Sect. 7.2] derives approximate measurement error models for (2) as summarized in Part 2 [3, Eqs. (70) - (75)]:

$$\phi_{-End}^{BStrt} \approx \sum_i C_{Bi,Strt}^{BStrt} \left\{ \begin{array}{l} \left[\kappa_{LinScal} + \kappa_{Asym} \text{Sign}(\dot{\beta}_i) \right] \underline{u}_i^{Bi,Strt} \theta_i \\ + \left[I \sin \theta_i + (1 - \cos \theta_i) \left(\underline{u}_i^{Bi,Strt} \times \right) \right] \left(\kappa_{Mis} \underline{u}_i^{Bi,Strt} \right) \end{array} \right\}$$

$$C_{B1,Strt}^{BStrt} = I \quad \text{Do } i=1 \text{ To } n : C_{Bi+1,Strt}^{BStrt} = C_{Bi,Strt}^{BStrt} C_{Bi+1,Strt}^{Bi,Strt} \quad (5)$$

$$C_{Bi+1,Strt}^{Bi,Strt} = I + \sin \theta_i \left(\underline{u}_i^{Bi,Strt} \times \right) + (1 - \cos \theta_i) \left(\underline{u}_i^{Bi,Strt} \times \right)^2$$

$$C_{BEnd}^{BStrt} = C_{Bn+1,Strt}^{BStrt}$$

$$\delta \hat{\underline{a}}_{SF Strt}^{BStrt} \approx -g \left(\lambda_{LinScal} + \lambda_{Mis} + \lambda_{Asym} A_{SFSign}^{BStrt} \right) \underline{u}_{Down}^{BStrt} + \underline{\lambda}_{Bias} \quad (6)$$

$$\delta \hat{\underline{a}}_{SF End}^{BEnd} \approx -g \left(\lambda_{LinScal} + \lambda_{Mis} + \lambda_{Asym} A_{SFSign}^{BEnd} \right) \underline{u}_{Down}^{BEnd} + \underline{\lambda}_{Bias}$$

$$\Delta \hat{\underline{a}}_H^{BStrt} \approx g \underline{u}_{Down}^{BStrt} \times \phi_{-End}^{BStrt} + \left(C_{BEnd}^{BStrt} \delta \hat{\underline{a}}_{SF End}^{BEnd} - \delta \hat{\underline{a}}_{SF Strt}^{BStrt} \right)_H$$

$$\hat{\underline{a}}_{Strt Down}^{BStrt} \approx \underline{u}_{Down}^{BStrt} \cdot \delta \hat{\underline{a}}_{SF Strt}^{BStrt} \quad \hat{\underline{a}}_{End Down}^{BEnd} \approx \underline{u}_{Down}^{BEnd} \cdot \delta \hat{\underline{a}}_{SF End}^{BEnd} \quad (7)$$

$$\underline{u}_{Down}^{BEnd} = \left(C_{BEnd}^{BStrt} \right)^T \underline{u}_{Down}^{BStrt}$$

where coordinate frames are defined in Section 3.0 and

$\kappa_{LinScal}$, κ_{Mis} , κ_{Asym} = Gyro triad residual linear scale factor error, misalignment, and asymmetrical scale-factor error matrices.

$\lambda_{LinScal}$, λ_{Mis} , λ_{Asym} = Accelerometer triad residual linear scale factor, misalignment, and asymmetrical scale-factor error matrices.

$\underline{\lambda}_{Bias}$ = Accelerometer triad bias error vector.

i = Subscript designating the rotation number in the particular SRT rotation sequence.

n = Subscript designating rotation number i for the last rotation in a particular SRT sequence.

$\underline{u}_i^{B_{i,Strt}}$ = Unit vector along the rotation axis for rotation i in the rotation sequence, also defined for the SRT to be a along a particular IMU B frame axis; e.g.,

$\underline{u}_i^{B_{i,Strt}} = [1 \ 0 \ 0]^T$, $[0 \ 1 \ 0]^T$, or $[0 \ 0 \ 1]^T$ for rotation i around B frame axis x , y , or z .

θ_i = Total angle traversed by rotation i in the rotation sequence.

$C_{B_{i,Strt}}^{B_{Strt}}$ = Direction cosine matrix that transforms vectors from $B_{i,Strt}$ to B_{Strt} frame coordinates.

$C_{B_{End}}^{B_{Strt}}$ = Direction cosine matrix that transforms vectors from B_{End} to B_{Strt} frame coordinates.

$\underline{\phi}_{-End}^{B_{Strt}}$ = Rotation angle error vector imbedded within the (4) measurement of $\hat{C}_B^{B_{Strt}}$ at the end of the rotation sequence.

$\underline{u}_{Dwn}^{B_{Strt}}$, $\underline{u}_{Dwn}^{B_{End}}$ = Unit vectors downward in the B_{Strt} and B_{End} frames.

$\hat{\delta}_{-SF_{Strt}}^{B_{Strt}}$, $\hat{\delta}_{-SF_{End}}^{B_{End}}$ = Errors in the (3) measurements of $\hat{\underline{a}}_{SF_{Strt}}^{B_{Strt}}$ and $\hat{\underline{a}}_{SF_{End}}^{B_{Strt}}$.

An important characteristic of the approximate (5) - (7) equations is that $\Delta \hat{\underline{a}}_H^{B_{Strt}}$ has no dependency on the misalignment of actual IMU B_{Strt} and B_{End} frames from their nominal orientations (Section 5.0 justifies (5) - (7) for sensor error determination by analytically

demonstrating these misalignments to have negligible impact on SRT test results). This is a direct result of defining $\hat{\Delta \underline{a}}_H^{B\text{Srt}}$ as the difference between ending and starting acceleration measurements. Only angular errors incurred during the rotation sequence (characterized by $\phi_{\underline{End}}^{B\text{Srt}}$) impact the $\hat{\Delta \underline{a}}_H^{B\text{Srt}}$ reading. This considerably simplifies the SRT setup because it allows each rotation sequence to begin from an approximate initial IMU attitude, thereby eliminating the requirement for precise IMU mounting on the rotation test fixture and orientation of the test fixture (and its rotation axes) relative to the local *NED* frame.

Elements within the (5) - (6) error parameters are defined as

$$\kappa_{LinScal} = \begin{bmatrix} \kappa_{xx} & 0 & 0 \\ 0 & \kappa_{yy} & 0 \\ 0 & 0 & \kappa_{zz} \end{bmatrix} \quad \kappa_{Mis} = \begin{bmatrix} 0 & \kappa_{xy} & \kappa_{xz} \\ \kappa_{yx} & 0 & \kappa_{yz} \\ \kappa_{zx} & \kappa_{zy} & 0 \end{bmatrix} \quad \kappa_{Asym} = \begin{bmatrix} \kappa_{xxx} & 0 & 0 \\ 0 & \kappa_{yyy} & 0 \\ 0 & 0 & \kappa_{zzz} \end{bmatrix} \quad (8)$$

$$\lambda_{LinScal} = \begin{bmatrix} \lambda_{xx} & 0 & 0 \\ 0 & \lambda_{yy} & 0 \\ 0 & 0 & \lambda_{zz} \end{bmatrix} \quad \lambda_{Mis} = \begin{bmatrix} 0 & \lambda_{xy} & \lambda_{xz} \\ \lambda_{yx} & 0 & \lambda_{yz} \\ \lambda_{zx} & \lambda_{zy} & 0 \end{bmatrix} \quad (9)$$

$$\lambda_{Asym} = \begin{bmatrix} \lambda_{xxx} & 0 & 0 \\ 0 & \lambda_{yyy} & 0 \\ 0 & 0 & \lambda_{zzz} \end{bmatrix} \quad \underline{\lambda}_{Bias} = \begin{bmatrix} \lambda_x \\ \lambda_y \\ \lambda_z \end{bmatrix}$$

where

κ_{ii} = Gyro *i* linear scale factor error (component of $\kappa_{LinScal}$).

κ_{iii} = Gyro *i* asymmetric scale factor error (component of κ_{Asym}).

κ_{ij} = Gyro *i* misalignment error coupling angular rate from axis *j* into the gyro *i* input axis (component of κ_{Mis}).

λ_i = Accelerometer *i* bias error (component of $\underline{\lambda}_{Bias}$).

λ_{ii} = Accelerometer *i* linear scale factor error (component of $\lambda_{LinScal}$).

λ_{iii} = Accelerometer *i* asymmetric scale factor error (component of λ_{Asym}).

λ_{ij} = Accelerometer i misalignment error coupling acceleration from axis j into the accelerometer i input axis (component of λ_{Mis}).

The gyro misalignments in (8) are relative to an arbitrary selected coordinate frame B representing IMU inertial sensor axes. To minimize second order error effects, it is expeditious to select the B frame to correspond with *MARS* (mean angular rate sensor) axes, the orthogonal frame that best fits around the actual gyro input axes. Fig. 3 illustrates the concept.

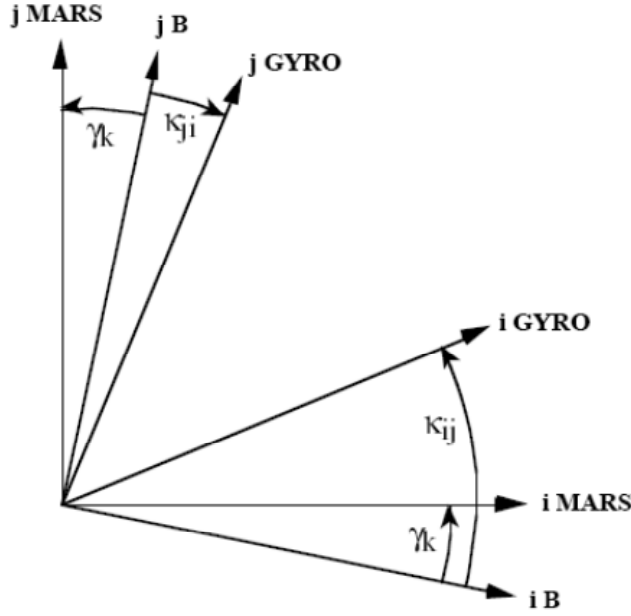


Fig. 3 - *MARS* Coordinates

In Fig. 3, γ_k is the angle between MARS and general B frame axes i and j . From Fig. 3, defining the B frame to be a *MARS* type is equivalent to setting $\gamma_k = 0$ for which

$$\kappa_{ij} = \kappa_{ji} \quad (10)$$

When adopting the *MARS* frame for B , it is also expedient to redefine κ_{ij} in terms of the angular orthogonality error between i and j , i.e., the angle between i and j gyro axes compared with the nominal orthogonal *MARS* axes equivalent of $\pi/2$. From Fig. 3, the conversion formula is

$$v_{ij} = \kappa_{ij} + \kappa_{ji} \quad (11)$$

or with (10),

$$\kappa_{ij} = \kappa_{ji} = \frac{1}{2} v_{ij} \quad (12)$$

where

v_{ij} = Orthogonality error between gyro axes i and j .

For a *MARS* defined B frame, the 6 accelerometer λ_{ij} misalignments in (9) will then automatically become *MARS* reference specialized. To identify *MARS* specialization and compatibility with *MARS* referenced gyro misalignments in (12), we will adopt the accelerometer misalignment definition formula

$$\lambda_{ij} = \mu_{ij} \quad (13)$$

where

μ_{ij} = Misalignment of accelerometer i relative to *MARS* B frame axis j .

Substituting the (12) and (13) conversion formulas in (8) and (9) then obtains the *MARS* B frame referenced equivalents:

$$\begin{aligned} \kappa_{LinScal} &= \begin{bmatrix} \kappa_{xx} & 0 & 0 \\ 0 & \kappa_{yy} & 0 \\ 0 & 0 & \kappa_{zz} \end{bmatrix} & \kappa_{Mis} &= \frac{1}{2} \begin{bmatrix} 0 & v_{xy} & v_{zx} \\ v_{xy} & 0 & v_{yz} \\ v_{zx} & v_{yz} & 0 \end{bmatrix} & \kappa_{Asym} &= \begin{bmatrix} \kappa_{xxx} & 0 & 0 \\ 0 & \kappa_{yyy} & 0 \\ 0 & 0 & \kappa_{zzz} \end{bmatrix} & (14) \\ \\ \lambda_{LinScal} &= \begin{bmatrix} \lambda_{xx} & 0 & 0 \\ 0 & \lambda_{yy} & 0 \\ 0 & 0 & \lambda_{zz} \end{bmatrix} & \lambda_{Mis} &= \begin{bmatrix} 0 & \mu_{xy} & \mu_{xz} \\ \mu_{yx} & 0 & \mu_{yz} \\ \mu_{zx} & \mu_{zy} & 0 \end{bmatrix} & & (15) \\ \\ \lambda_{Asym} &= \begin{bmatrix} \lambda_{xxx} & 0 & 0 \\ 0 & \lambda_{yyy} & 0 \\ 0 & 0 & \lambda_{zzz} \end{bmatrix} & \underline{\lambda}_{Bias} &= \begin{bmatrix} \lambda_x \\ \lambda_y \\ \lambda_z \end{bmatrix} \end{aligned}$$

4.5.1 SRT Measurements In Terms Of Sensor Compensation Coefficient Errors

Eqs. (5) - (7) with (8) - (9) or (14) - (15) are linearized approximations to the (4) and (3) measurements for each rotation sequence in the SRT. Section 6.0 presents a generic approach for SRT rotation sequence design, deriving formulas for generating a particular compensation coefficient error signature in one of the $\hat{\Delta a}_H^{B Strt}$, $\hat{a}_{Strt Down}^{B Strt}$, $\hat{a}_{End Down}^{B End}$ components of (7). The Section 6.0 process designed the Table 1 rotation sequences and the following analytical equivalents to (7) for the Table 1 measurements:

$$\begin{aligned}
\Delta a_{x1}^{BStirt} &= -2\pi g (\kappa_{yy} + \kappa_{yyy}) & \Delta a_{x2}^{BStirt} &= -2\pi g (\kappa_{xx} + \kappa_{xxx}) \\
\Delta a_{y3}^{BStirt} &= -2\pi g (\kappa_{zz} + \kappa_{zzz}) \\
\Delta a_{x1a}^{BStirt} &= 2\pi g (\kappa_{yy} - \kappa_{yyy}) & \Delta a_{x2a}^{BStirt} &= 2\pi g (\kappa_{xx} - \kappa_{xxx}) \\
\Delta a_{y3a}^{BStirt} &= 2\pi g (\kappa_{zz} - \kappa_{zzz}) \\
\Delta a_{y4}^{BStirt} &= 4g v_{yz} & \Delta a_{x5}^{BStirt} &= 4g v_{zx} & \Delta a_{y6}^{BStirt} &= 4g v_{xy} \\
\Delta a_{x7}^{BStirt} &= 2g (\mu_{xy} + v_{xy} / 2) & \Delta a_{z7}^{BStirt} &= -2 [\lambda_z + (\pi g / 2)(\kappa_{xx} + \kappa_{xxx})] & (16) \\
a_{Down7}^{BStirt} &= -g (\lambda_{yy} - \lambda_{yyy}) + \lambda_y & a_{Down7}^{BEnd} &= -g (\lambda_{yy} + \lambda_{yyy}) - \lambda_y \\
\Delta a_{x8}^{BStirt} &= 2g (\mu_{xz} + v_{zx} / 2) & \Delta a_{z9}^{BStirt} &= 2g (\mu_{zx} + v_{zx} / 2) \\
a_{Down8}^{BStirt} &= -g (\lambda_{zz} - \lambda_{zzz}) + \lambda_z & a_{Down8}^{BEnd} &= -g (\lambda_{zz} + \lambda_{zzz}) - \lambda_z \\
a_{Down9}^{BStirt} &= -g (\lambda_{xx} - \lambda_{xxx}) - \lambda_x & a_{Down9}^{BEnd} &= -g (\lambda_{xx} + \lambda_{xxx}) + \lambda_x \\
\Delta a_{z10}^{BStirt} &= 2g (\mu_{yz} + v_{yz} / 2) & \Delta a_{y11}^{BStirt} &= 2g (\mu_{yz} + v_{yz} / 2) \\
\Delta a_{y12}^{BStirt} &= 2g (\mu_{yx} + v_{xy} / 2) & \Delta a_{y13}^{BStirt} &= -2 (\lambda_y + g v_{yz}) & \Delta a_{x14}^{BStirt} &= -2 (\lambda_x + g v_{zx})
\end{aligned}$$

where

Δa_{jk}^{BStirt} = Analytical model approximation for the component j (x , y , or z) of the actual $\hat{\Delta a}_{jk}^{BStirt}$ measurement in (3) for rotation sequence k .

a_{Downk}^{BStirt} , a_{Downk}^{BEnd} = Analytical model approximations for the actual \hat{a}_{Downk}^{BStirt} , \hat{a}_{Downk}^{BEnd} measurements in (3) for rotation sequence k .

For confirmation of the Eqs. (16) general derivation approach in Section 6.0, Part 3 [4, Eqs. (18), (28), (43), (54) – (55) & (63)] derives the equivalent directly from (5) – (7), specifically for Table 1 Sequences 3, 5, 6, 7, and 13. Results are identical to (16).

4.5.2 Sensor Compensation Coefficient Errors In Terms Of SRT Measurements

SRT determination of errors in the Eqs. (2) compensation coefficients is based on the inverse of (16) with the actual Eq. (3) measurements substituted for Δa_{jk}^{BStirt} , a_{Downk}^{BStirt} , a_{Downk}^{BEnd} . Because Section 6.0 designed each of the Table 1 rotation sequences to excite a particular compensation error, the inversion process is trivial, yielding

$$\begin{aligned}
\kappa_{yy} &= -\frac{1}{4\pi g} \left(\Delta \hat{a}_{x1}^{BStrt} - \Delta \hat{a}_{x1a}^{BStrt} \right) & \kappa_{xx} &= -\frac{1}{4\pi g} \left(\Delta \hat{a}_{x2}^{BStrt} - \Delta \hat{a}_{x2a}^{BStrt} \right) \\
\kappa_{zz} &= -\frac{1}{4\pi g} \left(\Delta \hat{a}_{y3}^{BStrt} - \Delta \hat{a}_{y3a}^{BStrt} \right) \\
\kappa_{yyy} &= -\frac{1}{4\pi g} \left(\Delta \hat{a}_{x1}^{BStrt} + \Delta \hat{a}_{x1a}^{BStrt} \right) & \kappa_{xxx} &= -\frac{1}{4\pi g} \left(\Delta \hat{a}_{x2}^{BStrt} + \Delta \hat{a}_{x2a}^{BStrt} \right) \\
\kappa_{zzz} &= -\frac{1}{4\pi g} \left(\Delta \hat{a}_{y3}^{BStrt} + \Delta \hat{a}_{y3a}^{BStrt} \right) \\
v_{yz} &= \frac{1}{4g} \Delta \hat{a}_{y4}^{BStrt} & v_{zx} &= \frac{1}{4g} \Delta \hat{a}_{x5}^{BStrt} & v_{xy} &= \frac{1}{4g} \Delta \hat{a}_{y6}^{BStrt} \\
\mu_{xy} &= \frac{1}{2g} \left(\Delta \hat{a}_{x7}^{BStrt} - g v_{xy} \right) & \lambda_z &= -\frac{1}{2} \left(\Delta \hat{a}_{z7}^{BStrt} + \pi g \kappa_{xx} \right) \\
\mu_{xz} &= \frac{1}{2g} \left(\Delta \hat{a}_{x8}^{BStrt} - g v_{zx} \right) & \mu_{zx} &= \frac{1}{2g} \left(\Delta \hat{a}_{z9}^{BStrt} - g v_{zx} \right) \\
\mu_{zy} &= \frac{1}{2g} \left(\Delta \hat{a}_{z10}^{BStrt} - g v_{yz} \right) & \mu_{yz} &= \frac{1}{2g} \left(\Delta \hat{a}_{y11}^{BStrt} - g v_{yz} \right) \\
\mu_{yx} &= \frac{1}{2g} \left(\Delta \hat{a}_{y12}^{BStrt} - g v_{xy} \right) \\
\lambda_y &= -\frac{1}{2} \Delta \hat{a}_{y13}^{BStrt} - g v_{yz} & \lambda_x &= -\frac{1}{2} \Delta \hat{a}_{x14}^{BStrt} - g v_{zx} \\
\lambda_{yy} &= -\frac{1}{2g} \left(\hat{a}_{Down7}^{BEnd} + \hat{a}_{Down7}^{BStrt} \right) & \lambda_{yyy} &= -\frac{1}{2g} \left(\hat{a}_{Down7}^{BEnd} - \hat{a}_{Down7}^{BStrt} - 2 \lambda_y \right) \\
\lambda_{zz} &= -\frac{1}{2g} \left(\hat{a}_{Down8}^{BEnd} + \hat{a}_{Down8}^{BStrt} \right) & \lambda_{zzz} &= -\frac{1}{2g} \left(\hat{a}_{Down8}^{BEnd} - \hat{a}_{Down8}^{BStrt} - 2 \lambda_z \right) \\
\lambda_{xx} &= -\frac{1}{2g} \left(\hat{a}_{Down9}^{BEnd} + \hat{a}_{Down9}^{BStrt} \right) & \lambda_{xxx} &= -\frac{1}{2g} \left(\hat{a}_{Down9}^{BEnd} - \hat{a}_{Down9}^{BStrt} - 2 \lambda_x \right)
\end{aligned} \tag{17}$$

where

$\Delta \hat{a}_{jk}^{BStrt}$ = Component j (x , y , or z) of the actual $\Delta \hat{a}^{BStrt}$ measurement in (3) for rotation sequence k .

\hat{a}_{Downk}^{BStrt} , \hat{a}_{Downk}^{BEnd} = Actual \hat{a}_{Down}^{BStrt} , \hat{a}_{Down}^{BEnd} measurements in (3) for rotation sequence k .

If the gyros have no scale factor asymmetry (i.e., κ_{xxx} , κ_{yyy} , $\kappa_{zzz} = 0$), rotations sequences 1a - 3a would not be used, and the gyro linear scale factor terms in (17) would be computed as

$$\kappa_{yy} = -\frac{1}{2\pi g} \Delta \hat{a}_{x1}^{BStrt} \quad \kappa_{xx} = -\frac{1}{2\pi g} \Delta \hat{a}_{x2}^{BStrt} \quad \kappa_{zz} = -\frac{1}{2\pi g} \Delta \hat{a}_{y3}^{BStrt} \quad (18)$$

Note that accelerometer misalignment (μ_{ij}) and x, y bias (λ_x, λ_y) equations in (17) include $\frac{1}{2}v_{xy}$, $\frac{1}{2}v_{yz}$, and $\frac{1}{2}v_{zx}$ gyro-to-gyro orthogonality error offsets. The orthogonality errors are calculated in (18) from the rotation sequence 4 - 6 measurements, whence, they can be removed from the μ_{ij} and λ_x, λ_y equations. Similarly, z accelerometer bias (λ_z) in (17) includes a $\frac{1}{2}\pi g \kappa_{xx}$ gyro linear scale factor error offset. The κ_{xx} error calculated in (17) from rotation sequence 2 and 2a measurements can be removed from the λ_z equation. Finally, the λ_{xxx} , λ_{yyy} , λ_{zzz} accelerometer scale factor asymmetry equations in (17) include $\frac{1}{2}\lambda_x$, $\frac{1}{2}\lambda_y$, $\frac{1}{2}\lambda_z$ accelerometer bias offsets. After accelerometer biases are computed, they can be removed from the λ_{xxx} , λ_{yyy} , λ_{zzz} equations.

4.6 SENSOR COMPENSATION COEFFICIENT ERROR CORRECTION

Equations (17) represent the template for routines implemented in the SRT for evaluating error residuals in the Eqs. (2) $\hat{\kappa}$ and $\hat{\lambda}$ compensation coefficients. At SRT completion, the compensation coefficients would be corrected (re-calibrated) for the SRT determined error residuals - See Part 2 [3, Sects. A.5 & B.5] for rationale. When the (2) coefficient values are unknown (set to zero), the (17) template outputs represent updated values to be subsequently used in (2) for $\hat{\kappa}$ and $\hat{\lambda}$. When the (2) coefficients have non-zero values (i.e., from a previous calibration), the outputs from the (17) template represent the negative of errors in the (2) coefficients (to be used for (2) coefficient updating). In both cases, the updating operation consists of adding the (17) template outputs to the (2) coefficient values used during the SRT:

$$\begin{aligned} \hat{\lambda}_{LinScal}(+) &= \hat{\lambda}_{LinScal}(-) + \Delta \hat{\lambda}_{LinScal} & \hat{\lambda}_{Mis}(+) &= \hat{\lambda}_{Mis}(-) + \Delta \hat{\lambda}_{Mis} \\ \hat{\lambda}_{Asym}(+) &= \hat{\lambda}_{Asym}(-) + \Delta \hat{\lambda}_{Asym} & \hat{\lambda}_{Bias}(+) &= \hat{\lambda}_{Bias}(-) + \Delta \hat{\lambda}_{Bias} \end{aligned} \quad (19)$$

$$\begin{aligned} \hat{\kappa}_{LinScal}(+) &= \hat{\kappa}_{LinScal}(-) + \Delta \hat{\kappa}_{LinScal} & \hat{\kappa}_{Mis}(+) &= \hat{\kappa}_{Mis}(-) + \Delta \hat{\kappa}_{Mis} \\ \hat{\kappa}_{Asym}(+) &= \hat{\kappa}_{Asym}(-) + \Delta \hat{\kappa}_{Asym} \end{aligned}$$

where

(-), (+) = Designation for compensation coefficients in (2) before (-) SRT execution, and after (+) coefficient error determination/correction. The (-) coefficients are applied in (2) during the SRT.

$\Delta\hat{\kappa}$, $\Delta\hat{\lambda}$ = SRT determined corrections to the (2) coefficients, calculated using (17) as a template.

4.7 ITERATING THE SRT FOR ACCURACY ENHANCEMENT

The error analysis in Section 5.0 shows that the SRT is capable of determining sensor compensation errors to a few micro-radians accuracy (assuming pre-calibrating sensor scale factors to 1000 ppm accuracy, 1 milli-radian accuracy in executing the rotation sequences, and aligning the sensors within the IMU and the IMU on the rotation fixture to 1 milli-radian accuracy). If the mounting, rotation execution, and pre-calibration errors are larger, micro-radian accuracy can still be achieved by repeating the SRT following application of (19) to the results from the first SRT. Modern computer/memory technology makes this a trivial operation if the SRT computational process is structured as a batch-type post-data-collection operation on raw sensor data ($\underline{\omega}_{Raw}$ and $\underline{a}_{SF_{Raw}}$) recorded during the Table 1 SRT rotation-sequence/measurement process. SRT measurements would then be generated following data collection by “playing back” the recorded data in “simulated” past time through Eqs. (1) - (4). With this type of structure, an equivalent SRT is easily repeated by playing-back the originally recorded data through (1) - (4), without having to repeat the IMU data collection operation.

4.8 MITIGATING THE EFFECT OF RESIDUAL GYRO BIAS ON SRT ACCURACY

As with the original SRT, the improved SRT ignores the effect of residual gyro bias compensation error on SRT accuracy. Section 5.2.6 shows that for gyros having no g-sensitivity, improved SRT sensor error determination inaccuracy induced by 0.1 deg/hr residual gyro bias is approximately 1 micro-radians for gyro/accelerometer misalignment and 2 micro-gs for accelerometer bias. For gyros having larger bias error residuals (e.g., 1 to 50 deg/hr), a simple procedure can be included in the SRT for recalibrating gyro bias as part of SRT data collection operations. The method is to measure/recalibrate gyro biases at the start of the SRT as the average of the gyro output minus earth rate input (based on the approximately known orientation of the IMU on the rotation fixture relative to north, east, vertical). Errors incurred in the recalibration operation are due to uncertainty in earth rate input to the gyros and gyro random walk output noise during the averaging process.

For a large IMU/fixture alignment uncertainty of 10 milli-radians, the associated earth rate estimate would be 0.1 deg/hr, generating a bias recalibration error of 0.1 deg/hr, hence, 1 micro-radian SRT inaccuracy (as discussed previously). Recalibration error from gyro random walk output noise equals $60 \times \sigma_{RndmWalk} / \sqrt{T_{Avg}}$ deg/hr where $\sigma_{RndmWalk}$ is the gyro random walk coefficient in degrees per square-root of hour and T_{Avg} is the averaging time in seconds for bias measurement. Thus, for $\sigma_{RndmWalk} = 0.002$ deg/rt-hr (representative of ring laser gyros utilized in a standard accuracy military aircraft INS) and $T_{Avg} = 10$ seconds, the gyro bias recalibration error would be 0.038 deg/hr. The corresponding impact on SRT sensor error determination inaccuracy would be $0.038/0.1 = 0.38$ micro-radians (or micro-gs), generally negligible for a

standard accuracy INS. In contrast, for $\sigma_{RndmWalk} = 0.125$ deg/rt-hr (representative of a MEMS gyro) and $T_{Avg} = 10$ second, the calibration error would be 2.37 deg/hr, for a corresponding SRT inaccuracy of $2.37/0.1 = 24$ micro-radians = 0.024 milli-radians (or 0.024 milli-gs), generally acceptable for typical MEMS applications. These results can be reduced using a longer averaging time (e.g., by a factor of 3.2 for $T_{Avg} = 100$ seconds).

The method of implementing the gyro bias correction operation depends on whether or not the gyros have g-sensitivity, and whether the iteration process of the previous section is being applied. For gyros with no g-sensitivity, gyro biases can be measured during a single IMU static measurement period for which the 3 orthogonal IMU gyro biases are measured simultaneously. For gyros having g-sensitivity, 6 IMU static measurement periods would be required, each having the 3 orthogonal IMU gyro biases measured simultaneously, 3 of the 6 with each of the IMU axes up, the other 3 of the 6 with each of the IMU axes down. By summing and differencing the 6 measurements for each gyro, the g-sensitive and g-insensitive bias coefficients would then be determined. The bias errors so determined would then be used to update the $\underline{\kappa}_{Bias}$ coefficients in (2) prior to executing the SRT. (Note: As defined in (8) and (14), $\underline{\kappa}_{Bias}$ only includes g-insensitive coefficients. G-sensitive coefficients would be added, 3 for each gyro corresponding to specific force along the gyro input and cross-axes multiplying the corresponding coefficient.)

If the SRT is applied once without iteration, gyro bias measurements would be performed during a separate time period preceding the first measurement in the SRT sequence. If an SRT iteration process is employed (as in Section 4.7), gyro biases can be measured during the first pass through the SRT, then applied during the subsequent pass, requiring no additional time period for gyro bias measurement. Note also that for the Table 1 sequences, g-sensitive gyro bias measurements could be made as part of the normal SRT measurement process during the time periods used for accelerometer scale factor calibration (e.g., from Eqs. (17), during the start and end measurement periods for Sequences 7 - 9).

4.9 CALIBRATING MISALIGNMENTS BETWEEN THE IMU AND IMU MOUNT

For an IMU operated as an INS, unaided (free-inertial) velocity/position output accuracy is determined by inertial sensor error residuals and initial misalignment of the INS attitude reference B frame relative to earth referenced north/east/down coordinates. INS error contributions include the relative misalignments between the inertial sensors, but not B frame misalignment relative to its mount within the navigating vehicle. INS misalignment to the vehicle mount impacts the ability for attitude outputs to accurately represent vehicle angular orientation (roll, pitch, heading), an important secondary function of an INS. To mitigate mounting misalignment error, attitude outputs are compensated by correction coefficients determined by measurement/calibration test. The method to accurately calibrate INS to vehicle mount misalignment depends on the application. Many are based on the principal that while stationary and nominally horizontal, a non-zero output from a perfectly calibrated accelerometer will directly measure the accelerometer misalignment relative to the horizontal.

As an example, consider a test setup in which an IMU is mounted to a level test fixture with z axis down in the same manner as in the application vehicle. For the IMU having J_x, J_y misalignments relative to the mounting surface, the outputs from the nominally horizontal x and y accelerometers (divided by g) would respectively be J_y and minus J_x . The remaining J_z misalignment relative to a nominal mounting surface can be measured by repositioning the IMU to have x axis down, placing the y, z axes nominally horizontal. The output from the y accelerometer divided by g would then be J_z . If the rotation fixture has a pitch down capability about a horizontal axis, the IMU repositioning operation could be executed without remounting the IMU from its initial J_x, J_y measurement setup. The initial IMU mounting for this method would position the nominal IMU x axis perpendicular to the rotation fixture pitch down axis.

Once the J_x, J_y, J_z misalignment components are determined, attitude outputs generated from the INS would be compensated as in [2, Eqs.(8.3-1) - (8.3-2)] using

$(\hat{C}_B^N)_{Out} = \hat{C}_B^N [I + (\underline{J} \times)]$ where N is the INS reference navigation frame (e.g., azimuth wander), \hat{C}_B^N is the INS attitude matrix generated by integration from compensated gyro inputs, \underline{J} is the IMU B frame-to-mount misalignment vector (i.e., formed from J_x, J_y, J_z), and $(\hat{C}_B^N)_{Out}$ is the misalignment compensated \hat{C}_B^N matrix used to generate roll, pitch, heading outputs, e.g., as in [2, Sect. 4.1.2].

The accelerometer output measurements for the previous procedure would be generated using an averaging filter similar to the type used in the SRT for acceleration measurements. Note also that this procedure could also be imbedded within the SRT test itself as part of Section 4.7 batch-type iteration operations. Following the first sensor coefficient error measurement/correction cycle, the average of the Eqs. (2) compensated acceleration outputs would be used for \underline{J} misalignment component determination.

5.0 IMPROVED STRAPDOWN ROTATION TEST ERROR ANALYSIS

Eqs. (5) - (7) for sensor error determination are linearized approximations based on neglecting second order terms (products of sensor errors), rotation fixture imperfections in executing rotations, IMU mounting anomalies on the test fixture (to vertical and relative to north), gyro bias variations from initial calibration, and sensor noise effects. This section analytically defines the error induced by these approximations in determining sensor errors with the improved SRT. Of particular interest is the impact of initial IMU uncertainty relative to north/vertical and errors induced by rotation fixture imperfections, both ultimately affecting production cost.

The key sensor error parameters determined with the SRT are derived from the $\hat{\Delta a}_H^{B_{Strt}}$ horizontal acceleration measurement. The analysis in this section will be restricted to errors incurred using $\hat{\Delta a}_H^{B_{Strt}}$.

5.1 NOMINAL COORDINATE FRAMES FOR SECOND ORDER ERROR ANALYSIS

In addition to the coordinate frames described in Section 3.0, this section introduces the concept of “nominal” B frame coordinates to describe angular motion of an IMU under test having an idealized (error free) mounting on an idealized rotation-fixture that can execute prescribed rotations without error. Analogous to the Section 3.0 B frame, the nominal B frame (B^{Nom}) rotates relative to the earth (and inertial space) during rotation segments of each rotation sequence. All other nominal coordinate frames are fixed (non-rotating) relative to the earth, most defined to be aligned with B^{Nom} at the start and end of a rotation sequence, one defined to be aligned with north, east, down coordinates at the test site. Specific definitions for the nominal coordinate frame are as follows:

B^{Nom} = Nominal B frame defined as a hypothetical B frame that is nominally mounted on a nominal idealized rotation fixture that executes rotations exactly as prescribed, and which was installed in the test facility exactly as prescribed relative to local NED coordinates (i.e., so that the orientation of the B_{Nom} frame is known without error at any commanded rotation fixture gimbal angles).

B_{Strt}^{Nom} = Coordinate frame that is fixed (non-rotating) relative to the earth and aligned with the B^{Nom} frame at the start of the rotation sequence. Nominally, one of the B_{Strt}^{Nom} frame axes (x , y , or z) would be aligned with the local vertical if the inertial measurement unit (IMU being rotation tested is perfectly mounted on an idealized rotation fixture.

B_{End}^{Nom} = Coordinate frame that is fixed (non-rotating) relative to the earth and aligned with the B^{Nom} frame at the end of the rotation sequence.

$B_{i, Strt}^{Nom}$ = Coordinate frame that is fixed (non-rotating) relative to the earth and aligned with the B^{Nom} frame at the start of rotation i in a rotation sequence.

$B_{i, End}^{Nom}$ = Coordinate frame that is fixed (non-rotating) relative to the earth and aligned with the B^{Nom} frame at the end of rotation i in a rotation sequence.

5.2 IMPROVED SRT ERROR ANALYSIS

The error analysis begins by first defining the actual SRT measurement as the sum of the approximate version used in (7) plus terms neglected in the (7) derivation, Part 2 [3, Eq. (99)]:

$$\Delta \hat{\underline{a}}^{B Strt} = \Delta \hat{\underline{a}}_0^{B Strt} + e\left(\Delta \hat{\underline{a}}_0^{B Strt}\right) \quad (20)$$

where

$\Delta \hat{\underline{a}}^{B Strt}$ = Actual SRT measurement taken with (3) - (4) containing all error effects.

$\Delta \hat{\underline{a}}_0^{B Strt}$ = Approximate value of $\Delta \hat{\underline{a}}^{B Strt}$, the horizontal component for the (7) measurement model.

$e\left(\Delta \hat{\underline{a}}_0^{B Strt}\right)$ = Approximation error in $\Delta \hat{\underline{a}}_0^{B Strt}$.

0 = Subscript indicating approximate parameters used in the (5) - (7) error models.

From Part 2 [3, Eqs. (95)] we define the other error terms in (5) - (7) similarly:

$$\begin{aligned} \delta \hat{\underline{a}}_{SF Strt}^{B Strt} &= \delta \hat{\underline{a}}_{SF 0 Strt}^{B Strt} + e\left(\delta \hat{\underline{a}}_{SF 0 Strt}^{B Strt}\right) & \delta \hat{\underline{a}}_{SF End}^{B End} &= \delta \hat{\underline{a}}_{SF 0 End}^{B End} + e\left(\delta \hat{\underline{a}}_{SF 0 End}^{B End}\right) \\ \phi_{End}^{B Strt} &= \phi_{0 End}^{B Strt} + e\left(\phi_{0 End}^{B Strt}\right) \end{aligned} \quad (21)$$

where

$\delta \hat{\underline{a}}_{SF 0 Strt}^{B Strt}$, $\delta \hat{\underline{a}}_{SF 0 End}^{B End}$, $\phi_{0 End}^{B Strt}$ = Approximate error models in (5) - (7).

$\delta \hat{\underline{a}}_{SF Strt}^{B Strt}$, $\delta \hat{\underline{a}}_{SF End}^{B End}$, $\phi_{End}^{B Strt}$ = Actual error vectors containing terms neglecting in (5) - (7).

$e\left(\delta \hat{\underline{a}}_{SF 0 Strt}^{B Strt}\right)$, $e\left(\delta \hat{\underline{a}}_{SF 0 End}^{B End}\right)$, $e\left(\phi_{0 End}^{B Strt}\right)$ = Errors in the $\delta \hat{\underline{a}}_{SF 0 Strt}^{B Strt}$, $\delta \hat{\underline{a}}_{SF 0 End}^{B End}$, $\phi_{0 End}^{B Strt}$ approximate (5) - (7) error models.

Using the “0” parameter notation, the approximate $\Delta \hat{\underline{a}}_0^{B Strt}$ measurement in (20) is from the linearized form of Part 2 [3, Eq. (45)], the basis for (7):

$$\Delta \hat{\underline{a}}_0^{B Strt} \equiv \underline{g} \underline{u}_{Dwn}^{B Strt} \times \phi_{-0End}^{B Strt} + C_{B End}^{B Strt} \delta \hat{\underline{a}}_{SF 0End}^{B End} - \delta \hat{\underline{a}}_{SF 0Strt}^{B Strt} \quad (22)$$

Note that (22) uses the nominal B_{Nom} frame in contrast with (7) that approximates B_{Nom} as B . The (22) form is consistent with Part 2 which first derives the full (unapproximated) $\Delta \hat{\underline{a}}^{B Strt}$ model in the B_{Nom} frame, then in Part 2 [3, Eqs. (70) - (72)], approximates B_{Nom} as B for (5) - (7).

The accelerometer error terms in (22) are from (6):

$$\begin{aligned} \delta \hat{\underline{a}}_{SF 0Strt}^{B Strt} &\equiv -\underline{g} \left(\lambda_{LinScal} + \lambda_{Mis} + \lambda_{Asym} A_{SF Sign}^{B Strt} \right) \underline{u}_{Dwn}^{B Strt} + \underline{\lambda}_{Bias} \\ \delta \hat{\underline{a}}_{SF 0End}^{B End} &\equiv -\underline{g} \left(\lambda_{LinScal} + \lambda_{Mis} + \lambda_{Asym} A_{SF Sign}^{B End} \right) \underline{u}_{Dwn}^{B End} + \underline{\lambda}_{Bias} \end{aligned} \quad (23)$$

The $\phi_{-0End}^{B Strt}$ term in (22) can be defined similarly from (7) or alternatively, from Part 2 [3, Eq. (76)] from which (7) was derived in Part 2 [3, Sect. 6.1]:

$$\begin{aligned} \phi_{-0}^{B Strt} &= \int_{t_{Strt}}^t \dot{\phi}_{-0}^{B Strt} dt \\ \dot{\phi}_{-0}^{B Strt} &\equiv C_{B Nom}^{B Strt} \left(\kappa_{LinScal} + \kappa_{Mis} + \kappa_{Asym} \Omega_{EB Sign}^B \right) \underline{\omega}_{E: B Nom}^B \\ \phi_{-0End}^{B Strt} &= \phi_{-0}^{B Strt} \quad @ \quad t = t_{End} \end{aligned} \quad (24)$$

The analytical form of $e\left(\Delta \hat{\underline{a}}_0^{B Strt}\right)$ in (20) is derived in Part 2 as [3, Eq. (100) with Eqs. (101) - (102)] for the $e\left(\delta \hat{\underline{a}}_{SF 0Strt}^{B Strt}\right)$, $e\left(\delta \hat{\underline{a}}_{SF 0End}^{B End}\right)$, $e\left(\phi_{-0End}^{B Strt}\right)$ inputs:

$$\begin{aligned} e\left(\Delta \hat{\underline{a}}_0^{B Strt}\right) &= \underline{g} \underline{u}_{Dwn}^{B Strt} \times \left[e\left(\phi_{-0End}^{B Strt}\right) + \left(\frac{1}{2} \phi_{-0End}^{B Strt} - \underline{\alpha}_{Strt}^{B Strt}\right) \times \phi_{-0End}^{B Strt} \right] \\ + C_{B End}^{B Strt} &e\left(\delta \hat{\underline{a}}_{SF 0End}^{B End}\right) - e\left(\delta \hat{\underline{a}}_{SF 0Strt}^{B Strt}\right) + \left(\phi_{-0End}^{B Strt} + \underline{\alpha}_{End}^{B Strt} - \underline{\alpha}_{Strt}^{B Strt}\right) \times \left(C_{B End}^{B Strt} \delta \hat{\underline{a}}_{SF 0End}^{B End}\right) \end{aligned} \quad (25)$$

$$\begin{aligned}
e\left(\hat{\delta a}_{SF Strt}^{B Strt}\right) &= g\left(\lambda_{LinScal} + \lambda_{Mis} + \lambda_{Asym} A_{SF Sign}^{B Strt}\right)\left(\underline{\alpha}_{Strt}^{B Nom} \times \underline{u}_{Dwn}^{B Nom}\right) + \underline{\lambda}_{Quant Strt} + \underline{\lambda}_{Rndm Strt} \\
e\left(\hat{\delta a}_{SF End0}^{B End}\right) &= g\left(\lambda_{LinScal} + \lambda_{Mis} + \lambda_{Asym} A_{SF Sign}^{B End}\right)\left(\underline{\alpha}_{End}^{B Nom} \times \underline{u}_{Dwn}^{B Nom}\right) + \underline{\lambda}_{Quant End} + \underline{\lambda}_{Rndm End}
\end{aligned} \tag{26}$$

$$\begin{aligned}
e\left(\phi_{-0}^{B Strt}\right) &= \int_{t Strt}^t e\left(\dot{\phi}_{-0}^{B Strt}\right) dt \\
e\left(\dot{\phi}_{-0}^{B Strt}\right) &= C_{B Nom}^{B Strt} \left(\kappa_{LinScal} + \kappa_{Mis} + \kappa_{Asym} \Omega_{EB Sign}^B\right) \underline{\omega}_{I:E}^{B Nom} \\
&+ \left(\underline{\alpha}_{Strt}^{B Nom} - \underline{\alpha}_{Strt}^{B Nom}\right) \times \left[C_{B Nom}^{B Strt} \left(\kappa_{LinScal} + \kappa_{Mis} + \kappa_{Asym} \Omega_{EB Sign}^B\right) \underline{\omega}_{E:B}^{B Nom} \right] \\
&+ C_{B Nom}^{B Strt} \left[\left(\kappa_{LinScal} + \kappa_{Mis} + \kappa_{Asym} \Omega_{EB Sign}^B\right) \left(\dot{\underline{\alpha}}^{B Nom} - \underline{\alpha}^{B Nom} \times \underline{\omega}_{E:B}^{B Nom}\right) \right] \\
&+ C_{B Nom}^{B Strt} \left(\underline{\kappa}_{Bias} + \delta \underline{\omega}_{Quant} + \delta \underline{\omega}_{Rand}\right) + \left(\phi_{-0}^{B Strt} - \underline{\alpha}_{Strt}^{B Nom}\right) \times \underline{\omega}_{I:E}^{B Strt} \\
e\left(\phi_{-0 End}^{B Strt}\right) &= e\left(\phi_{-0}^{B Strt}\right) @ t = t End
\end{aligned} \tag{27}$$

The rotation sequences in Section 4.0 were designed so that one of the horizontal components of $\Delta \hat{a}^{B Strt}$ only responded to a particular sensor error. Thus, each component of (20) used for sensor error determination can be expressed by the scalar relationship

$$\Delta a_{jk}^{B Strt} = \pm H_k x_{0k} + e\left(\Delta a_{0jk}^{B Strt}\right) \tag{28}$$

where

$\Delta a_{jk}^{B Strt}$ = Horizontal component of $\Delta \hat{a}^{B Strt}$ from rotation sequence k along IMU axis j .

$e\left(\Delta a_{0jk}^{B Strt}\right)$ = Horizontal component of $e\left(\Delta \hat{a}_0^{B Strt}\right)$ along IMU axis j used for the $\Delta \hat{a}^{B Strt}$ measurement for rotation sequence k .

x_{0k} = Particular sensor component(s) measured by $\Delta a_{jk}^{B Strt}$ within the total error group determined by the SRT from (16).

H_k = Measurement sensitivity of Δa_{jk}^{BStirt} to x_{0k} . From (16), H_k for each x_{0k} is defined in Table 2.

x_{0k}	H_k
$(\kappa_{yy} + \kappa_{yyy}), (\kappa_{xx} + \kappa_{xxx}), (\kappa_{zz} + \kappa_{zzz})$ $(\kappa_{yy} - \kappa_{yyy}), (\kappa_{xx} - \kappa_{xxx}), (\kappa_{zz} - \kappa_{zzz})$	2 π g
v_{yz}, v_{zx}, v_{xy}	4 g
$(\mu_{xy} + v_{xy} / 2), (\mu_{xz} + v_{zx} / 2), (\mu_{zx} + v_{zx} / 2),$ $(\mu_{zy} + v_{yz} / 2), (\mu_{yz} + v_{yz} / 2), (\mu_{yx} + v_{xy} / 2),$ $(\lambda_y / g + v_{yz}), (\lambda_x / g + v_{zx}), [\lambda_z / g + (\pi / 2)(\kappa_{xx} + \kappa_{xxx})]$	2 g

Table 2 - Measurement Sensitivity To Sensor Errors

Sensor error determination for the improved SRT is based on (28) by neglecting $e(\Delta a_{0jk}^{BStirt})$:

$$\Delta a_{jk}^{BStirt} = \pm H_k \hat{x}_{0k} \quad (29)$$

where

$$\hat{x}_{0k} = \text{Value for } x_{0k} \text{ determined by SRT data processing.}$$

Equating (28) and (29) finds:

$$\pm H_k \hat{x}_{0k} = \pm H_k x_{0k} + e(\Delta a_{0jk}^{BStirt}) \rightarrow \hat{x}_{0k} = x_{0k} \pm \frac{1}{H_k} e(\Delta a_{0jk}^{BStirt}) \quad (30)$$

Thus

$$\delta \hat{x}_{0k} \equiv \hat{x}_{0k} - x_{0k} = \pm \frac{1}{H_k} e(\Delta a_{0jk}^{BStirt}) \quad (31)$$

where

$$\delta \hat{x}_{0k} = \text{Error in the SRT determined } \hat{x}_{0k} \text{ due to neglecting } e(\Delta a_{0jk}^{BStirt}) \text{ in (29).}$$

Equation (31) with Table 2 is in a convenient form for assessing the impact of particular elements of $e(\Delta a_{0jk}^{BStirt})$ on \hat{x}_{0k} determination accuracy.

5.2.1 Impact Of IMU Rotation And Mounting Error On SRT Accuracy

One of the principle advantages of the SRT concept is reduction in accuracy demands on rotation test fixtures and associated IMU mounting. These effects can be assessed by analyzing $\delta\hat{x}_k$ equation (31) for the impact of general IMU misalignment parameter α ; from $e\left(\Delta\hat{a}_0^{B\text{Strt}}\right)$ directly, and from the $e\left(\delta\hat{a}_{SF0\text{End}}^{B\text{End}}\right)$, $e\left(\delta\hat{a}_{SF0\text{Strt}}^{B\text{Strt}}\right)$, $e\left(\phi_{-0\text{End}}^{B\text{Strt}}\right)$ inputs to $e\left(\Delta\hat{a}_0^{B\text{Strt}}\right)$.

5.2.1.1 Direct Effect Of α In $e\left(\Delta\hat{a}_0^{B\text{Strt}}\right)$ On $\delta\hat{x}_{0k}$

From (25), α impacts $e\left(\Delta\hat{a}_0^{B\text{Strt}}\right)$ directly through the

$$\left(\underline{\alpha}_{\text{End}}^{B\text{Strt}\text{Nom}} - \underline{\alpha}_{\text{Strt}}^{B\text{Strt}\text{Nom}}\right) \times \left(C_{B\text{End}}^{B\text{Strt}\text{Nom}} \delta\hat{a}_{SF0\text{End}}^{B\text{End}}\right) \text{ and } g \underline{u}_{\text{Dwn}}^{B\text{Strt}\text{Nom}} \times e\left(\phi_{-0\text{End}}^{B\text{Strt}}\right) \text{ terms.}$$

From (23), the $\delta\hat{a}_{SF0\text{End}}^{B\text{End}}$ magnitude equals the uncertainty in accelerometer scale factor and bias errors. For $\left(\underline{\alpha}_{\text{End}}^{B\text{Strt}\text{Nom}} - \underline{\alpha}_{\text{Strt}}^{B\text{Strt}\text{Nom}}\right)$ and $\delta\hat{a}_{SF0\text{End}}^{B\text{End}}$ of 1 milli-rad and 1 milli-g magnitude, the magnitude of $\left(\underline{\alpha}_{\text{End}}^{B\text{Strt}\text{Nom}} - \underline{\alpha}_{\text{Strt}}^{B\text{Strt}\text{Nom}}\right) \times \left(C_{B\text{End}}^{B\text{Strt}\text{Nom}} \delta\hat{a}_{SF0\text{End}}^{B\text{End}}\right)$ will be 1 micro-g. From (31) and Table 2 for H_k , the maximum error in $\delta\hat{x}_{0k}$ will then be 0.5 micro-g.

From (24), the $\phi_{-0\text{End}}^{B\text{Strt}}$ magnitude equals the uncertainty in gyro scale-factor and misalignment error. For $\phi_{-0\text{End}}^{B\text{Strt}}$ and $\underline{\alpha}_{\text{Strt}}^{B\text{Strt}\text{Nom}}$ magnitudes of 1000 ppm and 1 milli-rad, the magnitude of $g \underline{u}_{\text{Dwn}}^{B\text{Strt}\text{Nom}} \times e\left(\phi_{-0\text{End}}^{B\text{Strt}}\right)$ will be 1 micro-g. From (31) and Table 2 for H_k , the corresponding maximum error in $\delta\hat{x}_{0k}$ will be 0.5 micro-g.

5.2.1.2 Effect Of α In $e\left(\delta\hat{a}_{SF0\text{Strt}}^{B\text{Strt}}\right)$ And $e\left(\delta\hat{a}_{SF0\text{End}}^{B\text{End}}\right)$ On $\delta\hat{x}_{0k}$

From (26), α impacts $e\left(\delta\hat{a}_{SF0\text{Strt}}^{B\text{Strt}}\right)$ and $e\left(\delta\hat{a}_{SF0\text{End}}^{B\text{End}}\right)$ through the

$$g\left(\lambda_{\text{LinScals}} + \lambda_{\text{Mis}} + \lambda_{\text{Asym}} A_{SF\text{Sign}}^{B\text{End}}\right) \left(\underline{\alpha}_{\text{Strt}}^{B\text{Strt}\text{Nom}} \times \underline{u}_{\text{Dwn}}^{B\text{Strt}\text{Nom}}\right) \text{ and}$$

$g \left(\lambda_{LinScals} + \lambda_{Mis} + \lambda_{Asym} A_{SFSign}^{BEnd} \right) \left(\underline{\alpha}_{End}^{BNom} \times \underline{u}_{Dwn}^{BNom} \right)$ terms. For α and accelerometer scale factor uncertainties of 1 milli-rad and 1000 ppm, the magnitude of these terms will be 1 micro-g. The impact on $e \left(\Delta \hat{\underline{a}}_0^{BStrt} \right)$ in (25) will also be on the order of 1 micro-g through the $C_{BEnd}^{BNom} e \left(\hat{\delta \underline{a}}_{SF0End}^{BEnd} \right) - e \left(\hat{\delta \underline{a}}_{SF0Strt}^{BStrt} \right)$ term. From (31) and Table 2 for H_k , the maximum error in $\delta \hat{x}_{0k}$ will then be on the order of 0.5 micro-g.

5.2.1.3 Impact Of α In $e \left(\phi_{-0End}^{BStrt} \right)$ On $\delta \hat{x}_{0k}$

From (27), α impacts $e \left(\phi_{-0End}^{BStrt} \right)$ through the integrated effect of

$$\left(\underline{\alpha}_{Strt}^{BNom} - \underline{\alpha}_{Strt}^{BNom} \right) \times \left[C_{BNom}^{BStrt} \left(\kappa_{LinScal} + \kappa_{Mis} + \kappa_{Asym} \Omega_{EBSign}^B \right) \underline{\omega}_{E:BNom}^{BNom} \right],$$

$$C_{BNom}^{BStrt} \left[\left(\kappa_{LinScal} + \kappa_{Mis} + \kappa_{Asym} \Omega_{EBSign}^B \right) \left(\dot{\underline{\alpha}}^{BNom} - \underline{\alpha}^{BNom} \times \underline{\omega}_{E:BNom}^{BNom} \right) \right], \text{ and}$$

$$\underline{\alpha}_{Strt}^{BNom} \times \underline{\omega}_{I:E}^{BStrt} \text{ in the (27) } e \left(\dot{\phi}_{-0}^{BStrt} \right) \text{ equation.}$$

For the rotation sequences in Table 1, the maximum value for the integral of $\underline{\omega}_{E:BNom}^{BNom}$ over a rotation sequence will be the H_k value in Table 2 divided by g. Hence, the maximum integral value into $e \left(\phi_{-0End}^{BStrt} \right)$ of terms multiplying $\underline{\omega}_{E:BNom}^{BNom}$ will be on the order of $\alpha \times$ gyro scale-factor/misalignment error $\times H_k / g$. For α and gyro scale-factor/misalignment errors on the order of 1 milli-rad, this translates into a maximum $e \left(\phi_{-0End}^{BStrt} \right)$ error of H_k / g micro-rad. The impact on $e \left(\Delta \hat{\underline{a}}_0^{BStrt} \right)$ in (25) through $g \underline{u}_{Dwn}^{BNom} \times e \left(\phi_{-0End}^{BStrt} \right)$ will then be H_k micro-g. Thus, from (31), the impact on $\delta \hat{x}_{0k}$ will be 1 micro-rad.

The integral of $\dot{\underline{\alpha}}^{BNom}$ over a rotation sequence is $\left(\underline{\alpha}_{End}^{BNom} - \underline{\alpha}_{Strt}^{BNom} \right)$. Thus the maximum integral value into $e \left(\phi_{-0End}^{BStrt} \right)$ of terms multiplying $\dot{\underline{\alpha}}^{BNom}$ will be on the order of $\alpha \times$ gyro scale-factor/misalignment error. For α and gyro scale-factor/misalignment errors on the order of 1000 ppm and 1 milli-rad, this translates into a maximum $e \left(\phi_{-0End}^{BStrt} \right)$ error of 1 micro-rad, impacting

$e\left(\Delta\hat{a}_0^{B\text{Strt}}\right)$ in (25) by 1 micro-g. From (31) and Table 2 for H_k , the maximum error in $\delta\hat{x}_{0k}$ will then be 0.5 micro-rad.

An important new advantage of the improved SRT is elimination of the requirement for inertial self-alignment of the IMU prior to rotation sequence execution, a problem area for IMUs with lesser accuracy gyros. This requires a reasonably accurate initial physical alignment of the IMU on the test fixture relative to north (e.g., 1 milli-radian). The $\underline{\alpha}_{\text{Strt}}^{B\text{Nom}} \times \underline{\omega}_{I:E}^{B\text{Strt}}$ term in (27) becomes the error introduced in $e\left(\dot{\phi}_0^{B\text{Strt}}\right)$ with this approach. The impact on sensor error determination accuracy depends on the total time over a rotation sequence for the error to integrate into $e\left(\phi_{-0\text{End}}^{B\text{Strt}}\right)$. If we assume that 10 seconds each will be used for acceleration measurement before and after rotation sequence execution, and 20 seconds for rotation sequence execution, the total time for a rotation sequence will be 40 seconds. Then the integral of the $\underline{\alpha}_{\text{Strt}}^{B\text{Nom}} \times \underline{\omega}_{I:E}^{B\text{Strt}}$ over the rotation sequence will be $\alpha \times \text{earth rate} \times 40$. For α of 1 milli-rad and earth rate = 15 deg/hr (0.000073 rad/sec), this translates into an $e\left(\phi_{-0\text{End}}^{B\text{Strt}}\right)$ value of $0.001 \times 0.000073 \times 40 = 2.9\text{E-}6$ rad = 2.9 micro-rad, thereby impacting $e\left(\Delta\hat{a}_0^{B\text{Strt}}\right)$ in (25) by 2.9 micro-g. From (31) and Table 2 for H_k , the maximum error in $\delta\hat{x}_{0k}$ will then be 1.5 micro-rad.

5.2.1.4 Summary Of Rotation Fixture And IMU Mounting Error Effects On SRT Sensor Error Determination Accuracy

Sections 5.2.1.1 - 5.2.1.3 show that for 1 milli-rad IMU mounting and rotation fixture errors, the impact on SRT sensor error determination accuracy will be on the order of 1 micro-rad. It is important to recognize, however, that except for the earth rate coupling effect discussed at the end of Section 5.2.1.3, each of the micro-rad errors is proportional to sensor errors being determined by the SRT. Hence, a repeated SRT using updated sensor calibration coefficients (updated from the previous SRT result), will eliminate these sources of sensor error determination in-accuracy (See Section 4.7 for further discussion). The only remaining error would be the 1.5 micro-rad earth rate coupling error induced by the integral of $\underline{\alpha}_{\text{Strt}}^{B\text{Nom}} \times \underline{\omega}_{I:E}^{B\text{Strt}}$ in the $e\left(\dot{\phi}_0^{B\text{Strt}}\right)$ equation.

5.2.2 Impact Of Gyro Output Noise On SRT Accuracy

The impact of gyro output noise on SRT accuracy can be assessed by analyzing how $\delta\underline{\omega}_{\text{Rand}}$ random noise and $\delta\underline{\omega}_{\text{Quant}}$ quantization noise in (27) propagate into $e\left(\phi_{-0\text{End}}^{B\text{Strt}}\right)$, then

into $e\left(\Delta\hat{a}_0^{B\text{Strt}}\right)$ equation (25).

On a root-mean-square (rms) average basis, integrated $\delta\omega_{Rand}$ random noise propagates as the square root of the integration time. For a 40 second rotation sequence time interval and 0.002 deg/ $\sqrt{\text{hr}}$ gyro random noise, the rms build-up in $e\left(\phi_{-0\text{End}}^{B\text{Strt}}\right)$ will be $[0.002 / (57.3 \times \sqrt{3600})] \times \sqrt{40} = 3.7$ micro-rad. The effect on $e\left(\Delta\hat{a}_0^{B\text{Strt}}\right)$ in (25) will then be 3.7 micro-gs. From (31) and Table 2, this translates into a maximum $\delta\hat{x}_{0k}$ sensor error determination error of 1.8 micro-rad.

The integral of $\delta\omega_{Quant}$ quantization noise over any time interval is the rms (root-mean-square) difference between integrated gyro output pulse quantization error at the start and end of the rotation sequence. For ε output pulse size, this translates into an rms quantization error of $\sqrt{(\varepsilon^2 / 12)} \times 2 = 0.4 \varepsilon$. For a 0.5 arc-sec pulse size, the rms impact on $e\left(\phi_{-0\text{End}}^{B\text{Strt}}\right)$ would be $0.4 \times [(0.5 / 3600) / 57.3] = 9.7 \text{ E-}7$ rad = 0.97 micro-rad. The rms effect on $e\left(\Delta\hat{a}_0^{B\text{Strt}}\right)$ in (25) would then be 0.97 micro-gs. From (31) and Table 2, this translates into an rms $\delta\hat{x}_{0k}$ sensor error determination error of 0.5 micro-rad.

5.2.3 Impact Of Output Accelerometer Noise On SRT Accuracy

The impact of accelerometer output noise on SRT accuracy can be assessed by analyzing how $\underline{\lambda}_{Quant\text{Strt}}$, $\underline{\lambda}_{Rndm\text{Strt}}$ at the start of a rotation sequence and $\underline{\lambda}_{Quant\text{End}}$, $\underline{\lambda}_{Rndm\text{End}}$ at the end of the rotation sequence impact $e\left(\delta\hat{a}_{SF\ 0\text{Strt}}^{B\text{Strt}}\right)$, $e\left(\delta\hat{a}_{SF\ 0\text{End}}^{B\text{End}}\right)$ in (26), hence, $e\left(\Delta\hat{a}_0^{B\text{Strt}}\right)$ in (25). The start and end effects are analyzed separately, each using an approach similar to that taken in 5.2.2 for gyro output noise impact analysis. The difference is that the integration time interval would be the averaging time to measure $\hat{a}_{SF\ \text{Strt}}^{B\text{Strt}}$ and $\hat{a}_{SF\ \text{End}}^{B\text{Strt}}$ in (3) using an appropriate noise reduction algorithm. Propagation of $\underline{\lambda}_{Rndm\text{Strt}}$ and $\underline{\lambda}_{Rndm\text{End}}$ over the averaging time is unaffected by the averaging algorithm, generating the same rms error as a simple integration process (i.e., to the random noise coefficient in fps/square-root-sec multiplied by the square-root of the integration time). Some averaging algorithms are designed to reduce the $\underline{\lambda}_{Quant}$ errors from what they would have been using an integration process for averaging (e.g., an average-of-averages algorithm - [2, Sect. 18.4.7.3]).

5.2.4 Impact Of Second Order Sensor Error Effects On SRT Accuracy

The impact of second order error effects (i.e., products of sensor error) on SRT accuracy are generated by the $\frac{g}{2} \left(\underline{u}_{Down}^{B\text{Strt}} \times \underline{\phi}_{0End}^{B\text{Strt}} \right) \times \underline{\phi}_{0End}^{B\text{Strt}}$ and $\underline{\phi}_{0End}^{B\text{Strt}} \times \left(C_{B\text{End}}^{B\text{Strt}} \delta \hat{\underline{a}}_{SF\text{0End}}^{B\text{End}} \right)$ terms in the (25) $e \left(\Delta \hat{\underline{a}}_0^{B\text{Strt}} \right)$ equation. From (24), $\underline{\phi}_{0End}^{B\text{Strt}}$ is proportional to gyro scale-factor and misalignment errors. From (23), $\delta \hat{\underline{a}}_{SF\text{0End}}^{B\text{End}}$ is proportional to accelerometer scale-factor, misalignment, and bias errors. Thus, for scale-factor, misalignment, and accelerometer bias errors on the order of 1 milli-rad and milli-g, $\frac{g}{2} \left(\underline{u}_{Down}^{B\text{Strt}} \times \underline{\phi}_{0End}^{B\text{Strt}} \right) \times \underline{\phi}_{0End}^{B\text{Strt}}$ and $\underline{\phi}_{0End}^{B\text{Strt}} \times \left(C_{B\text{End}}^{B\text{Strt}} \delta \hat{\underline{a}}_{SF\text{0End}}^{B\text{End}} \right)$ will be on the order of 1 micro-g, thus impacting $\delta \hat{x}_{0k}$ sensor error determination accuracy in (31) by 1 micro-rad.

It is also to be noted that the basic derivation of (25) for $e \left(\Delta \hat{\underline{a}}_0^{B\text{Strt}} \right)$ was based on complete (not linearized) sensor error models in the Part 2 appendices [3, Eqs. (A-15) & (B-15)]. Thus, there are no second order error effects within the sensor error models.

5.2.5 Impact Of $\underline{\phi}_{0End}^{B\text{Strt}} \times \underline{\omega}_{I:E}^{B\text{Strt}}$ In $e \left(\dot{\underline{\phi}}_{0End}^{B\text{Strt}} \right)$ On SRT Accuracy

The $\underline{\phi}_{0End}^{B\text{Strt}} \times \underline{\omega}_{I:E}^{B\text{Strt}}$ term in the (27) $e \left(\dot{\underline{\phi}}_{0End}^{B\text{Strt}} \right)$ equation builds into $e \left(\underline{\phi}_{0End}^{B\text{Strt}} \right)$ and then into $e \left(\Delta \hat{\underline{a}}_0^{B\text{Strt}} \right)$ through (23). From (24), $\underline{\phi}_{0End}^{B\text{Strt}}$ is proportional to gyro scale-factor and misalignment errors. For a 40 second rotation sequence time interval, gyro scale-factor/misalignment errors of 1-milli-rad/1000-ppm, and $\underline{\omega}_{I:E}^{B\text{Strt}}$ earth rate = 15 deg/hr (0.000073 rad/sec), this translates into an $e \left(\underline{\phi}_{0End}^{B\text{Strt}} \right)$ value of $0.001 \times 0.000073 \times 40 = 2.9\text{E-}6$ rad = 2.9 micro-rad, impacting $e \left(\Delta \hat{\underline{a}}_0^{B\text{Strt}} \right)$ in (25) by 2.9 micro-g. From (31) and Table 2 for H_k , the maximum error in $\delta \hat{x}_{0k}$ will then be 1.5 micro-rad. Similar to the second order error source discussion in the previous section, this particular error can be eliminated using a second SRT after sensor calibration coefficient updating with error determinations from the first SRT (See Section 4.7 for further discussion).

5.2.6 Impact Of Gyro Bias Calibration Error Residual On SRT Accuracy

The original and improved SRT were based on calibrating gyro bias to reasonable accuracy before the test so that it could be safely neglected in the Part 2 design of sensor error

determination equations. Thus, residual gyro bias errors following calibration will impact SRT sensor error determination accuracy. The impact of gyro bias $\underline{\kappa}_{Bias}$ on SRT accuracy can be assessed by analyzing how the $C_{B^{Nom}}^{B^{Strt}} \underline{\kappa}_{Bias}$ term in (27) propagates into $e\left(\underline{\phi}_0^{B^{Strt}}\right)$, then into $e\left(\Delta \hat{\underline{a}}_0^{B^{Strt}}\right)$ equation (25). For the analysis it is important to recognize that the sequences in Table 1 generate a changing $C_{B^{Nom}}^{B^{Strt}} \underline{\kappa}_{Bias}$ in the SRT measurement due to rotation induced $C_{B^{Nom}}^{B^{Strt}}$ changes. Additionally, the analysis should include the gyro bias cancellation effect in forming the $\Delta \hat{\underline{a}}^{B^{Strt}}$ measurement as the difference between acceleration measurements made before and after rotation sequence execution. For gyros having no g-sensitive bias error, the remainder of this section addresses these considerations, providing a rigorous analytical assessment of gyro bias impact on $e\left(\Delta \hat{\underline{a}}_0^{B^{Strt}}\right)$. The results demonstrate that uncompensated 0.1 deg/hr gyro biases induce SRT sensor determination errors on the order of 1 micro-radians and 1 micro-g, generally negligible for most applications. Section 4.8 shows how gyro bias induced SRT errors can be mitigated (if necessary) for fixed and g-sensitive gyro bias errors.

The contribution to measurement modeling error $e\left(\Delta \hat{\underline{a}}^{B^{Strt}}\right)$ caused by neglecting constant gyro bias in the $\Delta \hat{\underline{a}}_0^{B^{Strt}}$ derivation is derived as $\Delta \hat{\underline{a}}_{GyroBias}^{B^{Strt}}$ in Part 2 [3, Eq. (126) with Eqs. (131) & (120)]. Identifying $C_{B^{Meas2}}^{B^{Strt}}$ in [3, Eq. (126)] as $C_{B^{End}}^{B^{Strt}}$ obtains

$$e\left(\Delta \hat{\underline{a}}_0^{B^{Strt}}\right)_{GyroBias} = g \underline{u}_{Dwn}^{B^{Strt}} \times \left\{ \Delta \phi_{GyroBias Rot}^{B^{Strt}} + T_{Meas} \left[I + F_{Meas} \left(C_{B^{End}}^{B^{Strt}} - I \right) \right] \underline{\kappa}_{Bias} \right\} \quad (32)$$

$$\Delta \phi_{GyroBias Rot}^{B^{Strt}} = \sum_i C_{B_i^{Strt}}^{B^{Strt}} \left[I + \frac{(1 - \cos \theta_i)}{\theta_i} \left(\underline{u}_i^{B_i^{Strt}} \times \right) + \left(1 - \frac{\sin \theta_i}{\theta_i} \right) \left(\underline{u}_i^{B_i^{Strt}} \times \right)^2 \right] \frac{\theta_i}{\dot{\beta}_i} \underline{\kappa}_{Bias} \quad (33)$$

$$F_{Meas} \equiv \frac{1}{T_{Meas}} \int_{t_{Meas Strt}}^{t_{Meas End}} \zeta\left(t, t_{Meas End}\right) (t - t_{Meas Strt}) dt \quad (34)$$

where

$\underline{\kappa}_{Bias}$ = Gyro bias error vector residual which is assumed constant over the rotation sequence time period (and without “g-sensitive” variations dependent on gyro orientation relative to the local vertical).

T_{Meas} = Time interval for making each of the $\hat{\underline{a}}^{BStrt}$ SRT measurements at the start and end of the rotation sequence.

$e\left(\Delta\hat{\underline{a}}_0^{BStrt}\right)_{GyroBias}$ = Component $e\left(\Delta\hat{\underline{a}}_0^{BStrt}\right)$ caused by neglecting the effect of gyro bias in the Part 2 derivation of $\Delta\hat{\underline{a}}_H^{BStrt}$ for (7).

θ_i = Signed magnitude of total angular traversal around rotation axis i .

$\dot{\beta}_i$ = Angular rate of rotation i .

$t_{MeasStrt}, t_{MeasEnd}$ = Time at the start and end of the $\hat{\underline{a}}^{BStrt}$ measurement time.

$\zeta(t, t_{MeasEnd})$ = Measurement averaging algorithm weighting function: The algorithm response at $t_{MeasEnd}$ from a unit impulse input to the averaging algorithm at time t during the measurement period. Typical averaging algorithms are a simple linear average or an average of successive overlapping averages (“average-of-averages”) [2, Sect. 18.4.7.3].

Part 3 [4] evaluates (32) - (34) showing the impact on the Eq. (16) results [4, Eqs. (20), (34), (48), (57), & (65)] to be:

$$\begin{aligned}
e\left(\Delta a_{y3}^{BStrt}\right)_{GyroBias} &= -2\pi g \left[1/\dot{\beta} + T_{Meas}/(2\pi) \right] \kappa_z \quad \text{Similarly For Seqs. 1, 2, and 1a - 3a} \\
e\left(\Delta a_{x5}^{BStrt}\right)_{GyroBias} &= 4g \left[(\kappa_x + \kappa_z)/\dot{\beta} - T_{Meas} \kappa_y/4 \right] \quad \text{Similarly For Seq. 4} \\
e\left(\Delta a_{y6}^{BStrt}\right)_{GyroBias} &= 4g \left[(\kappa_x + \kappa_y)/\dot{\beta} - T_{Meas} \kappa_z/4 \right] \\
e\left(\Delta a_{x7}^{BStrt}\right)_{GyroBias} &= 2g \left[\kappa_y/\dot{\beta} + T_{Meas} (1 - 2F_{Meas}) \kappa_z/2 \right] \quad \text{Similarly For Seqs. 8 - 12} \\
e\left(\Delta a_{z7}^{BStrt}\right)_{GyroBias} &= -\pi g \left(1/\dot{\beta} + T_{Meas}/\pi \right) \kappa_x \\
e\left(\Delta a_{y13}^{BStrt}\right)_{GyroBias} &= -2g \left[(\kappa_z + \kappa_y)/\dot{\beta} - T_{Meas} \kappa_x/2 \right] \quad \text{Similarly For Seq. 14}
\end{aligned} \tag{35}$$

where

$e\left(\Delta a_{jk}^{BStrt}\right)_{GyroBias}$ = Component j (x , y , or z) of the $e\left(\Delta \hat{a}_0^{BStrt}\right)_{GyroBias}$ error in the $\Delta \hat{a}_0^{BStrt}$ measurement approximation for rotation sequence k produced by fixed gyro bias.

κ_i = Gyro bias component i (x , y , or z) in $\underline{\kappa}_{Bias}$ - as in (8) or (14).

To assess the impact of (35) on SRT sensor error determination accuracy we write, analogous to (31):

$$\left(\delta \hat{x}_{jk}\right)_{GyroBias} = \pm \frac{1}{H_k} e\left(\Delta a_{jk}^{BStrt}\right)_{GyroBias} \quad (36)$$

where

$e\left(\Delta a_{jk}^{BStrt}\right)_{GyroBias}$ = Horizontal component of $e\left(\Delta \hat{a}_0^{BStrt}\right)$ along IMU axis j used for the $\Delta \hat{a}_0^{BStrt}$ measurement for rotation sequence k - caused by neglecting gyro bias in (29).

$\left(\delta \hat{x}_{jk}\right)_{GyroBias}$ = Error in the SRT rotation k determined sensor error $\delta \hat{x}_{jk}$ along IMU axis j , caused by neglecting gyro bias in (29).

The (36) H_k s for the $e\left(\Delta a_{jk}^{BStrt}\right)_{GyroBias}$ errors in (35) are, from (16), the same as in Table 2:

$2\pi g$ for $e\left(\Delta a_{y3}^{BStrt}\right)_{GyroBias}$; $4g$ for $e\left(\Delta a_{x5}^{BStrt}\right)_{GyroBias}$ and $e\left(\Delta a_{y6}^{BStrt}\right)_{GyroBias}$; and $2g$ for $e\left(\Delta a_{x7}^{BStrt}\right)_{GyroBias}$, $e\left(\Delta a_{z7}^{BStrt}\right)_{GyroBias}$, and $e\left(\Delta a_{y13}^{BStrt}\right)_{GyroBias}$. Substitution in (36) then

finds for the sensor determination errors in (17) generated by the (35) gyro bias induced errors in (16):

$$\begin{aligned}
e(\kappa_{zz} - \kappa_{zzz})_{GyroBias} &= - \left[1 / \dot{\beta} + T_{Meas} / (2\pi) \right] \kappa_z \quad \text{Similarly For Seqs. 1, 2, and 1a - 3a} \\
e(v_{zx})_{GyroBias} &= (\kappa_x + \kappa_z) / \dot{\beta} - T_{Meas} \kappa_y / 4 \quad \text{Similarly For Seq. 4} \\
e(v_{xy})_{GyroBias} &= (\kappa_x + \kappa_y) / \dot{\beta} - T_{Meas} \kappa_z / 4 \\
e(\mu_{xy} + v_{xy}/2)_{GyroBias} &= \kappa_y / \dot{\beta} + T_{Meas} (1 - 2 F_{Meas}) \kappa_z / 2 \quad \text{Similarly For Seqs. 8 - 12} \\
e[\lambda_z + (\pi g / 2)(\kappa_{xx} + \kappa_{xxx})]_{GyroBias} &= -(\pi g / 2) \left(1 / \dot{\beta} + T_{Meas} / \pi \right) \kappa_x \\
e(\lambda_y + g v_{yz})_{GyroBias} &= -g \left[(\kappa_z + \kappa_y) / \dot{\beta} - T_{Meas} \kappa_x / 2 \right] \quad \text{Similarly For Seq. 14}
\end{aligned} \tag{37}$$

Part 2 [3, Sect. 8.4] shows that F_{Meas} in (34) is 1/2, both for a simple averaging algorithm and for an average-of-averages algorithm. Using $F_{Meas} = 1/2$ and representative values for $\dot{\beta}$ and T_{Meas} , (37) enables evaluation of the effect of neglecting the $\kappa_x, \kappa_y, \kappa_z$ gyro bias calibration errors. For example, for $\dot{\beta} = 1$ rad/sec, $T_{Meas} = 10$ sec, $\kappa_x + \kappa_y = 0.1$ deg/hr = $4.85e-7$ rad/sec, and $\kappa_z = -0.1$ deg/hr = $-4.85e-7$ rad/sec, the $e(v_{xy})_{GyroBias}$ gyro orthogonality error determination error in (37) would be 1.70 micro-radians. As another example, for $\dot{\beta} = 1$ rad/sec, $T_{Meas} = 10$ sec, $\kappa_z + \kappa_y = -4.85e-7$ rad/sec, $\kappa_x = 4.85e-7$ rad/sec, and $g = 32.2$ ft/sec², the $e(\lambda_y + g v_{yz})_{GyroBias}$ accelerometer bias determination error in (37) would be $9.37e-5$ ft/sec² = 2.91 micro-gs. Finally, for $\dot{\beta} = 1$ rad/sec and $\kappa_y = 4.85e-7$ rad/sec, the $e(\mu_{xy} + v_{xy}/2)_{GyroBias}$ accelerometer misalignment error in (37) would be 0.49 micro-radians. The induced errors in these examples are acceptable for most applications.

For larger than 0.1 deg/hr gyro bias calibration errors, the effect may not be negligible, requiring the Section 4.8 mitigation process for reduction.

6.0 DESIGNING THE IMPROVED SRT ROTATION SEQUENCES

As with the original SRT, rotation sequences for the improved SRT are designed to achieve the following objectives:

- 1) The rotation sequences should excite all sensor calibration errors so they are made visible within transformed acceleration measurements.
- 2) A sufficient number and type of rotation sequences should be executed so that the acceleration measurements taken between rotations have distinctive responses such that the instrument errors can be ascertained by measurement data analysis.

- 3) The rotations and measurements should be executed fairly rapidly (e.g., 50 deg/sec rotation rates) to assure that sensor outputs are stable over the test period, and to limit attitude error buildup (from gyro bias and heading uncertainty) from producing significant acceleration measurement errors.
- 4) Accelerometer bias calibration errors should be determined from measurements taken with the accelerometer being measured in a horizontal attitude. This eliminates the possibility of accelerometer scale factor modeling uncertainties coupling vertical specific force into the acceleration measurement, potentially corrupting bias determination accuracy.
- 5) The rotation sequences should be designed so that the fewest number of error sources are excited for each rotation sequence (between measurements). Ideally, each sequence should excite only one particular error source.

Because of the improved SRT analytical format, objective 5) is readily achieved by designing each rotation sequence to determine a particular sensor compensation error (i.e., gyro-to-gyro misalignment, gyro scale-factor-error, accelerometer-to-gyro misalignment, accelerometer bias error, and accelerometer scale-factor-error). The following subsections describe the rotation sequence design process based on the approximation that gyro bias calibration errors are negligible. Section 5.2.6 analytically demonstrates the impact of neglecting gyro bias calibration error on SRT results. If problematic, Section 4.8 shows how the gyro bias error effect can be mitigated with an easily executed measurement/correction operation.

The following classical vector product identities [2, Eqs. (3.1.1-16) & (3.1.1-35)] will be useful in the rotation sequence design process:

$$\underline{V}_1 \times (\underline{V}_2 \times \underline{V}_3) = \underline{V}_2 (\underline{V}_1 \cdot \underline{V}_3) - \underline{V}_3 (\underline{V}_1 \cdot \underline{V}_2) \quad (38)$$

$$(\underline{V}_1 \times \underline{V}_2) \cdot \underline{V}_3 = (\underline{V}_2 \times \underline{V}_3) \cdot \underline{V}_1 = (\underline{V}_3 \times \underline{V}_1) \cdot \underline{V}_2 \quad (39)$$

where

$$\underline{V}_1, \underline{V}_2, \underline{V}_3 = \text{Arbitrary vectors.}$$

The following general IMU axis and unit vector definitions will also prove useful:

$$\underline{u}_{\nu B}^B, \underline{u}_{\xi B}^B, \underline{u}_{\sigma B}^B = \text{Unit vectors along IMU general } B \text{ frame axes } \nu, \xi, \sigma.$$

From the previous definition, it follows that for a particular B_i type of B frame,

$$\underline{u}_{\nu B_i}^{B_i}, \underline{u}_{\xi B_i}^{B_i}, \underline{u}_{\sigma B_i}^{B_i} = \underline{u}_{\nu B}^B, \underline{u}_{\xi B}^B, \underline{u}_{\sigma B}^B \quad (40)$$

6.1 GYRO ERROR SIGNATURES ON THE SRT MEASUREMENT

To achieve the previous Item 5) goal in the SRT rotation sequence design process, this introductory subsection is included to provide an understanding of how rotation induced gyro errors impact the measurement.

Eqs. (5) - (7) show that SRT horizontal acceleration measurements are functions of accelerometer errors and $\underline{\phi}_{End}^{B Strt}$ attitude errors, the latter induced by gyro misalignment/scale-factor error during each of the sequence rotations. From Part 2 [3, Eqs. (58) & (77)], $\underline{\phi}_{End}^{B Strt}$ can be defined by

$$\underline{\phi}_{End}^{B Strt} = \sum_i \Delta \underline{\phi}_i^{B Strt} \quad \Delta \underline{\phi}_i^{B Strt} = \int_{t_{iStrt}}^{t_{iEnd}} C_B^{B Strt} \delta \underline{\omega}_{Gyro_i}^B dt \quad (41)$$

where

t_{iStrt}, t_{iEnd} = Time at the start and end of rotation i in a rotation sequence.

$\delta \underline{\omega}_{Gyro_i}^B$ = IMU gyro error vector in B frame coordinates during rotation i .

$C_B^{B Strt}$ = Direction cosine matrix that transforms vectors from the instantaneous IMU B frame axes into B_{Strt} coordinates.

Eq. (41) shows that gyro B frame errors generate error buildup during rotation segment i as $\Delta \underline{\phi}_i^{B Strt}$, the integral of $\delta \underline{\omega}_{Gyro_i}^B$ projections on B_{Strt} frame axes (through the $C_B^{B Strt}$ matrix).

The $\Delta \underline{\phi}_i^{B Strt}$ errors then sum into the total $\underline{\phi}_{End}^{B Strt}$ for the sequence. This basic concept is used extensively in this section in designing rotation sequences to meet the previous stated goals.

The angular rate $\underline{\omega}_i^B$ during rotation i is around a particular axis so that neglecting gyro bias errors,

$$\begin{aligned} \delta \underline{\omega}_{Gyro_i}^B &= \kappa_{Scal/Mis} \underline{\omega}_i^B = \kappa_{Scal/Mis} \underline{u}_i^B \dot{\beta}_i \\ \Delta \underline{\phi}_i^{B Strt} &= \int_0^{\theta_i} C_B^{B Strt} \kappa_{Scal/Mis} \underline{u}_i^B \dot{\beta}_i dt = \left(\int_0^{\theta_i} C_B^{B Strt} d\beta_i \right) \kappa_{Scal/Mis} \underline{u}_i^B \end{aligned} \quad (42)$$

in which

$$\begin{aligned} \kappa_{Scal/Mis} &= \kappa_{Scal} + \kappa_{Mis} \quad \text{with} \quad \kappa_{Scal} \equiv \kappa_{LinScal} + \kappa_{Asym} \text{Sign}(\dot{\beta}_i) \\ \kappa_{Scal/Mis} \underline{u}_i^B &= \kappa_{Scal} \underline{u}_i^B + \kappa_{Mis} \underline{u}_i^B \end{aligned} \quad (43)$$

where

\underline{u}_i^B = Unit vector in B frame coordinates along the rotation axis for rotation i .

$\dot{\beta}_i$ = Signed magnitude of angular rate $\underline{\omega}_i^B$.

θ_i = Total angular traversal of rotation i around \underline{u}_i^B .

Recognizing that $C_B^{BStrt} = C_{BiStrt}^{BStrt} C_B^{BiStrt}$, (42) for $\Delta\phi_i^{BStrt}$ is equivalently:

$$\begin{aligned} \Delta\phi_i^{BStrt} &= C_{BiStrt}^{BStrt} \left(\int_0^{\theta_i} C_B^{BiStrt} d\beta_i \right) \kappa_{Scal/Mis} \underline{u}_i^B = C_{BiStrt}^{BStrt} \Delta\phi_i^{BiStrt} \\ &\text{in which } \Delta\phi_i^{BiStrt} \equiv \left(\int_0^{\theta_i} C_B^{BiStrt} d\beta_i \right) \kappa_{Scal/Mis} \underline{u}_i^B \end{aligned} \quad (44)$$

where

B_{iStrt} = IMU B frame attitude at the start of rotation i .

As in the original SRT, each \underline{u}_i^B rotation axis is around one of the IMU axes. Thus, in (43) from (8) and (14), $\kappa_{Scal} \underline{u}_i^B$ will be along \underline{u}_i^B , $\kappa_{Mis} \underline{u}_i^B$ will be perpendicular to \underline{u}_i^B , hence, $\kappa_{Scal/Mis} \underline{u}_i^B$ can be written in the alternate form:

$$\kappa_{Scal/Mis} \underline{u}_i^B = \kappa_{Scal\mu} \underline{u}_{\mu B_i}^B + \kappa_{\zeta\mu} \underline{u}_{\zeta B_i}^B + \kappa_{\eta\mu} \underline{u}_{\eta B_i}^B \quad (45)$$

where

μ = IMU axis along \underline{u}_i^B .

ζ, η = IMU axes perpendicular to axis μ .

$\underline{u}_{\mu B_i}^B, \underline{u}_{\zeta B_i}^B, \underline{u}_{\eta B_i}^B$ = Mutually orthogonal unit vectors along IMU B Frame axes μ, ζ, η during rotation i .

$\kappa_{Scal\mu}$ = Eqs. (8) or (14) diagonal element in $\kappa_{LinScal} + \kappa_{Asym} \text{Sign}(\dot{\beta}_i)$ corresponding to IMU axis μ .

$\kappa_{\zeta\mu}, \kappa_{\eta\mu}$ = Eqs. (8) or (14) κ_{Mis} elements in column μ and rows ζ, η .

With (45), (44) becomes

$$\begin{aligned} \Delta \underline{\phi}_{-i}^{B_i Strt} &\equiv \left(\int_0^{\theta_i} C_B^{B_i Strt} d\beta_i \right) \left(\kappa_{Scal} \underline{u}_{\mu B_i}^B + \kappa_{\zeta \mu} \underline{u}_{\zeta B_i}^B + \kappa_{\eta \mu} \underline{u}_{\eta B_i}^B \right) \\ \Delta \underline{\phi}_{-i}^{B_i Strt} &= C_{B_i Strt}^{B_i Strt} \Delta \underline{\phi}_{-i}^{B_i Strt} \end{aligned} \quad (46)$$

The $C_B^{B_i Strt}$ matrix in (46) is from Part 2 [3, Eq. (84)]:

$$C_B^{B_i Strt} = I + \sin \beta_i \left(\underline{u}_{\mu B_i}^B \times \right) + (1 - \cos \beta_i) \left(\underline{u}_{\mu B_i}^B \times \right)^2 \quad (47)$$

from which $\left(\int_0^{\theta_i} C_B^{B_i Strt} d\beta_i \right)$ in (46) becomes

$$\int_0^{\theta_i} C_B^{B_i Strt} d\beta_i = \theta_i \left[I + \left(\underline{u}_{\mu B_i}^B \times \right)^2 \right] + (1 - \cos \theta_i) \left(\underline{u}_{\mu B_i}^B \times \right) - \sin \theta_i \left(\underline{u}_{\mu B_i}^B \times \right)^2 \quad (48)$$

Note from (38) and the definitions of $\underline{u}_{\mu B_i}^B$, $\underline{u}_{\zeta B_i}^B$, $\underline{u}_{\eta B_i}^B$ being mutually orthogonal unit vectors that

$$\left(\underline{u}_{\mu B_i}^B \times \right)^2 \underline{u}_{\mu B_i}^B = 0 \quad \left(\underline{u}_{\mu B_i}^B \times \right)^2 \underline{u}_{\zeta B_i}^B = -\underline{u}_{\zeta B_i}^B \quad \left(\underline{u}_{\mu B_i}^B \times \right)^2 \underline{u}_{\eta B_i}^B = -\underline{u}_{\eta B_i}^B \quad (49)$$

With (48) and (49) $\Delta \underline{\phi}_{-i}^{B_i Strt}$ in (46) then becomes

$$\begin{aligned} \Delta \underline{\phi}_{-i}^{B_i Strt} &= \theta_i \kappa_{Scal} \underline{u}_{\mu B_i}^B + (1 - \cos \theta_i) \left(\kappa_{\zeta \mu} \underline{u}_{\mu B_i}^B \times \underline{u}_{\zeta B_i}^B + \kappa_{\eta \mu} \underline{u}_{\mu B_i}^B \times \underline{u}_{\eta B_i}^B \right) \\ &\quad + \sin \theta_i \left(\kappa_{\zeta \mu} \underline{u}_{\zeta B_i}^B + \kappa_{\eta \mu} \underline{u}_{\eta B_i}^B \right) \end{aligned} \quad (50)$$

Because by definition, $\underline{u}_{\mu B_i}^B$, $\underline{u}_{\zeta B_i}^B$, $\underline{u}_{\eta B_i}^B$ are constant throughout rotation i , we can also write as in (40) for more specificity at the start of the rotation:

$$\underline{u}_{\mu B_i}^B = \underline{u}_{\mu B_i Strt}^{B_i Strt} \quad \underline{u}_{\zeta B_i}^B = \underline{u}_{\zeta B_i Strt}^{B_i Strt} \quad \underline{u}_{\eta B_i}^B = \underline{u}_{\eta B_i Strt}^{B_i Strt} \quad (51)$$

where

$\underline{u}_{\mu B_i Strt}^{B_i Strt}$, $\underline{u}_{\zeta B_i Strt}^{B_i Strt}$, $\underline{u}_{\eta B_i Strt}^{B_i Strt}$ = Unit vectors $\underline{u}_{\mu B_i}^B$, $\underline{u}_{\zeta B_i}^B$, $\underline{u}_{\eta B_i}^B$ at the start of rotation i as projected on IMU $B_i Strt$ frame axes.

Substituting (51) in (50) gives

$$\begin{aligned} \Delta \underline{\phi}_i^{B_{iStrt}} = & \theta_i \kappa_{Scal} \mu \underline{u}_{\mu B_{iStrt}}^{B_{iStrt}} + (1 - \cos \theta_i) \left(\kappa_{\zeta \mu} \underline{u}_{\mu B_{iStrt}}^{B_{iStrt}} \times \underline{u}_{\zeta B_{iStrt}}^{B_{iStrt}} + \kappa_{\eta \mu} \underline{u}_{\mu B_{iStrt}}^{B_{iStrt}} \times \underline{u}_{\eta B_{iStrt}}^{B_{iStrt}} \right) \\ & + \sin \theta_i \left(\kappa_{\zeta \mu} \underline{u}_{\zeta B_{iStrt}}^{B_{iStrt}} + \kappa_{\eta \mu} \underline{u}_{\eta B_{iStrt}}^{B_{iStrt}} \right) \end{aligned} \quad (52)$$

Lastly, (52) is transformed through $C_{B_{iStrt}}^{B_{iStrt}}$ in (46), and the result summed in (41) to obtain

$$\begin{aligned} \underline{\phi}_{End}^{B_{iStrt}} : \\ \Delta \underline{\phi}_i^{B_{iStrt}} = & C_{B_{iStrt}}^{B_{iStrt}} \Delta \underline{\phi}_i^{B_{iStrt}} \\ = & \theta_i \kappa_{Scal} \mu \underline{u}_{\mu B_{iStrt}}^{B_{iStrt}} + (1 - \cos \theta_i) \left(\kappa_{\zeta \mu} \underline{u}_{\mu B_{iStrt}}^{B_{iStrt}} \times \underline{u}_{\zeta B_{iStrt}}^{B_{iStrt}} + \kappa_{\eta \mu} \underline{u}_{\mu B_{iStrt}}^{B_{iStrt}} \times \underline{u}_{\eta B_{iStrt}}^{B_{iStrt}} \right) \\ & + \sin \theta_i \left(\kappa_{\zeta \mu} \underline{u}_{\zeta B_{iStrt}}^{B_{iStrt}} + \kappa_{\eta \mu} \underline{u}_{\eta B_{iStrt}}^{B_{iStrt}} \right) \end{aligned} \quad (53)$$

$$\underline{\phi}_{End}^{B_{iStrt}} = \sum_i \Delta \underline{\phi}_i^{B_{iStrt}}$$

where

$$\underline{u}_{\mu B_{iStrt}}^{B_{iStrt}}, \underline{u}_{\zeta B_{iStrt}}^{B_{iStrt}}, \underline{u}_{\eta B_{iStrt}}^{B_{iStrt}} = \text{Unit vectors } \underline{u}_{\mu B_i}^B, \underline{u}_{\zeta B_i}^B, \underline{u}_{\eta B_i}^B \text{ at the start of rotation } i \text{ as projected on } B_{iStrt} \text{ frame axes.}$$

For each rotation i , Eqs. (53) show how rotation angle θ_i and IMU $\underline{u}_{\mu B_{iStrt}}^{B_{iStrt}}, \underline{u}_{\zeta B_{iStrt}}^{B_{iStrt}}, \underline{u}_{\eta B_{iStrt}}^{B_{iStrt}}$ axis orientations at the start of rotation i impact how $\kappa_{Scal} \mu$ scale-factor error and $\kappa_{\zeta \mu}, \kappa_{\eta \mu}$ misalignments register in $\underline{\phi}_{End}^{B_{iStrt}}$. The result then translates into the $\Delta \hat{a}_H^{B_{iStrt}}$ measurement through the $g \underline{u}_{Dwn}^{B_{iStrt}} \times \left(\underline{\phi}_{End}^{B_{iStrt}} \right)$ term in (7).

Based on (53), the design goal for each rotation sequence in the SRT is to define a set of i rotations that will generate a particular gyro scale-factor-error or misalignment term onto the measurement while rejecting others. Included must be the selection of a starting and ending orientation for the IMU that will generate a particular Eqs. (6) accelerometer error component on the (7) measurement. Both objectives must also be compatible with rotation limitations associated with a two-axis rotation fixture.

To help visualize attitude orientations during rotation sequence design, the Fig. 4 cutout design tool has proven to be a useful design aid.

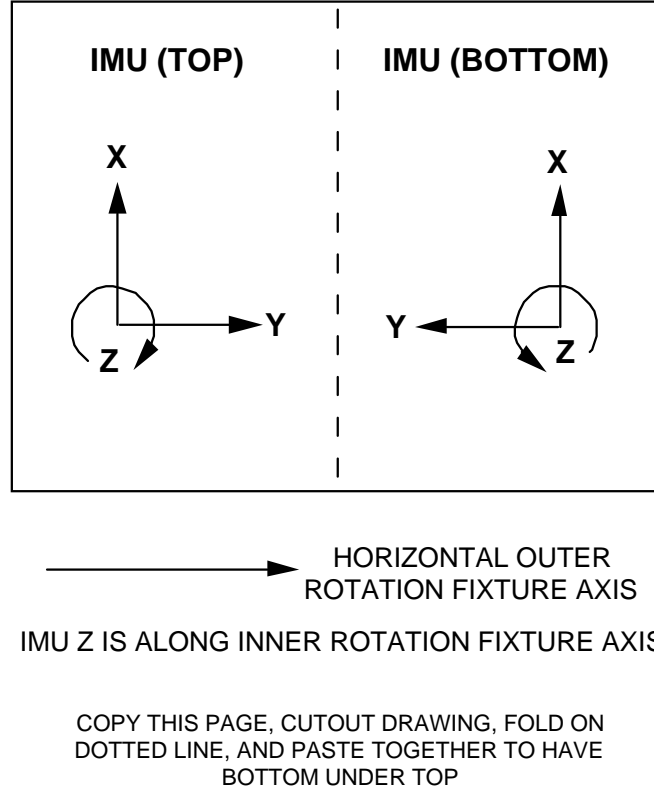


Fig. 4 - Rotation Sequence Cutout Design Tool

6.2 ROTATION SEQUENCES FOR GYRO CALIBRATION ERROR DETERMINATION

Based on the $\hat{\Delta \underline{a}}_H^{BStrt}$ expression in (7), the accelerometer error contribution can be eliminated from $\hat{\Delta \underline{a}}_H^{BStrt}$ by designing the rotation sequence for B frame attitude at sequence end to be the same as at the beginning. Then C_{BEnd}^{BStrt} in (7) will be identity, $\underline{u}_{Dwn}^{BEnd}$ will equal $\underline{u}_{Dwn}^{BStrt}$, $\delta \hat{\underline{a}}_{SFEnd}^{BEnd}$ in (6) will equal $\delta \hat{\underline{a}}_{SFStrt}^{BStrt}$, and $\hat{\Delta \underline{a}}_H^{BStrt}$ in (7) will simplify to

$$\hat{\Delta \underline{a}}_H^{BStrt} = g \underline{u}_{Dwn}^{BStrt} \times \underline{\phi}_{End}^{BStrt} \quad (54)$$

Thus, rotation sequence design for gyro calibration error determination can focus on (54), using $\underline{\phi}_{End}^{BStrt}$ from (53) to assess how gyro errors impact the $\hat{\Delta \underline{a}}_H^{BStrt}$ SRT measurement.

6.2.1 Sequences To Determine Gyro Scale-Factor Calibration Errors

Eq. (53) shows that only gyro scale factor errors will be generated in ϕ_{End}^{BStrt} for a single 360 degree IMU θ_i rotation, while returning the IMU to its initial attitude for (54) compatibility. Then with (43) for κ_{Scal} definition and (8) or (14) for scale-factor error components, (53) using $\theta_i = 2\pi$ reduces to

$$\phi_{End}^{BStrt} = \Delta\phi_{-1}^{BStrt} = 2\pi \kappa_{Scal} \mu \underline{u}_{\mu B1Strt}^{BStrt} = 2\pi \left[\kappa_{\mu\mu} + \kappa_{\mu\mu\mu} \text{Sign}(\dot{\beta}_1) \right] \underline{u}_{\mu B1Strt}^{BStrt} \quad (55)$$

With (55), $\Delta\hat{a}_H^{BStrt}$ in (54) becomes:

$$\Delta\hat{a}_H^{BStrt} = g \underline{u}_{Dwn}^{BStrt} \times \left(\phi_{End}^{BStrt} \right) = 2\pi g \left[\kappa_{\mu\mu} + \kappa_{\mu\mu\mu} \text{Sign}(\dot{\beta}_1) \right] \underline{u}_{Dwn}^{BStrt} \times \underline{u}_{\mu B1Strt}^{BStrt} \quad (56)$$

Rotation sequences 1 - 3 and 1a - 3a in Table 1 are based on (56) for κ_{Scal} error determination.

As an example of (56) applied to gyro scale-factor error determination, consider rotation sequence 3 in Table 1 for which $\underline{u}_{1Strt}^{BStrt}$ is along the IMU z axis, the rotation is positive, and the starting IMU x axis orientation is down. Then $\underline{u}_{Dwn}^{BStrt} \times \underline{u}_{\mu B1Strt}^{BStrt} = \underline{u}_{xBStrt}^{BStrt} \times \underline{u}_{zBStrt}^{BStrt} = -\underline{u}_{yBStrt}^{BStrt}$ and (56) becomes $\Delta\hat{a}_H^{BStrt} = -2\pi g (\kappa_{yy} + \kappa_{yyy}) \underline{u}_{yBStrt}^{BStrt}$, corresponding to $\Delta a_{y3}^{BStrt} = -2\pi g (\kappa_{zz} + \kappa_{zzz})$ in (16) for Sequence 3 in Table 1. For assurance, the identical result for Sequence 3 was generated directly from (7) with (6) in Part 3 [4, Eq. (18)].

Section 4.2 defines the IMU/rotation-fixture axis convention as having the IMU mounted with z axis along the fixture inner rotation axis (and IMU x and y axes perpendicular to the inner rotation axis), with gimbal angles at zero when the IMU z axis is down and the IMU y axis is along the fixture outer rotation axis. Based on this convention, to generate IMU z axis rotation around a horizontal $\underline{u}_{1Strt}^{BStrt}$ rotation axis, the inner gimbal angle would be set to zero (placing IMU axis y along the fixture horizontal outer axis), the fixture outer rotation angle would be set to minus 90 degrees (placing IMU axis z horizontal and axis x down as in Table 1 for Sequence 3), and the single +360 degree rotation for the sequence executed around the fixture inner rotation axis. (Note - Use of the Fig. 4 cutout design tool makes rotation setup/execution operations more easily visually).

6.2.2 Sequences To Determine Gyro Orthogonality Calibration Errors

One of the principle benefits of the SRT procedure is the ability to directly determine sensor-to-sensor misalignments. For the IMU gyros, misalignment between two gyro axes is the

orthogonality error shown in (11) as the sum of the gyro misalignment calibration coefficient errors (e.g., $\kappa_{ij} + \kappa_{ji}$ for the i and j axis gyros). Structuring a rotation sequence to measure the orthogonality error between two gyros entails positioning the IMU so that κ_{ij} and κ_{ji}

misalignments both register on one of the $\underline{\phi}_{End}^{B\text{Strt}}$ components, thereby assuring presence in the

(7) sequence measurement: $\Delta \hat{\underline{a}}_H^{B\text{Strt}} = \underline{g}_{Dwn}^{B\text{Strt}} \times \underline{\phi}_{End}^{B\text{Strt}}$. To this end, a four-rotation sequence can be structured using a two-axis rotation fixture, enabling direct measurement of orthogonality error between gyros having input axes perpendicular to the inner rotation fixture axis. (As will be explained subsequently, limitations of a two-axis fixture require an alternative eight-rotation sequence to measure orthogonality between gyro axes perpendicular to the inner rotation axis.)

To aid in the analytics, parameters ν, ξ, σ will be used to represent IMU axes in general, and chosen to correspond with axes μ, ζ, η during a particular rotation i . (Note: ν, ξ, σ IMU axes will also be utilized later to distinguish μ, ζ, η from IMU parameters used to characterize accelerometer errors).

6.2.2.1 Four-Rotation Sequences For Gyro Orthogonality Error Determination

The four-rotation sequence design process is simplified by structuring the sequence as a series of 180 degree rotations (plus or minus) for which (53) becomes for $\underline{\phi}_{End}^{B\text{Strt}}$:

$$\begin{aligned} \Delta \underline{\phi}_i^{B\text{Strt}} &= C_{Bi\text{Strt}}^{B\text{Strt}} \Delta \underline{\phi}_i^{Bi\text{Strt}} \\ &= \pm \pi \kappa_{Scal} \underline{u}_{\mu Bi\text{Strt}}^{B\text{Strt}} + 2 \left(\kappa_{\zeta\mu} \underline{u}_{\mu Bi\text{Strt}}^{B\text{Strt}} \times \underline{u}_{\zeta Bi\text{Strt}}^{B\text{Strt}} + \kappa_{\eta\mu} \underline{u}_{\mu Bi\text{Strt}}^{B\text{Strt}} \times \underline{u}_{\eta Bi\text{Strt}}^{B\text{Strt}} \right) \quad (57) \\ \underline{\phi}_{End}^{B\text{Strt}} &= \sum_i \Delta \underline{\phi}_i^{B\text{Strt}} \end{aligned}$$

Now consider rotations required to register orthogonality error $\nu_{\xi\sigma}$ between the IMU ξ and σ axis gyros into $\underline{\phi}_{End}^{B\text{Strt}}$. From (11), $\nu_{\xi\sigma} = \kappa_{\xi\sigma} + \kappa_{\sigma\xi}$, thus to generate $\nu_{\xi\sigma}$ requires a rotation around axis σ to excite $\kappa_{\sigma\xi}$ and a rotation around ξ to excite $\kappa_{\xi\sigma}$. To assure that only $\kappa_{\xi\sigma}$ and $\kappa_{\sigma\xi}$ are excited, no other rotations in the sequence should be around axis ν , the third in the ν, ξ, σ IMU 3-axis set. So that the $\Delta \hat{\underline{a}}_H^{B\text{Strt}}$ measurement for the sequence does not include accelerometer errors, we also specify that the IMU orientation at sequence end matches the orientation at sequence start, assuring that accelerometer-error-free (54) applies for $\Delta \hat{\underline{a}}_H^{B\text{Strt}}$.

Based on the previous discussion, consider a sequence of 180 degree rotations, the first (rotation 1) around axis ξ , the second (rotation 2) about axis ν . For rotation 1 around ξ , we set rotation axis μ in (57) to $\mu = \xi$, and arbitrarily assign ζ, η in (57) to, respectively, σ, ν . For

rotation 2 around ν , we set μ in (57) to $\mu = \nu$, and arbitrarily assign ζ, η in (57) to, respectively, ξ, σ . Thus, for rotations 1 and 2,

$$\begin{aligned} \mu, \underline{u}_{\mu B_{1Strt}}^{B Strt} &= \xi, \underline{u}_{\xi B_{1Strt}}^{B Strt} & \zeta, \underline{u}_{\zeta B_{1Strt}}^{B Strt} &= \sigma, \underline{u}_{\sigma B_{1Strt}}^{B Strt} & \eta, \underline{u}_{\eta B_{1Strt}}^{B Strt} &= \nu, \underline{u}_{\nu B_{1Strt}}^{B Strt} \\ \mu, \underline{u}_{\mu B_{2Strt}}^{B Strt} &= \nu, \underline{u}_{\nu B_{2Strt}}^{B Strt} & \zeta, \underline{u}_{\zeta B_{2Strt}}^{B Strt} &= \xi, \underline{u}_{\xi B_{2Strt}}^{B Strt} & \eta, \underline{u}_{\eta B_{2Strt}}^{B Strt} &= \sigma, \underline{u}_{\sigma B_{2Strt}}^{B Strt} \end{aligned} \quad (58)$$

Then (57) obtains for $\Delta\phi_{-1}^{B Strt}$ and $\Delta\phi_{-2}^{B Strt}$:

$$\begin{aligned} \Delta\phi_{-1}^{B Strt} &= \pm \pi \kappa_{Scal \xi} \underline{u}_{\xi B_{1Strt}}^{B Strt} + 2 \left(\kappa_{\sigma \xi} \underline{u}_{\xi B_{1Strt}}^{B Strt} \times \underline{u}_{\sigma B_{1Strt}}^{B Strt} + \kappa_{\nu \xi} \underline{u}_{\xi B_{1Strt}}^{B Strt} \times \underline{u}_{\nu B_{1Strt}}^{B Strt} \right) \\ \Delta\phi_{-2}^{B Strt} &= \pm \pi \kappa_{Scal \nu} \underline{u}_{\nu B_{2Strt}}^{B Strt} + 2 \left(\kappa_{\xi \nu} \underline{u}_{\nu B_{2Strt}}^{B Strt} \times \underline{u}_{\xi B_{2Strt}}^{B Strt} + \kappa_{\sigma \nu} \underline{u}_{\nu B_{2Strt}}^{B Strt} \times \underline{u}_{\sigma B_{2Strt}}^{B Strt} \right) \end{aligned} \quad (59)$$

The first rotation is 180 degrees around axis ξ , reversing the direction of the σ, ν axes so that following rotation 1,

$$\begin{aligned} \underline{u}_{\nu B_{1End}}^{B Strt} &= \underline{u}_{\nu B_{2Strt}}^{B Strt} = -\underline{u}_{\nu B_{1Strt}}^{B Strt} & \underline{u}_{\xi B_{1End}}^{B Strt} &= \underline{u}_{\xi B_{2Strt}}^{B Strt} = \underline{u}_{\xi B_{1Strt}}^{B Strt} \\ \underline{u}_{\sigma B_{1End}}^{B Strt} &= \underline{u}_{\sigma B_{2Strt}}^{B Strt} = -\underline{u}_{\sigma B_{1Strt}}^{B Strt} \end{aligned} \quad (60)$$

Hence,

$$\underline{u}_{\nu B_{2Strt}}^{B Strt} \times \underline{u}_{\xi B_{2Strt}}^{B Strt} = -\underline{u}_{\nu B_{1Strt}}^{B Strt} \times \underline{u}_{\xi B_{1Strt}}^{B Strt} \quad \underline{u}_{\nu B_{2Strt}}^{B Strt} \times \underline{u}_{\sigma B_{2Strt}}^{B Strt} = \underline{u}_{\nu B_{1Strt}}^{B Strt} \times \underline{u}_{\sigma B_{1Strt}}^{B Strt} \quad (61)$$

Substituting (61) and $\underline{u}_{\nu B_{2Strt}}^{B Strt}$ from (60) into (59) and summing for $\phi_{-End}^{B Strt}$ in (57) obtains

$$\begin{aligned} \Delta\phi_{-1}^{B Strt} + \Delta\phi_{-2}^{B Strt} &= \pm \pi \kappa_{Scal \xi} \underline{u}_{\xi B_{1Strt}}^{B Strt} - \left(\pm \pi \kappa_{Scal \nu} \right) \underline{u}_{\nu B_{1Strt}}^{B Strt} \\ + 2 \left(\kappa_{\nu \xi} + \kappa_{\xi \nu} \right) \underline{u}_{\xi B_{1Strt}}^{B Strt} \times \underline{u}_{\nu B_{1Strt}}^{B Strt} &+ 2 \kappa_{\sigma \xi} \underline{u}_{\xi B_{1Strt}}^{B Strt} \times \underline{u}_{\sigma B_{1Strt}}^{B Strt} + 2 \kappa_{\sigma \nu} \underline{u}_{\nu B_{1Strt}}^{B Strt} \times \underline{u}_{\sigma B_{1Strt}}^{B Strt} \end{aligned} \quad (62)$$

As discussed earlier, to avoid generating accelerometer errors on the measurement, the remaining rotations in the sequence must return the IMU to it starting orientation (the basis for the simplified (54) version of $\Delta\hat{a}_H^{B Strt}$ in (7) for gyro scale-factor/misalignment error determination). This is easily achieved by performing two additional rotations (rotations 3 and 4) as a repeat of the 180 degree ξ followed by ν rotations executed for rotations 1 and 2. The result will be the same form as (62) but with 1, 2 replaced by 3, 4:

$$\begin{aligned} \Delta\phi_{\underline{3}}^{B\text{Strt}} + \Delta\phi_{\underline{4}}^{B\text{Strt}} &= \pm\pi \kappa_{Scal\xi} \underline{u}_{\xi B3\text{Strt}}^{B\text{Strt}} - \left(\pm\pi \kappa_{Scal\nu}\right) \underline{u}_{\nu B3\text{Strt}}^{B\text{Strt}} \\ +2\left(\kappa_{\nu\xi} + \kappa_{\xi\nu}\right) \underline{u}_{\xi B3\text{Strt}}^{B\text{Strt}} \times \underline{u}_{\nu B3\text{Strt}}^{B\text{Strt}} &+ 2\kappa_{\sigma\xi} \underline{u}_{\xi B3\text{Strt}}^{B\text{Strt}} \times \underline{u}_{\sigma B3\text{Strt}}^{B\text{Strt}} + 2\kappa_{\sigma\nu} \underline{u}_{\nu B3\text{Strt}}^{B\text{Strt}} \times \underline{u}_{\sigma B3\text{Strt}}^{B\text{Strt}} \end{aligned} \quad (63)$$

But by definition, $\underline{u}_{\nu B3\text{Strt}}^{B\text{Strt}}, \underline{u}_{\xi B3\text{Strt}}^{B\text{Strt}}, \underline{u}_{\sigma B3\text{Strt}}^{B\text{Strt}} = \underline{u}_{\nu B2\text{End}}^{B\text{Strt}}, \underline{u}_{\xi B2\text{End}}^{B\text{Strt}}, \underline{u}_{\sigma B2\text{End}}^{B\text{Strt}}$. Additionally, rotation 2 was around IMU axis ν , reversing the direction of the IMU σ, ξ axes, so that following rotation 1,

$$\begin{aligned} \underline{u}_{\nu B2\text{End}}^{B\text{Strt}} &= \underline{u}_{\nu B2\text{Strt}}^{B\text{Strt}} = \underline{u}_{\nu B1\text{End}}^{B\text{Strt}} & \underline{u}_{\xi B2\text{End}}^{B\text{Strt}} &= -\underline{u}_{\xi B2\text{Strt}}^{B\text{Strt}} = -\underline{u}_{\xi B1\text{End}}^{B\text{Strt}} \\ \underline{u}_{\sigma B2\text{End}}^{B\text{Strt}} &= -\underline{u}_{\sigma B2\text{Strt}}^{B\text{Strt}} = -\underline{u}_{\sigma B1\text{End}}^{B\text{Strt}} \end{aligned} \quad (64)$$

Thus,

$$\begin{aligned} \underline{u}_{\nu B3\text{Strt}}^{B\text{Strt}} &= \underline{u}_{\nu B2\text{End}}^{B\text{Strt}} = \underline{u}_{\nu B1\text{End}}^{B\text{Strt}} & \underline{u}_{\xi B3\text{Strt}}^{B\text{Strt}} &= \underline{u}_{\xi B2\text{End}}^{B\text{Strt}} = -\underline{u}_{\xi B1\text{End}}^{B\text{Strt}} \\ \underline{u}_{\sigma B3\text{Strt}}^{B\text{Strt}} &= \underline{u}_{\sigma B2\text{End}}^{B\text{Strt}} = -\underline{u}_{\sigma B1\text{End}}^{B\text{Strt}} \end{aligned} \quad (65)$$

or with (60):

$$\begin{aligned} \underline{u}_{\nu B3\text{Strt}}^{B\text{Strt}} &= \underline{u}_{\nu B2\text{End}}^{B\text{Strt}} = -\underline{u}_{\nu B1\text{Strt}}^{B\text{Strt}} & \underline{u}_{\xi B3\text{Strt}}^{B\text{Strt}} &= \underline{u}_{\xi B2\text{End}}^{B\text{Strt}} = -\underline{u}_{\xi B1\text{Strt}}^{B\text{Strt}} \\ \underline{u}_{\sigma B3\text{Strt}}^{B\text{Strt}} &= \underline{u}_{\sigma B2\text{End}}^{B\text{Strt}} = \underline{u}_{\sigma B1\text{Strt}}^{B\text{Strt}} \end{aligned} \quad (66)$$

Hence,

$$\begin{aligned} \underline{u}_{\xi B3\text{Strt}}^{B\text{Strt}} \times \underline{u}_{\nu B3\text{Strt}}^{B\text{Strt}} &= \underline{u}_{\xi B1\text{Strt}}^{B\text{Strt}} \times \underline{u}_{\nu B1\text{Strt}}^{B\text{Strt}} & \underline{u}_{\xi B3\text{Strt}}^{B\text{Strt}} \times \underline{u}_{\sigma B3\text{Strt}}^{B\text{Strt}} &= -\underline{u}_{\xi B1\text{Strt}}^{B\text{Strt}} \times \underline{u}_{\sigma B1\text{Strt}}^{B\text{Strt}} \\ \underline{u}_{\nu B3\text{Strt}}^{B\text{Strt}} \times \underline{u}_{\sigma B3\text{Strt}}^{B\text{Strt}} &= -\underline{u}_{\nu B1\text{Strt}}^{B\text{Strt}} \times \underline{u}_{\sigma B1\text{Strt}}^{B\text{Strt}} \end{aligned} \quad (67)$$

Substituting (67) and $\underline{u}_{\xi B3\text{Strt}}^{B\text{Strt}}, \underline{u}_{\nu B3\text{Strt}}^{B\text{Strt}}$ from (66) into (63) yields

$$\begin{aligned} \Delta\phi_{\underline{3}}^{B\text{Strt}} + \Delta\phi_{\underline{4}}^{B\text{Strt}} &= -\left(\pm\pi \kappa_{Scal\xi}\right) \underline{u}_{\xi B1\text{Strt}}^{B\text{Strt}} + \left(\pm\pi \kappa_{Scal\nu}\right) \underline{u}_{\nu B1\text{Strt}}^{B\text{Strt}} \\ +2\left(\kappa_{\nu\xi} + \kappa_{\xi\nu}\right) \underline{u}_{\xi B1\text{Strt}}^{B\text{Strt}} \times \underline{u}_{\nu B1\text{Strt}}^{B\text{Strt}} &- 2\kappa_{\sigma\xi} \underline{u}_{\xi B1\text{Strt}}^{B\text{Strt}} \times \underline{u}_{\sigma B1\text{Strt}}^{B\text{Strt}} - 2\kappa_{\sigma\nu} \underline{u}_{\nu B1\text{Strt}}^{B\text{Strt}} \times \underline{u}_{\sigma B1\text{Strt}}^{B\text{Strt}} \end{aligned} \quad (68)$$

Lastly, recognizing by definition that $\underline{u}_{\nu B1\text{Strt}}^{B\text{Strt}}, \underline{u}_{\xi B1\text{Strt}}^{B\text{Strt}} = \underline{u}_{\nu B\text{Strt}}^{B\text{Strt}}, \underline{u}_{\xi B\text{Strt}}^{B\text{Strt}}$, we combine (68) with (62) in (57) to obtain for $\phi_{\underline{End}}^{B\text{Strt}}$:

$$\begin{aligned} \underline{\phi}_{-End}^{B Strt} = \sum_i \Delta \underline{\phi}_{-i}^{B Strt} = & \left[\left(\pm \pi \kappa_{Scal \xi_1} \right) - \left(\pm \pi \kappa_{Scal \xi_3} \right) \right] \underline{u}_{\xi B Strt}^{B Strt} \\ & - \left[\left(\pm \pi \kappa_{Scal v_1} \right) - \left(\pm \pi \kappa_{Scal v_3} \right) \right] \underline{u}_{v B Strt}^{B Strt} + 4 \left(\kappa_{v \xi} + \kappa_{\xi v} \right) \underline{u}_{\xi B Strt}^{B Strt} \times \underline{u}_{v B Strt}^{B Strt} \end{aligned} \quad (69)$$

where

$\kappa_{Scal \xi_1}$, $\kappa_{Scal v_1}$, $\kappa_{Scal \xi_3}$, $\kappa_{Scal v_3}$ = $\kappa_{Scal \xi}$, $\kappa_{Scal v}$ respectively for rotations 1 - 2 and 3 - 4, the distinction attributable to potentially different angular rate directions (plus or minus) for each of the 1 - 4 rotations. If all rotations are in the same direction, $\kappa_{Scal \xi_1}$ = $\kappa_{Scal \xi_3}$ = $\kappa_{Scal v_1}$, $\kappa_{Scal v_3}$ = $\kappa_{Scal v_1}$, and the scale factor effects in (69) would cancel.

To translate $\underline{\phi}_{-End}^{B Strt}$ into the $\hat{\Delta \underline{a}}_H^{B Strt}$ measurement in (54), we select $\underline{u}_{v B Strt}^{B Strt}$ to be vertical which sets $\underline{u}_{Dwn}^{B Strt} = \left(\underline{u}_{v B Strt}^{B Strt} \cdot \underline{u}_{Dwn}^{B Strt} \right) \underline{u}_{v B Strt}^{B Strt}$. Then (54) with (69) becomes

$$\begin{aligned} \hat{\Delta \underline{a}}_H^{B Strt} &= g \underline{u}_{Dwn}^{B Strt Nom} \times \underline{\phi}_{-End}^{B Strt} = g \left(\underline{u}_{v B Strt}^{B Strt} \cdot \underline{u}_{Dwn}^{B Strt} \right) \underline{u}_{v B Strt}^{B Strt} \times \underline{\phi}_{-End}^{B Strt} \\ &= g \left(\underline{u}_{v B Strt}^{B Strt} \cdot \underline{u}_{Dwn}^{B Strt} \right) \underline{u}_{v B Strt}^{B Strt} \times \left\{ \left[\left(\pm \pi \kappa_{Scal \xi_1} \right) - \left(\pm \pi \kappa_{Scal \xi_3} \right) \right] \underline{u}_{\xi B Strt}^{B Strt} \right. \\ & \quad \left. + 4 \left(\kappa_{v \xi} + \kappa_{\xi v} \right) \underline{u}_{\xi B Strt}^{B Strt} \times \underline{u}_{v B Strt}^{B Strt} \right\} \quad (70) \\ &= g \left(\underline{u}_{v B Strt}^{B Strt} \cdot \underline{u}_{Dwn}^{B Strt} \right) \left[\left(\pm \pi \kappa_{Scal \xi_1} \right) - \left(\pm \pi \kappa_{Scal \xi_3} \right) \right] \underline{u}_{v B Strt}^{B Strt} \times \underline{u}_{\xi B Strt}^{B Strt} \\ & \quad + 4 \left(\kappa_{v \xi} + \kappa_{\xi v} \right) \underline{u}_{\xi B Strt}^{B Strt} \end{aligned}$$

or with gyro orthogonality error Eq. (11),

$$\begin{aligned} \hat{\Delta \underline{a}}_H^{B Strt} &= g \left(\underline{u}_{v B Strt}^{B Strt} \cdot \underline{u}_{Dwn}^{B Strt} \right) \left[\left(\pm \pi \kappa_{Scal \xi_1} \right) - \left(\pm \pi \kappa_{Scal \xi_3} \right) \right] \underline{u}_{v B Strt}^{B Strt} \times \underline{u}_{\xi B Strt}^{B Strt} \\ & \quad + 4 \nu_{v \xi} \underline{u}_{\xi B Strt}^{B Strt} \end{aligned} \quad (71)$$

Eq. (71) shows that to determine $\nu_{v \xi}$, the differential acceleration measurement for the sequence should be the $\underline{u}_{\xi B}^B$ component of $\hat{\Delta \underline{a}}_H^{B Strt}$:

$$\underline{u}_{\xi B}^B \cdot \hat{\Delta \underline{a}}_H^{B Strt} = 4g \left(\underline{u}_{v B Strt}^{B Strt} \cdot \underline{u}_{Dwn}^{B Strt} \right) \nu_{v \xi} \quad (72)$$

Eq. (72) was used for Table 1 for rotation sequences 4 and 5 in which the initial IMU ν axis is downward along z (along $\underline{u}_{\nu}^{BStrt} = \underline{u}_{Dwn}^{BStrt} = \underline{u}_{z}^{BStrt}$). For Sequence 4, the IMU ξ rotation axis is y ($\underline{u}_{\xi}^{BStrt} = \underline{u}_{y}^{BStrt}$); for Sequence 5, the IMU ξ rotation axis is x ($\underline{u}_{\xi}^{BStrt} = \underline{u}_{x}^{BStrt}$). The (72) measurement formula for these sequences is shown in Eqs. (16) as $\Delta a_{y4}^{BStrt} = 4 g v_{yz}$ and $\Delta a_{x5}^{BStrt} = 4 g v_{zx}$. For assurance, the identical result for Sequence 5 was generated directly from (7) with (6) in Part 3 [4, Eq. (28)].

The four-rotation ξ, ν, ξ, ν sequence is executable with a two-axis rotation fixture having the IMU mounted with ν axis along the fixture inner gimbal axis, the outer gimbal angle initialized to have IMU axis ν vertical, and the inner gimbal angle initialized to have IMU axis ξ along the outer (horizontal) gimbal axis. The rotation sequence would be executed using four sequential 180 degree rotations, the first two around the outer, then inner gimbal axes, the second two a repeat of the first two.

6.2.2.2 Eight-Rotation Sequence For Gyro Orthogonality Error Determination

In principle, a four-rotation sequence analogous to ξ, ν, ξ, ν in Section 6.2.2.1 could also be structured to measure the $v_{\xi\sigma}$ gyro ξ, σ axis orthogonality error; i.e., a ξ, σ, ξ, σ sequence of 180 degree rotations starting with σ axis vertical. However, for an IMU mounted with ν along a two-axis fixture inner gimbal axis (as in Section 6.2.2.1), this is not possible. The reason is that the IMU mounting places both the ξ and σ axes perpendicular to the inner gimbal axis, restricting rotations about ξ or σ to be generated around only the outer gimbal axis. If the inner gimbal angle is initialized to have IMU ξ axis along the outer gimbal axis (enabling the first rotation in the sequence to be around ξ), rotation 2 could not be executed around σ because after rotation 1 completion, the IMU σ axis will not be aligned with the outer gimbal axis. To enable IMU σ axis rotation following a ξ rotation, the inner gimbal angle would have to be changed by 90 degrees (around IMU axis ν) to bring the σ axis into alignment with the outer gimbal axis. Similarly, to enable another ξ rotation, a 90 degree ν rotation would be required to align ξ with the outer gimbal axis, etc. to bring the IMU back to the starting attitude. Thus, to generate a $v_{\xi\sigma}$ signature on the measurement using an IMU mounting for $v_{\xi\nu}$ determination, an eight-rotation sequence is required; $180\xi, +90\nu, 180\sigma, +90\nu$ followed by a repeated $180\xi, +90\nu, 180\sigma, +90\nu$. (The + designation for the ν rotations is important as will be discussed subsequently). It remains to be found whether the added ν rotations excite other unwanted gyro error signatures onto the $\Delta \hat{a}_H^{BStrt}$ measurement used for $v_{\xi\sigma}$ determination.

Rotations 1, 3, 5, and 7 are 180 degrees for which (57) applies. For rotation 1 around the IMU ξ axis, we set rotation axis μ in (57) to $\mu = \xi$, and arbitrarily assign ζ, η in (57) to,

respectively, σ, ν . For rotation 3 around the IMU σ axis, we set rotation axis μ in (57) to $\mu = \sigma$, and arbitrarily assign ζ, η in (57) to, respectively, ξ, ν . Thus, for rotations 1 and 3,

$$\begin{aligned} \mu, \underline{u}_{\mu B_{1Strt}}^{B Strt} &= \xi, \underline{u}_{\xi B_{1Strt}}^{B Strt} & \zeta, \underline{u}_{\zeta B_{1Strt}}^{B Strt} &= \sigma, \underline{u}_{\sigma B_{1Strt}}^{B Strt} & \eta, \underline{u}_{\eta B_{1Strt}}^{B Strt} &= \nu, \underline{u}_{\nu B_{1Strt}}^{B Strt} \\ \mu, \underline{u}_{\mu B_{3Strt}}^{B Strt} &= \sigma, \underline{u}_{\sigma B_{3Strt}}^{B Strt} & \zeta, \underline{u}_{\zeta B_{3Strt}}^{B Strt} &= \xi, \underline{u}_{\xi B_{3Strt}}^{B Strt} & \eta, \underline{u}_{\eta B_{3Strt}}^{B Strt} &= \nu, \underline{u}_{\nu B_{3Strt}}^{B Strt} \end{aligned} \quad (73)$$

and (57) obtains for $\Delta\phi_{\underline{1}}^{B Strt}$ and $\Delta\phi_{\underline{3}}^{B Strt}$:

$$\begin{aligned} \Delta\phi_{\underline{1}}^{B Strt} &= \pm \pi \kappa_{Scal \xi} \underline{u}_{\xi B_{1Strt}}^{B Strt} + 2 \left(\kappa_{\sigma \xi} \underline{u}_{\xi B_{1Strt}}^{B Strt} \times \underline{u}_{\sigma B_{1Strt}}^{B Strt} + \kappa_{\nu \xi} \underline{u}_{\xi B_{1Strt}}^{B Strt} \times \underline{u}_{\nu B_{1Strt}}^{B Strt} \right) \\ \Delta\phi_{\underline{3}}^{B Strt} &= \pm \pi \kappa_{Scal \sigma} \underline{u}_{\sigma B_{3Strt}}^{B Strt} + 2 \left(\kappa_{\xi \sigma} \underline{u}_{\sigma B_{3Strt}}^{B Strt} \times \underline{u}_{\xi B_{3Strt}}^{B Strt} + \kappa_{\nu \sigma} \underline{u}_{\sigma B_{3Strt}}^{B Strt} \times \underline{u}_{\nu B_{3Strt}}^{B Strt} \right) \end{aligned} \quad (74)$$

We now find expressions for $\underline{u}_{\nu B_{3Strt}}^{B Strt}, \underline{u}_{\xi B_{3Strt}}^{B Strt}, \underline{u}_{\sigma B_{3Strt}}^{B Strt}$ in (74) as a function of $\underline{u}_{\nu B_{Strt}}^{B Strt}, \underline{u}_{\xi B_{Strt}}^{B Strt}, \underline{u}_{\sigma B_{Strt}}^{B Strt}$ by successive transformation backwards from frame B_{3Strt} to B_{Strt} through the first two rotations, $180\xi, +90\nu$. Since the ξ rotation is 180 degrees and the ν rotation is 90 degrees, (47) with (51) shows that

$$\begin{aligned} C_{B_{3Strt}}^{B_{2Strt}} &= I + \left(\underline{u}_{\nu B_{2Strt}}^{B_{2Strt}} \times \right) + \left(\underline{u}_{\nu B_{2Strt}}^{B_{2Strt}} \times \right)^2 = I + \left(\underline{u}_{\nu B_{Strt}}^{B_{Strt}} \times \right) + \left(\underline{u}_{\nu B_{Strt}}^{B_{Strt}} \times \right)^2 \\ C_{B_{2Strt}}^{B_{1Strt}} &= I + 2 \left(\underline{u}_{\xi B_{1Strt}}^{B_{1Strt}} \times \right)^2 = I + 2 \left(\underline{u}_{\xi B_{Strt}}^{B_{Strt}} \times \right)^2 \end{aligned} \quad (75)$$

Then:

$$\begin{aligned} \underline{u}_{\nu B_{3Strt}}^{B_{2Strt}} &= C_{B_{3Strt}}^{B_{2Strt}} \underline{u}_{\nu B_{3Strt}}^{B_{3Strt}} = C_{B_{3Strt}}^{B_{2Strt}} \underline{u}_{\nu B_{Strt}}^{B_{Strt}} \\ &= \left[I + \left(\underline{u}_{\nu B_{Strt}}^{B_{Strt}} \times \right) + \left(\underline{u}_{\nu B_{Strt}}^{B_{Strt}} \times \right)^2 \right] \underline{u}_{\nu B_{Strt}}^{B_{Strt}} = \underline{u}_{\nu B_{Strt}}^{B_{Strt}} \\ \underline{u}_{\nu B_{3Strt}}^{B_{Strt}} &= C_{B_{2Strt}}^{B_{Strt}} \underline{u}_{\nu B_{3Strt}}^{B_{2Strt}} = \left[I + 2 \left(\underline{u}_{\xi B_{Strt}}^{B_{Strt}} \times \right)^2 \right] \underline{u}_{\nu B_{Strt}}^{B_{Strt}} = -\underline{u}_{\nu B_{Strt}}^{B_{Strt}} \end{aligned} \quad (76)$$

$$\begin{aligned} \underline{u}_{\xi B_{3Strt}}^{B_{2Strt}} &= C_{B_{3Strt}}^{B_{2Strt}} \underline{u}_{\xi B_{3Strt}}^{B_{3Strt}} = C_{B_{3Strt}}^{B_{2Strt}} \underline{u}_{\xi B_{Strt}}^{B_{Strt}} \\ &= \left[I + \left(\underline{u}_{\nu B_{Strt}}^{B_{Strt}} \times \right) + \left(\underline{u}_{\nu B_{Strt}}^{B_{Strt}} \times \right)^2 \right] \underline{u}_{\xi B_{Strt}}^{B_{Strt}} = \underline{u}_{\nu B_{Strt}}^{B_{Strt}} \times \underline{u}_{\xi B_{Strt}}^{B_{Strt}} \end{aligned} \quad (77)$$

$$\underline{u}_{\xi B_{3Strt}}^{B_{Strt}} = C_{B_{2Strt}}^{B_{Strt}} \underline{u}_{\xi B_{3Strt}}^{B_{2Strt}} = \left[I + 2 \left(\underline{u}_{\xi B_{Strt}}^{B_{Strt}} \times \right)^2 \right] \left(\underline{u}_{\nu B_{Strt}}^{B_{Strt}} \times \underline{u}_{\xi B_{Strt}}^{B_{Strt}} \right) = -\underline{u}_{\nu B_{Strt}}^{B_{Strt}} \times \underline{u}_{\xi B_{Strt}}^{B_{Strt}}$$

$$\begin{aligned} \underline{u}_{\sigma B_{3Stt}}^{B_{2Stt}} &= C_{B_{3Stt}}^{B_{2Stt}} \underline{u}_{\sigma B_{3Stt}}^{B_{3Stt}} = C_{B_{3Stt}}^{B_{2Stt}} \underline{u}_{\sigma B_{Stt}}^{B_{Stt}} \\ &= \left[I + \left(\underline{u}_{vB_{Stt}}^{B_{Stt}} \times \right) + \left(\underline{u}_{vB_{Stt}}^{B_{Stt}} \times \right)^2 \right] \underline{u}_{\sigma B_{Stt}}^{B_{Stt}} = \underline{u}_{vB_{Stt}}^{B_{Stt}} \times \underline{u}_{\sigma B_{Stt}}^{B_{Stt}} \end{aligned} \quad (78)$$

$$\underline{u}_{\sigma B_{3Stt}}^{B_{Stt}} = C_{B_{2Stt}}^{B_{Stt}} \underline{u}_{\sigma B_{3Stt}}^{B_{2Stt}} = \left[I + 2 \left(\underline{u}_{\xi B_{Stt}}^{B_{Stt}} \times \right)^2 \right] \left(\underline{u}_{vB_{Stt}}^{B_{Stt}} \times \underline{u}_{\sigma B_{Stt}}^{B_{Stt}} \right) = \underline{u}_{vB_{Stt}}^{B_{Stt}} \times \underline{u}_{\sigma B_{Stt}}^{B_{Stt}}$$

or in summary

$$\underline{u}_{vB_{3Stt}}^{B_{Stt}} = -\underline{u}_{vB_{Stt}}^{B_{Stt}} \quad \underline{u}_{\xi B_{3Stt}}^{B_{Stt}} = -\underline{u}_{vB_{Stt}}^{B_{Stt}} \times \underline{u}_{\xi B_{Stt}}^{B_{Stt}} \quad \underline{u}_{\sigma B_{3Stt}}^{B_{Stt}} = \underline{u}_{vB_{Stt}}^{B_{Stt}} \times \underline{u}_{\sigma B_{Stt}}^{B_{Stt}} \quad (79)$$

With (79), the $\underline{u}_{\sigma B_{3Stt}}^{B_{Stt}} \times \underline{u}_{\xi B_{3Stt}}^{B_{Stt}}$ and $\underline{u}_{\sigma B_{3Stt}}^{B_{Stt}} \times \underline{u}_{vB_{3Stt}}^{B_{Stt}}$ terms in (74) become

$$\begin{aligned} \underline{u}_{\sigma B_{3Stt}}^{B_{Stt}} \times \underline{u}_{vB_{3Stt}}^{B_{Stt}} &= -\left(\underline{u}_{vB_{Stt}}^{B_{Stt}} \times \underline{u}_{\sigma B_{Stt}}^{B_{Stt}} \right) \times \underline{u}_{vB_{Stt}}^{B_{Stt}} = -\underline{u}_{\sigma B_{Stt}}^{B_{Stt}} \\ \underline{u}_{\sigma B_{3Stt}}^{B_{Stt}} \times \underline{u}_{\xi B_{3Stt}}^{B_{Stt}} &= -\left(\underline{u}_{vB_{Stt}}^{B_{Stt}} \times \underline{u}_{\sigma B_{Stt}}^{B_{Stt}} \right) \times \left(\underline{u}_{vB_{Stt}}^{B_{Stt}} \times \underline{u}_{\xi B_{Stt}}^{B_{Stt}} \right) \\ &= -\underline{u}_{vB_{Stt}}^{B_{Stt}} \left[\left(\underline{u}_{vB_{Stt}}^{B_{Stt}} \times \underline{u}_{\sigma B_{Stt}}^{B_{Stt}} \right) \cdot \underline{u}_{\xi B_{Stt}}^{B_{Stt}} \right] + \underline{u}_{\xi B_{Stt}}^{B_{Stt}} \left[\left(\underline{u}_{vB_{Stt}}^{B_{Stt}} \times \underline{u}_{\sigma B_{Stt}}^{B_{Stt}} \right) \cdot \underline{u}_{vB_{Stt}}^{B_{Stt}} \right] \\ &= -\underline{u}_{vB_{Stt}}^{B_{Stt}} \left[\left(\underline{u}_{vB_{Stt}}^{B_{Stt}} \times \underline{u}_{\sigma B_{Stt}}^{B_{Stt}} \right) \cdot \underline{u}_{\xi B_{Stt}}^{B_{Stt}} \right] = \underline{u}_{vB_{Stt}}^{B_{Stt}} \left[\left(\underline{u}_{\xi B_{Stt}}^{B_{Stt}} \times \underline{u}_{\sigma B_{Stt}}^{B_{Stt}} \right) \cdot \underline{u}_{vB_{Stt}}^{B_{Stt}} \right] \\ &= \underline{u}_{\xi B_{Stt}}^{B_{Stt}} \times \underline{u}_{\sigma B_{Stt}}^{B_{Stt}} \end{aligned} \quad (80)$$

The last equality in (80) stems from the general identity that for any vector \underline{V} :

$$\underline{V} = \left(\underline{V} \cdot \underline{u}_{vB_{Stt}}^{B_{Stt}} \right) \underline{u}_{vB_{Stt}}^{B_{Stt}} + \left(\underline{V} \cdot \underline{u}_{\xi B_{Stt}}^{B_{Stt}} \right) \underline{u}_{\xi B_{Stt}}^{B_{Stt}} + \left(\underline{V} \cdot \underline{u}_{\sigma B_{Stt}}^{B_{Stt}} \right) \underline{u}_{\sigma B_{Stt}}^{B_{Stt}}. \text{ Thus, for}$$

$$\underline{V} = \underline{u}_{\xi B_{Stt}}^{B_{Stt}} \times \underline{u}_{\sigma B_{Stt}}^{B_{Stt}}, \text{ it follows that}$$

$$\begin{aligned} \underline{u}_{\xi B_{Stt}}^{B_{Stt}} \times \underline{u}_{\sigma B_{Stt}}^{B_{Stt}} &= \left[\left(\underline{u}_{\xi B_{Stt}}^{B_{Stt}} \times \underline{u}_{\sigma B_{Stt}}^{B_{Stt}} \right) \cdot \underline{u}_{vB_{Stt}}^{B_{Stt}} \right] \underline{u}_{vB_{Stt}}^{B_{Stt}} \\ &+ \left[\left(\underline{u}_{\xi B_{Stt}}^{B_{Stt}} \times \underline{u}_{\sigma B_{Stt}}^{B_{Stt}} \right) \cdot \underline{u}_{\xi B_{Stt}}^{B_{Stt}} \right] \underline{u}_{\xi B_{Stt}}^{B_{Stt}} + \left[\left(\underline{u}_{\xi B_{Stt}}^{B_{Stt}} \times \underline{u}_{\sigma B_{Stt}}^{B_{Stt}} \right) \cdot \underline{u}_{\sigma B_{Stt}}^{B_{Stt}} \right] \underline{u}_{\sigma B_{Stt}}^{B_{Stt}} \\ &= \left[\left(\underline{u}_{\xi B_{Stt}}^{B_{Stt}} \times \underline{u}_{\sigma B_{Stt}}^{B_{Stt}} \right) \cdot \underline{u}_{vB_{Stt}}^{B_{Stt}} \right] \underline{u}_{vB_{Stt}}^{B_{Stt}} \end{aligned} \quad (81)$$

Substituting (80) in (74) with (51), obtains

$$\begin{aligned}
\Delta\phi_{-1}^{B\text{Strt}} &= \pm\pi \kappa_{Scal\xi} \underline{u}_{\xi}^{B\text{Strt}} + 2\left(\kappa_{\sigma\xi} \underline{u}_{\xi}^{B\text{Strt}} \times \underline{u}_{\sigma}^{B\text{Strt}} + \kappa_{\nu\xi} \underline{u}_{\xi}^{B\text{Strt}} \times \underline{u}_{\nu}^{B\text{Strt}}\right) \\
\Delta\phi_{-3}^{B\text{Strt}} &= \pm\pi \kappa_{Scal\sigma} \underline{u}_{\nu}^{B\text{Strt}} \times \underline{u}_{\sigma}^{B\text{Strt}} + 2\left(\kappa_{\xi\sigma} \underline{u}_{\xi}^{B\text{Strt}} \times \underline{u}_{\sigma}^{B\text{Strt}} - \kappa_{\nu\sigma} \underline{u}_{\sigma}^{B\text{Strt}}\right)
\end{aligned} \tag{82}$$

Combining $\Delta\phi_{-1}^{B\text{Strt}}$ and $\Delta\phi_{-3}^{B\text{Strt}}$ from (82) then yields for $\phi_{-End}^{B\text{Strt}}$ in (53):

$$\begin{aligned}
\Delta\phi_{-1}^{B\text{Strt}} + \Delta\phi_{-3}^{B\text{Strt}} &= \pm\pi \kappa_{Scal\xi} \underline{u}_{\xi}^{B\text{Strt}} \pm\pi \kappa_{Scal\sigma} \underline{u}_{\nu}^{B\text{Strt}} \times \underline{u}_{\sigma}^{B\text{Strt}} \\
&+ 2\left(\kappa_{\sigma\xi} + \kappa_{\xi\sigma}\right) \underline{u}_{\xi}^{B\text{Strt}} \times \underline{u}_{\sigma}^{B\text{Strt}} + 2\kappa_{\nu\xi} \underline{u}_{\xi}^{B\text{Strt}} \times \underline{u}_{\nu}^{B\text{Strt}} - 2\kappa_{\nu\sigma} \underline{u}_{\sigma}^{B\text{Strt}}
\end{aligned} \tag{83}$$

Note that because $\underline{u}_{\nu}^{B\text{Strt}}, \underline{u}_{\xi}^{B\text{Strt}}, \underline{u}_{\sigma}^{B\text{Strt}}$ are mutually perpendicular,

$2\left(\kappa_{\sigma\xi} + \kappa_{\xi\sigma}\right) \underline{u}_{\xi}^{B\text{Strt}} \times \underline{u}_{\sigma}^{B\text{Strt}}$ is the only term in (83) parallel to $\underline{u}_{\nu}^{B\text{Strt}}$. This will ultimately be the component used through $\Delta\hat{\underline{a}}_H^{B\text{Strt}} = g \underline{u}_{Dwn}^{B\text{Strt}} \times \left(\phi_{-End}^{B\text{Strt}}\right)$ in (54) that determines the relative misalignment $\left(\kappa_{\sigma\xi} + \kappa_{\xi\sigma}\right)$ between the IMU σ and ξ axis gyros.

Given that rotation sequences 5 - 8 are identical to rotation sequences 1 - 4, the same methodology used to find finding expressions for $\Delta\phi_{-1}^{B\text{Strt}} + \Delta\phi_{-3}^{B\text{Strt}}$ in (83) can be used to find $\Delta\phi_{-5}^{B\text{Strt}} + \Delta\phi_{-7}^{B\text{Strt}}$ by substituting the IMU unit vectors at the start of rotation 5 (i.e., $\underline{u}_{\nu}^{B\text{Strt}}, \underline{u}_{\xi}^{B\text{Strt}}, \underline{u}_{\sigma}^{B\text{Strt}}$) for IMU unit vectors at the start of rotation 1 (i.e., $\underline{u}_{\nu}^{B\text{Strt}}, \underline{u}_{\xi}^{B\text{Strt}}, \underline{u}_{\sigma}^{B\text{Strt}}$). Thus, we can immediately write from (83):

$$\begin{aligned}
\Delta\phi_{-5}^{B\text{Strt}} + \Delta\phi_{-7}^{B\text{Strt}} &= \pm\pi \kappa_{Scal\xi} \underline{u}_{\xi}^{B\text{Strt}} + \left(\pm\pi \kappa_{Scal\sigma}\right) \left(\underline{u}_{\nu}^{B\text{Strt}} \times \underline{u}_{\sigma}^{B\text{Strt}}\right) \\
&+ 2\left(\kappa_{\sigma\xi} + \kappa_{\xi\sigma}\right) \underline{u}_{\xi}^{B\text{Strt}} \times \underline{u}_{\sigma}^{B\text{Strt}} + 2\kappa_{\nu\xi} \underline{u}_{\xi}^{B\text{Strt}} \times \underline{u}_{\nu}^{B\text{Strt}} - 2\kappa_{\nu\sigma} \underline{u}_{\sigma}^{B\text{Strt}}
\end{aligned} \tag{84}$$

To complete the $\Delta\phi_{-5}^{B\text{Strt}} + \Delta\phi_{-7}^{B\text{Strt}}$ derivation, we must now find expressions for $\underline{u}_{\nu}^{B\text{Strt}}, \underline{u}_{\xi}^{B\text{Strt}}, \underline{u}_{\sigma}^{B\text{Strt}}$ in (84) as a function of $\underline{u}_{\nu}^{B\text{Strt}}, \underline{u}_{\xi}^{B\text{Strt}}, \underline{u}_{\sigma}^{B\text{Strt}}$. Following the same methodology that led to (80), since ξ, σ rotations are 180 degrees and the ν rotations are 90 degrees, (47) shows that

$$\begin{aligned}
C_{B3Strt}^{B2Strt} &= C_{B5Strt}^{B4Strt} = I + \left(\underline{u}_{vBStrt}^{BStrt} \times \right) + \left(\underline{u}_{vBStrt}^{BStrt} \times \right)^2 \\
C_{B2Strt}^{BStrt} &= I + 2 \left(\underline{u}_{\xi BStrt}^{BStrt} \times \right)^2 \quad C_{B4Strt}^{B3Strt} = I + 2 \left(\underline{u}_{\sigma BStrt}^{BStrt} \times \right)^2
\end{aligned} \tag{85}$$

Then:

$$\begin{aligned}
\underline{u}_{vB5Strt}^{B4Strt} &= C_{B5Strt}^{B4Strt} \underline{u}_{vB5Strt}^{B5Strt} = C_{B5Strt}^{B4Strt} \underline{u}_{vBStrt}^{BStrt} \\
&= \left[I + \left(\underline{u}_{vBStrt}^{BStrt} \times \right) + \left(\underline{u}_{vBStrt}^{BStrt} \times \right)^2 \right] \underline{u}_{vBStrt}^{BStrt} = \underline{u}_{vBStrt}^{BStrt} \\
\underline{u}_{vB5Strt}^{B3Strt} &= C_{B4Strt}^{B3Strt} \underline{u}_{vB5Strt}^{B4Strt} = \left[I + 2 \left(\underline{u}_{\sigma BStrt}^{BStrt} \times \right)^2 \right] \underline{u}_{vBStrt}^{BStrt} = -\underline{u}_{vBStrt}^{BStrt} \\
\underline{u}_{vB5Strt}^{B2Strt} &= C_{B3Strt}^{B2Strt} \underline{u}_{vB5Strt}^{B3Strt} = \left[I + \left(\underline{u}_{vBStrt}^{BStrt} \times \right) + \left(\underline{u}_{vBStrt}^{BStrt} \times \right)^2 \right] \left(-\underline{u}_{vBStrt}^{BStrt} \right) = -\underline{u}_{vBStrt}^{BStrt} \\
\underline{u}_{vB5Strt}^{BStrt} &= C_{B2Strt}^{BStrt} \underline{u}_{vB5Strt}^{B2Strt} = \left[I + 2 \left(\underline{u}_{\xi BStrt}^{BStrt} \times \right)^2 \right] \left(-\underline{u}_{vBStrt}^{BStrt} \right) = \underline{u}_{vBStrt}^{BStrt} \\
\underline{u}_{\xi B5Strt}^{B4Strt} &= C_{B5Strt}^{B4Strt} \underline{u}_{\xi B5Strt}^{B5Strt} = C_{B5Strt}^{B4Strt} \underline{u}_{\xi BStrt}^{BStrt} \\
&= \left[I + \left(\underline{u}_{vBStrt}^{BStrt} \times \right) + \left(\underline{u}_{vBStrt}^{BStrt} \times \right)^2 \right] \underline{u}_{\xi BStrt}^{BStrt} = \underline{u}_{vBStrt}^{BStrt} \times \underline{u}_{\xi BStrt}^{BStrt} \\
\underline{u}_{\xi B5Strt}^{B3Strt} &= C_{B4Strt}^{B3Strt} \underline{u}_{\xi B5Strt}^{B4Strt} = \left[I + 2 \left(\underline{u}_{\sigma BStrt}^{BStrt} \times \right)^2 \right] \left(\underline{u}_{vBStrt}^{BStrt} \times \underline{u}_{\xi BStrt}^{BStrt} \right) = \underline{u}_{vBStrt}^{BStrt} \times \underline{u}_{\xi BStrt}^{BStrt} \\
\underline{u}_{\xi B5Strt}^{B2Strt} &= C_{B3Strt}^{B2Strt} \underline{u}_{\xi B5Strt}^{B3Strt} = \left[I + \left(\underline{u}_{vBStrt}^{BStrt} \times \right) + \left(\underline{u}_{vBStrt}^{BStrt} \times \right)^2 \right] \left(\underline{u}_{vBStrt}^{BStrt} \times \underline{u}_{\xi BStrt}^{BStrt} \right) \\
&= \underline{u}_{vBStrt}^{BStrt} \times \left(\underline{u}_{vBStrt}^{BStrt} \times \underline{u}_{\xi BStrt}^{BStrt} \right) = -\underline{u}_{\xi BStrt}^{BStrt} \\
\underline{u}_{\xi B5Strt}^{BStrt} &= C_{B2Strt}^{BStrt} \underline{u}_{\xi B5Strt}^{B2Strt} = \left[I + 2 \left(\underline{u}_{\xi BStrt}^{BStrt} \times \right)^2 \right] \left(-\underline{u}_{\xi BStrt}^{BStrt} \right) = -\underline{u}_{\xi BStrt}^{BStrt}
\end{aligned} \tag{87}$$

$$\begin{aligned}
\underline{u}_{\sigma B 5 Strt}^{B 4 Strt} &= C_{B 5 Strt}^{B 4 Strt} \underline{u}_{\sigma B 5 Strt}^{B 5 Strt} = C_{B 5 Strt}^{B 4 Strt} \underline{u}_{\sigma B Strt}^{B Strt} \\
&= \left[I + \left(\underline{u}_{\nu B Strt}^{B Strt} \times \right) + \left(\underline{u}_{\nu B Strt}^{B Strt} \times \right)^2 \right] \underline{u}_{\sigma B Strt}^{B Strt} = \underline{u}_{\nu B Strt}^{B Strt} \times \underline{u}_{\sigma B Strt}^{B Strt} \\
\underline{u}_{\sigma B 5 Strt}^{B 3 Strt} &= C_{B 4 Strt}^{B 3 Strt} \underline{u}_{\sigma B 5 Strt}^{B 4 Strt} = \left[I + 2 \left(\underline{u}_{\sigma B Strt}^{B Strt} \times \right)^2 \right] \left(\underline{u}_{\nu B Strt}^{B Strt} \times \underline{u}_{\sigma B Strt}^{B Strt} \right) = -\underline{u}_{\nu B Strt}^{B Strt} \times \underline{u}_{\sigma B Strt}^{B Strt} \\
\underline{u}_{\sigma B 5 Strt}^{B 2 Strt} &= C_{B 3 Strt}^{B 2 Strt} \underline{u}_{\sigma B 5 Strt}^{B 3 Strt} = \left[I + \left(\underline{u}_{\nu B Strt}^{B Strt} \times \right) + \left(\underline{u}_{\nu B Strt}^{B Strt} \times \right)^2 \right] \left(-\underline{u}_{\nu B Strt}^{B Strt} \times \underline{u}_{\sigma B Strt}^{B Strt} \right) \\
&= \underline{u}_{\nu B Strt}^{B Strt} \times \left(-\underline{u}_{\nu B Strt}^{B Strt} \times \underline{u}_{\sigma B Strt}^{B Strt} \right) = \underline{u}_{\sigma B Strt}^{B Strt} \\
\underline{u}_{\xi B 5 Strt}^{B Strt} &= C_{B 2 Strt}^{B Strt} \underline{u}_{\xi B 5 Strt}^{B 2 Strt} = \left[I + 2 \left(\underline{u}_{\xi B Strt}^{B Strt} \times \right)^2 \right] \underline{u}_{\sigma B Strt}^{B Strt} = -\underline{u}_{\sigma B Strt}^{B Strt}
\end{aligned} \tag{88}$$

or in summary:

$$\underline{u}_{\nu B 5 Strt}^{B Strt} = \underline{u}_{\nu B Strt}^{B Strt} \quad \underline{u}_{\xi B 5 Strt}^{B Strt} = -\underline{u}_{\xi B Strt}^{B Strt} \quad \underline{u}_{\sigma B 5 Strt}^{B Strt} = -\underline{u}_{\sigma B Strt}^{B Strt} \tag{89}$$

Eqs. (89) show that at rotation 4 completion, $\underline{u}_{\nu B}^B$ will be at its starting orientation and $\underline{u}_{\xi B}^B, \underline{u}_{\sigma B}^B$ will be reversed from their starting orientations. (Note: It follows then that since rotations 5 - 8 are a repeat of rotations 1 - 4, at rotation 8 completion, $\underline{u}_{\nu B}^B$ will be at its rotation 4 completion orientation and $\underline{u}_{\xi B}^B, \underline{u}_{\sigma B}^B$ will be reversed from their rotation 4 completion orientations. Thus, at completion of rotation 8, $\underline{u}_{\nu B}^B$ and $\underline{u}_{\xi B}^B, \underline{u}_{\sigma B}^B$ will have returned to their starting orientations. (This confirms our original premise that the selected $180 \xi, +90 \nu, 180 \sigma, +90 \nu, 180 \xi, +90 \nu, 180 \sigma, +90 \nu$ rotation sequence returns the IMU to its starting orientation.) Substituting (89) in (84) yields for $\Delta \phi_{\underline{5}}^{B Strt} + \Delta \phi_{\underline{7}}^{B Strt}$:

$$\begin{aligned}
\Delta \phi_{\underline{5}}^{B Strt} + \Delta \phi_{\underline{7}}^{B Strt} &= -\left(\pm \pi \kappa_{Scal \xi} \right) \underline{u}_{\xi Strt}^{B Strt} - \left(\pm \pi \kappa_{Scal \sigma} \right) \left(\underline{u}_{\nu B Strt}^{B Strt} \times \underline{u}_{\sigma B Strt}^{B Strt} \right) \\
&+ 2 \left(\kappa_{\sigma \xi} + \kappa_{\xi \sigma} \right) \underline{u}_{\xi B Strt}^{B Strt} \times \underline{u}_{\sigma B Strt}^{B Strt} - 2 \kappa_{\nu \xi} \underline{u}_{\xi B Strt}^{B Strt} \times \underline{u}_{\nu B Strt}^{B Strt} + 2 \kappa_{\nu \sigma} \underline{u}_{\sigma B Strt}^{B Strt}
\end{aligned} \tag{90}$$

Finally, we combine (90) with (83) to obtain for $\phi_{\underline{End}}^{B Strt}$ in (53):

$$\Delta \phi_{\underline{1}}^{B Strt} + \Delta \phi_{\underline{3}}^{B Strt} + \Delta \phi_{\underline{5}}^{B Strt} + \Delta \phi_{\underline{7}}^{B Strt} = 4 \left(\kappa_{\sigma \xi} + \kappa_{\xi \sigma} \right) \underline{u}_{\xi B Strt}^{B Strt} \times \underline{u}_{\sigma B Strt}^{B Strt} \tag{91}$$

or with (11) for ξ gyro to σ gyro orthogonality error definition

$$\phi_{\underline{1}}^{B\text{Strt}} + \Delta\phi_{\underline{3}}^{B\text{Strt}} + \Delta\phi_{\underline{5}}^{B\text{Strt}} + \Delta\phi_{\underline{7}}^{B\text{Strt}} = 4 \nu_{\xi\sigma} \underline{u}_{\xi B\text{Strt}}^{B\text{Strt}} \times \underline{u}_{\sigma B\text{Strt}}^{B\text{Strt}} \quad (92)$$

Equation (92) shows that orthogonality error $\nu_{\xi\sigma}$ only appears along $\underline{u}_{\xi B\text{Strt}}^{B\text{Strt}} \times \underline{u}_{\sigma B\text{Strt}}^{B\text{Strt}}$, and since axes ν , ξ , σ are mutually perpendicular, along an axis parallel to $\underline{u}_{\nu B\text{Strt}}^{B\text{Strt}}$. To obtain the total $\phi_{\underline{End}}^{B\text{Strt}}$ for (53), $\Delta\phi_{\underline{2}}^{B\text{Strt}} + \Delta\phi_{\underline{4}}^{B\text{Strt}} + \Delta\phi_{\underline{6}}^{B\text{Strt}} + \Delta\phi_{\underline{8}}^{B\text{Strt}}$ generated by 90 degree ν rotations must be added to $\Delta\phi_{\underline{1}}^{B\text{Strt}} + \Delta\phi_{\underline{3}}^{B\text{Strt}} + \Delta\phi_{\underline{5}}^{B\text{Strt}} + \Delta\phi_{\underline{7}}^{B\text{Strt}}$ in (90). It remains to determine whether the added ν rotations excite other unwanted gyro error signatures onto $\phi_{\underline{End}}^{B\text{Strt}}$, hence, onto the $\Delta\hat{a}_H^{B\text{Strt}}$ measurement in (53) for $\nu_{\xi\sigma}$ determination.

Because rotation 1 is 180 degrees around ξ , $\underline{u}_{\nu B}^B$ at rotation 2 start will be oppositely directed from $\underline{u}_{\nu B}^B$ at rotation sequence start ($\underline{u}_{\nu B 2\text{Strt}}^{B\text{Strt}} = -\underline{u}_{\nu B\text{Strt}}^{B\text{Strt}}$). Rotation 2 is around ν , leaving $\underline{u}_{\nu B}^B$ unaffected ($\underline{u}_{\nu B 3\text{Strt}}^{B\text{Strt}} = \underline{u}_{\nu B 2\text{Strt}}^{B\text{Strt}} = -\underline{u}_{\nu B\text{Strt}}^{B\text{Strt}}$). Rotation 3 is around σ , again reversing the direction of $\underline{u}_{\nu B}^B$ ($\underline{u}_{\nu B 4\text{Strt}}^{B\text{Strt}} = -\underline{u}_{\nu B 3\text{Strt}}^{B\text{Strt}} = \underline{u}_{\nu B\text{Strt}}^{B\text{Strt}}$). Rotation 4 is around ν , leaving $\underline{u}_{\nu B}^B$ unaffected ($\underline{u}_{\nu B 5\text{Strt}}^{B\text{Strt}} = \underline{u}_{\nu B 4\text{Strt}}^{B\text{Strt}} = \underline{u}_{\nu B\text{Strt}}^{B\text{Strt}}$). Thus, over the rotation 1 - 4 sequence, the first axis for ν rotation (rotation 2) is around $-\underline{u}_{\nu B\text{Strt}}^{B\text{Strt}}$ with the second (rotation 4) around $\underline{u}_{\nu B\text{Strt}}^{B\text{Strt}}$. The ν rotation axis direction pattern repeats for the remainder of the eight rotation sequence, i.e., around $-\underline{u}_{\nu B\text{Strt}}^{B\text{Strt}}$ for rotation 6 and around $\underline{u}_{\nu B\text{Strt}}^{B\text{Strt}}$. The impact on $\Delta\phi_{\underline{2}}^{B\text{Strt}} + \Delta\phi_{\underline{4}}^{B\text{Strt}} + \Delta\phi_{\underline{6}}^{B\text{Strt}} + \Delta\phi_{\underline{8}}^{B\text{Strt}}$ can be deduced from (53).

Equation (53) shows that only gyro scale factor errors appear along the rotation axis. Since rotations 2 and 4 are +90 degrees around oppositely directed ν axes, the scale factor composite $\Delta\phi_{\underline{2}}^{B\text{Strt}} + \Delta\phi_{\underline{4}}^{B\text{Strt}}$ effect along $\underline{u}_{\nu B\text{Strt}}^{B\text{Strt}}$ will cancel (and similarly for $\Delta\phi_{\underline{6}}^{B\text{Strt}} + \Delta\phi_{\underline{8}}^{B\text{Strt}}$). Because the ξ , σ axes are oppositely directed at rotation 5 start compared to rotation 1 start, and the ν axis at rotation 5 start is the same as at rotation 1, the misalignment coupling effect of ν axis rotation on $\Delta\phi_{\underline{6}}^{B\text{Strt}} + \Delta\phi_{\underline{8}}^{B\text{Strt}}$ components perpendicular to $\underline{u}_{\nu B\text{Strt}}^{B\text{Strt}}$ will be opposite from those for the $\Delta\phi_{\underline{2}}^{B\text{Strt}} + \Delta\phi_{\underline{4}}^{B\text{Strt}}$ components. The overall result is that the composite effect of ν axis rotations on $\Delta\phi_{\underline{2}}^{B\text{Strt}} + \Delta\phi_{\underline{4}}^{B\text{Strt}} + \Delta\phi_{\underline{6}}^{B\text{Strt}} + \Delta\phi_{\underline{8}}^{B\text{Strt}}$ will be zero, hence, $\phi_{\underline{End}}^{B\text{Strt}}$ for (53) will be from (92):

$$\underline{\phi}_{End}^{B Strt} = \sum_i \Delta \underline{\phi}_i^{B Strt} = 4 \nu_{\xi\sigma} \underline{u}_{\xi B Strt}^{B Strt} \times \underline{u}_{\sigma B Strt}^{B Strt} \quad (93)$$

It is important to recognize that Eq. (93) is based on rotations 2, 4, 6, and 8 being in the same direction (+90 degrees). As a result, ν axis gyro scale factor asymmetry errors are excited identically around the rotation axes, enabling them to cancel in the final (93) result.

With $\underline{u}_{\sigma B Strt}^{B Strt}$ selected to be vertical, $\underline{u}_{Dwn}^{B Strt} = \left(\underline{u}_{Dwn}^{B Strt} \cdot \underline{u}_{\sigma B Strt}^{B Strt} \right) \underline{u}_{\sigma B Strt}^{B Strt}$. Applying $\underline{\phi}_{End}^{B Strt}$ from (93), the $\hat{\Delta \underline{a}}_H^{B Strt}$ measurement in (54) then becomes for the eight rotation sequence:

$$\begin{aligned} \hat{\Delta \underline{a}}_H^{B Strt} &= g \underline{u}_{Dwn}^{B Strt} \times \underline{\phi}_{End}^{B Strt} = 4g \nu_{\xi\sigma} \left(\underline{u}_{Dwn}^{B Strt} \cdot \underline{u}_{\sigma B Strt}^{B Strt} \right) \underline{u}_{\sigma B Strt}^{B Strt} \times \left(\underline{u}_{\xi B Strt}^{B Strt} \times \underline{u}_{\sigma B Strt}^{B Strt} \right) \\ &= 4g \nu_{\xi\sigma} \left(\underline{u}_{Dwn}^{B Strt} \cdot \underline{u}_{\sigma B Strt}^{B Strt} \right) \underline{u}_{\xi B Strt}^{B Strt} \end{aligned} \quad (94)$$

The (94) measurement formula was used with $\underline{u}_{\sigma B Strt}^{B Strt} = \underline{u}_{Dwn}^{B Strt}$ for the Sequence 6 measurement in Table 1, with vertical axis σ corresponding to IMU axis x, and horizontal axis ξ corresponding to IMU y. With $\nu_{\xi\sigma} = \nu_{\sigma\xi}$ from (10), the result in (16) for rotation 6 in Table 1 is $\Delta a_{y6}^{B Strt} = 4 g \nu_{xy}$. For assurance, the identical result for Sequence 6 was generated directly from (7) with (6) in Part 3, [4, Eq. (43)].

6.3 ROTATION SEQUENCES FOR ACCELEROMETER CALIBRATION ERROR DETERMINATION

SRT determination of accelerometer misalignment and bias errors are based on the $\hat{\Delta \underline{a}}_H^{B Strt}$ differential type measurement in (7). Accelerometer scale factor error determination uses the $\hat{a}_{Strt Down}^{B Strt}$ and $\hat{a}_{End Down}^{B Strt}$ measurements in (7).

6.3.1 Determining Accelerometer Misalignment And Bias Calibration Errors

SRT sequence design for accelerometer misalignment and bias determination is easily accomplished based on 180 degree rotations for which $\hat{\Delta \underline{a}}_H^{B Strt}$ in (7) with (53) and (6) become

$$\hat{\Delta \underline{a}}_H^{B Strt} = \hat{\Delta \underline{a}}_H^{B Strt} \phi + \hat{\Delta \underline{a}}_H^{B Strt} SF \quad (95)$$

$$\Delta \hat{\underline{a}}_{H\phi}^{BStrt} = g \underline{u}_{Dwn}^{BNom} \times \phi_{End}^{BStrt} \quad \phi_{End}^{BStrt} = \sum_i \Delta \phi_i^{BStrt}$$

$$\Delta \phi_i^{BStrt} = C_{BiStrt}^{BStrt} \Delta \phi_i^{BiStrt} \quad (96)$$

$$= \pm \pi \kappa_{Scal} \mu \underline{u}_{\mu BiStrt}^{BStrt} + 2 \left(\kappa_{\zeta \mu} \underline{u}_{\mu BiStrt}^{BStrt} \times \underline{u}_{\zeta BiStrt}^{BStrt} + \kappa_{\eta \mu} \underline{u}_{\mu BiStrt}^{BStrt} \times \underline{u}_{\eta BiStrt}^{BStrt} \right)$$

$$\Delta \hat{\underline{a}}_{HSF}^{BStrt} = \left(C_{BEnd}^{BStrt} \delta \hat{\underline{a}}_{SFEnd}^{BEnd} - \delta \hat{\underline{a}}_{SFStrt}^{BStrt} \right)_H \quad (97)$$

$$\delta \hat{\underline{a}}_{SFStrt}^{BStrt} = -g \lambda_{Scal/Mis} \underline{u}_{Dwn}^{BStrt} + \underline{\lambda}_{Bias} \quad \delta \hat{\underline{a}}_{SFEnd}^{BEnd} = -g \lambda_{Scal/Mis} \underline{u}_{Dwn}^{BEnd} + \underline{\lambda}_{Bias}$$

in which

$$\lambda_{Scal/Mis} = \lambda_{Scal} + \lambda_{Mis} \quad \text{with} \quad \lambda_{Scal} \equiv \lambda_{LinScal} + \lambda_{Asym} A_{SFSign}^B$$

$$\lambda_{Scal/Mis} \underline{u}_{Dwn}^{BStrt} = \lambda_{Scal} \underline{u}_{Dwn}^{BStrt} + \lambda_{Mis} \underline{u}_{Dwn}^{BStrt} \quad (98)$$

$$\lambda_{Scal/Mis} \underline{u}_{Dwn}^{BEnd} = \lambda_{Scal} \underline{u}_{Dwn}^{BEnd} + \lambda_{Mis} \underline{u}_{Dwn}^{BEnd}$$

and where

$\Delta \hat{\underline{a}}_{H\phi}^{BStrt}$ = Component of $\Delta \hat{\underline{a}}_H^{BStrt}$ generated by gyro error.

$\Delta \hat{\underline{a}}_{HSF}^{BStrt}$ = Component of $\Delta \hat{\underline{a}}_H^{BStrt}$ generated by accelerometer error.

A_{SFSign}^B = Diagonal matrix with unity magnitude elements having the sign of the specific force acceleration component along the corresponding IMU axes.

As in the original SRT, one of the IMU axes will be vertical at the start and end of the rotation sequence. Thus, in (98) from (9) and (15), $\lambda_{Scal} \underline{u}_{Dwn}^{BStrt}$, $\lambda_{Scal} \underline{u}_{Dwn}^{BEnd}$ will be vertical and $\lambda_{Mis} \underline{u}_{Dwn}^{BStrt}$, $\lambda_{Mis} \underline{u}_{Dwn}^{BEnd}$ will be horizontal. Thus, $\lambda_{Scal/Mis} \underline{u}_{Dwn}^{BEnd}$, $\lambda_{Scal/Mis} \underline{u}_{Dwn}^{BEnd}$ can be written in the alternate form:

$$\lambda_{Scal/Mis} \underline{u}_{Dwn}^{BStrt} = \underline{u}_{Dwn}^{BStrt} \cdot \underline{u}_{\nu BStrt}^{BStrt} \left(\lambda_{Scal\nu} \underline{u}_{\nu BStrt}^{BStrt} + \lambda_{\xi\nu} \underline{u}_{\xi BStrt}^{BStrt} + \lambda_{\sigma\nu} \underline{u}_{\sigma BStrt}^{BStrt} \right) \quad (99)$$

$$\lambda_{Scal/Mis} \underline{u}_{Dwn}^{BEnd} = \underline{u}_{Dwn}^{BEnd} \cdot \underline{u}_{\nu BEnd}^{BEnd} \left(\lambda_{Scal\nu} \underline{u}_{\nu BEnd}^{BEnd} + \lambda_{\xi\nu} \underline{u}_{\xi BEnd}^{BEnd} + \lambda_{\sigma\nu} \underline{u}_{\sigma BEnd}^{BEnd} \right)$$

where

ν = Vertical IMU axis.

ξ, σ = Horizontal IMU axes (perpendicular to axis ν).

$\underline{u}_{\nu}^{BStrt}, \underline{u}_{\xi}^{BStrt}, \underline{u}_{\sigma}^{BStrt}, \underline{u}_{\nu}^{BEnd}, \underline{u}_{\xi}^{BEnd}, \underline{u}_{\sigma}^{BEnd}$ = Mutually orthogonal unit vectors in B frame coordinates along IMU ν, ξ, σ B Frame axes at the start and end of the rotation sequence.

$\lambda_{Scal\nu}$ = Diagonal element in column and row ν of $\lambda_{LinScal} + \lambda_{Asym} A_{SF}^B$ with $\lambda_{LinScal}$ and λ_{Asym} from (9) or (15).

$\lambda_{\xi\nu}, \lambda_{\sigma\nu}$ = Elements in column ν and rows ξ, σ of λ_{Mis} in (9) or (15).

Similarly, $\underline{\lambda}_{Bias}$ in (97) can be written as

$$\underline{\lambda}_{Bias} = \lambda_{\nu} \underline{u}_{\nu}^{BStrt} + \lambda_{\xi} \underline{u}_{\xi}^{BStrt} + \lambda_{\sigma} \underline{u}_{\sigma}^{BStrt} = \lambda_{\nu} \underline{u}_{\nu}^{BEnd} + \lambda_{\xi} \underline{u}_{\xi}^{BEnd} + \lambda_{\sigma} \underline{u}_{\sigma}^{BEnd} \quad (100)$$

where

$\lambda_{\nu}, \lambda_{\xi}, \lambda_{\sigma}$ = Elements in locations $\nu, \xi,$ and σ of $\underline{\lambda}_{Bias}$ in (9) or (15).

With (99) and (100), $\hat{\delta}_{SF}^{BStrt}$ and $\hat{\delta}_{SF}^{BEnd}$ in (97) become

$$\begin{aligned} \hat{\delta}_{SF}^{BStrt} &= -g \lambda_{Scal/Mis} \underline{u}_{Dwn}^{BStrt} + \underline{\lambda}_{Bias} \\ &= -g \underline{u}_{Dwn}^{BStrt} \cdot \underline{u}_{\nu}^{BStrt} \left(\lambda_{Scal\nu} \underline{u}_{\nu}^{BStrt} + \lambda_{\xi\nu} \underline{u}_{\xi}^{BStrt} + \lambda_{\sigma\nu} \underline{u}_{\sigma}^{BStrt} \right) \\ &\quad + \lambda_{\nu} \underline{u}_{\nu}^{BStrt} + \lambda_{\xi} \underline{u}_{\xi}^{BStrt} + \lambda_{\sigma} \underline{u}_{\sigma}^{BStrt} \\ &= \left(-g \lambda_{Scal\nu} \underline{u}_{Dwn}^{BStrt} \cdot \underline{u}_{\nu}^{BStrt} + \lambda_{\nu} \right) \underline{u}_{\nu}^{BStrt} + \left(-g \lambda_{\xi\nu} \underline{u}_{Dwn}^{BStrt} \cdot \underline{u}_{\nu}^{BStrt} + \lambda_{\xi} \right) \underline{u}_{\xi}^{BStrt} \\ &\quad + \left(-g \lambda_{\sigma\nu} \underline{u}_{Dwn}^{BStrt} \cdot \underline{u}_{\nu}^{BStrt} + \lambda_{\sigma} \right) \underline{u}_{\sigma}^{BStrt} \quad (101) \\ \hat{\delta}_{SF}^{BEnd} &= -g \lambda_{Scal/Mis} \underline{u}_{Dwn}^{BEnd} + \underline{\lambda}_{Bias} \\ &= \left(-g \lambda_{Scal\nu} \underline{u}_{Dwn}^{BEnd} \cdot \underline{u}_{\nu}^{BEnd} + \lambda_{\nu} \right) \underline{u}_{\nu}^{BEnd} + \left(-g \lambda_{\xi\nu} \underline{u}_{Dwn}^{BEnd} \cdot \underline{u}_{\nu}^{BEnd} + \lambda_{\xi} \right) \underline{u}_{\xi}^{BEnd} \\ &\quad + \left(-g \lambda_{\sigma\nu} \underline{u}_{Dwn}^{BEnd} \cdot \underline{u}_{\nu}^{BEnd} + \lambda_{\sigma} \right) \underline{u}_{\sigma}^{BEnd} \end{aligned}$$

With (101) while recognizing that $\underline{u}_{vBStrt}^{BStrt}$ and $\underline{u}_{vBEnd}^{BEnd}$ are vertical, we obtain for the horizontal $\Delta \hat{\underline{a}}_{HSF}^{BStrt}$ measurement component in (95):

$$\begin{aligned} \Delta \hat{\underline{a}}_{HSF}^{BStrt} = & \left(-g \lambda_{\xi v} \underline{u}_{Dwn}^{BEnd} \cdot \underline{u}_{vBEnd}^{BEnd} + \lambda_{\xi} \right) \underline{u}_{\xi BEnd}^{BStrt} + \left(-g \lambda_{\sigma v} \underline{u}_{Dwn}^{BEnd} \cdot \underline{u}_{vBEnd}^{BEnd} + \lambda_{\sigma} \right) \underline{u}_{\sigma BEnd}^{BStrt} \\ & - \left(-g \lambda_{\xi v} \underline{u}_{Dwn}^{BStrt} \cdot \underline{u}_{vBStrt}^{BStrt} + \lambda_{\xi} \right) \underline{u}_{\xi BStrt}^{BStrt} - \left(-g \lambda_{\sigma v} \underline{u}_{Dwn}^{BStrt} \cdot \underline{u}_{vBStrt}^{BStrt} + \lambda_{\sigma} \right) \underline{u}_{\sigma BStrt}^{BStrt} \end{aligned} \quad (102)$$

Collecting contributions from each error source while recognizing that the dot product between two vectors is identical in any coordinate frame, (102) becomes the final form:

$$\begin{aligned} \Delta \hat{\underline{a}}_{HSF}^{BStrt} = & -g \lambda_{\xi v} \left[\left(\underline{u}_{Dwn}^{BStrt} \cdot \underline{u}_{vBEnd}^{BStrt} \right) \underline{u}_{\xi BEnd}^{BStrt} - \left(\underline{u}_{Dwn}^{BStrt} \cdot \underline{u}_{vBStrt}^{BStrt} \right) \underline{u}_{\xi BStrt}^{BStrt} \right] \\ & - g \lambda_{\sigma v} \left[\left(\underline{u}_{Dwn}^{BStrt} \cdot \underline{u}_{vBEnd}^{BStrt} \right) \underline{u}_{\sigma BEnd}^{BStrt} - \left(\underline{u}_{Dwn}^{BStrt} \cdot \underline{u}_{vBStrt}^{BStrt} \right) \underline{u}_{\sigma BStrt}^{BStrt} \right] \\ & + \lambda_{\xi} \left(\underline{u}_{\xi BEnd}^{BStrt} - \underline{u}_{\xi BStrt}^{BStrt} \right) + \lambda_{\sigma} \left(\underline{u}_{\sigma BEnd}^{BStrt} - \underline{u}_{\sigma BStrt}^{BStrt} \right) \end{aligned} \quad (103)$$

Eq. (103) can now be used for IMU orientation definition at the start and end of the rotation sequence to generate a signature from only one of the accelerometer bias or misalignment errors on one of the $\Delta \hat{\underline{a}}_{HSF}^{BStrt}$ components. Having defined all rotations in the sequence to be 180

degrees considerably simplifies the design process. Then the $\underline{u}_{vBEnd}^{BStrt}$, $\underline{u}_{vBStrt}^{BStrt}$, $\underline{u}_{\sigma BEnd}^{BStrt}$ unit vectors will be parallel (directed along or oppositely) to their $\underline{u}_{vBStrt}^{BStrt}$, $\underline{u}_{vBStrt}^{BStrt}$, $\underline{u}_{\sigma BStrt}^{BStrt}$ starting equivalents.

6.3.1.1 Accelerometer Misalignment Error Determination

A principle advantage of the SRT is the ability to directly determine sensor-to-sensor misalignment errors, the groupings that directly impact inertial navigation accuracy. For the accelerometers, the misalignment of interest is between the accelerometer and gyro triads. For each accelerometer there are two such misalignments; between the accelerometer input axis and the two gyro input axes perpendicular to the accelerometer input axis. Fig. 5 shows that the relative misalignment between an i axis accelerometer and a j axis gyro is $\lambda_{ij} + \kappa_{ji}$ where λ_{ij} and κ_{ji} are i, j elements in the (8) - (9) κ_{Mis} and λ_{Mis} matrices. Selecting the B frame selected to be a *MARS* type equates λ_{ij} to μ_{ij} , thus with (12), the relative accelerometer-to-gyro misalignment becomes $\lambda_{ij} + \kappa_{ji} = \mu_{ij} + \frac{1}{2} v_{ij}$ where v_{ij} is the orthogonality error between the i and j axis gyros.

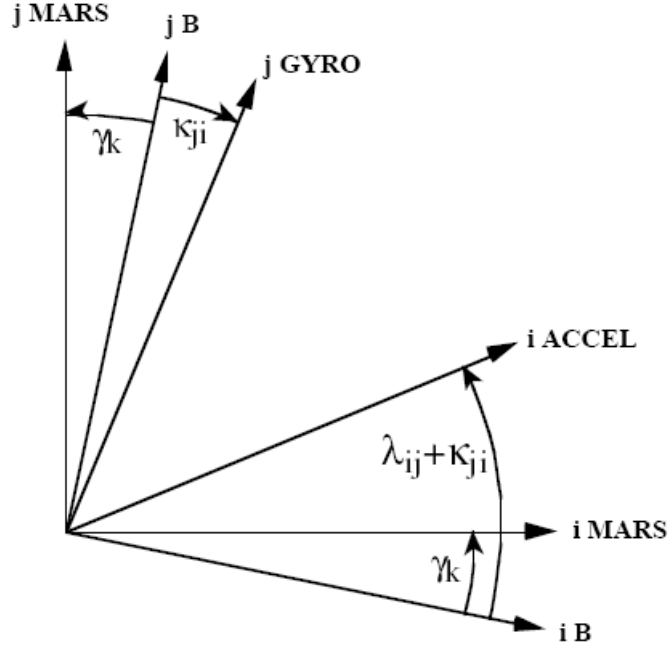


Fig. 5 - Accelerometer-To-Gyro Misalignment

The previous discussion shows that for an SRT rotation sequence designed to determine accelerometer-to-gyro misalignment, a signature of $\lambda_{ij} + \kappa_{ji}$ (or $\mu_{ij} + \frac{1}{2} v_{ij}$) must appear in (97) measurement $\Delta \hat{\underline{a}}_{H SF}^{B Strt}$. Thus, $\Delta \hat{\underline{a}}_{H \phi}^{B Strt}$ in (96) must excite κ_{ji} and $\Delta \hat{\underline{a}}_{H SF}^{B Strt}$ in (103) must excite λ_{ij} so they combine in (95) for the $\Delta \hat{\underline{a}}_H^{B Strt}$ measurement component. Ideally, this should be accomplished without additional errors entering the measurement. Both of these objectives can be achieved with a single 180 degree rotation around a horizontal axis.

Consider the 180 degree rotation to be around $\underline{u}_{\xi}^{B Strt}$. Then $\underline{u}_{\xi}^{B Strt} = \underline{u}_{\xi}^{B Strt}$, $\underline{u}_{\sigma}^{B Strt} = -\underline{u}_{\sigma}^{B Strt}$, $\underline{u}_{\nu}^{B Strt} = -\underline{u}_{\nu}^{B Strt}$, and (103) simplifies to

$$\Delta \hat{\underline{a}}_{H SF}^{B Strt} = 2g \lambda_{\xi \nu} \left(\underline{u}_{Dwn}^{B Strt} \cdot \underline{u}_{\nu}^{B Strt} \right) \underline{u}_{\xi}^{B Strt} - 2 \lambda_{\sigma} \underline{u}_{\sigma}^{B Strt} \quad (104)$$

Eq. (104) shows that accelerometer misalignment can be determined from the component of $\Delta \hat{\underline{a}}_{H SF}^{B Strt}$ along rotation axis $\underline{u}_{\xi}^{B Strt}$.

The $\Delta \hat{\underline{a}}_{H SF}^{B Strt}$ accelerometer error driven component from (104) combines in (95) with gyro error driven component $\Delta \hat{\underline{a}}_{H \phi}^{B Strt}$ from (96) to form the $\Delta \hat{\underline{a}}_H^{B Strt}$ horizontal differential measurement. For the 180 degree (plus or minus) single rotation selected for this sequence, $\Delta \hat{\underline{a}}_{H \phi}^{B Strt}$ in (96) simplifies:

$$\begin{aligned} \phi_{End}^{B Strt} &= \pm \pi \kappa_{Scal} \mu \underline{u}_{\mu B1Strt}^{B Strt} + 2 \left(\kappa_{\zeta \mu} \underline{u}_{\mu B1Strt}^{B Strt} \times \underline{u}_{\zeta B1Strt}^{B Strt} + \kappa_{\eta \mu} \underline{u}_{\mu B1Strt}^{B Strt} \times \underline{u}_{\eta B1Strt}^{B Strt} \right) \\ \Delta \hat{\underline{a}}_{H \phi}^{B Strt} &= g \underline{u}_{Down}^{B Strt} \times \phi_{End}^{B Strt} \end{aligned} \quad (105)$$

Having defined $\underline{u}_{\xi BStrt}^{B Strt}$ in (104) as the rotation axis sets rotation axis $\underline{u}_{\mu B1Strt}^{B Strt}$ in (105) to $\underline{u}_{\mu B1Strt}^{B Strt} = \underline{u}_{\xi BStrt}^{B Strt}$ and $\mu = \xi$. For (105) we then arbitrarily assign $\zeta, \underline{u}_{\zeta B1Strt}^{B Strt} = \nu, \underline{u}_{\nu BStrt}^{B Strt}$ which sets the remaining third axis to $\eta, \underline{u}_{\eta B1Strt}^{B Strt} = \sigma, \underline{u}_{\sigma BStrt}^{B Strt}$. Substituting these equalities in (105) converts $\phi_{End}^{B Strt}$ to the equivalent:

$$\phi_{End}^{B Strt} = \pm \pi \kappa_{Scal} \xi \underline{u}_{\xi BStrt}^{B Strt} + 2 \left(\kappa_{\nu \xi} \underline{u}_{\xi BStrt}^{B Strt} \times \underline{u}_{\nu BStrt}^{B Strt} + \kappa_{\sigma \xi} \underline{u}_{\xi BStrt}^{B Strt} \times \underline{u}_{\sigma BStrt}^{B Strt} \right) \quad (106)$$

Because $\underline{u}_{\nu BStrt}^{B Strt}$ has been defined in Section 6.3.1 to be vertical,

$\underline{u}_{Down}^{B Strt} = \left(\underline{u}_{\nu BStrt}^{B Strt} \cdot \underline{u}_{Down}^{B Strt} \right) \underline{u}_{\nu BStrt}^{B Strt}$ and $\Delta \hat{\underline{a}}_{H \phi}^{B Strt}$ in (105) becomes with (106):

$$\begin{aligned} \Delta \hat{\underline{a}}_{H \phi}^{B Strt} &= g \left(\underline{u}_{\nu BStrt}^{B Strt} \cdot \underline{u}_{Down}^{B Strt} \right) \underline{u}_{\nu BStrt}^{B Strt} \times \phi_{End}^{B Strt} \\ &= g \left(\underline{u}_{\nu BStrt}^{B Strt} \cdot \underline{u}_{Down}^{B Strt} \right) \left\{ \begin{array}{l} \pm \pi \kappa_{Scal} \xi \underline{u}_{\nu BStrt}^{B Strt} \times \underline{u}_{\xi BStrt}^{B Strt} \\ + 2 \left[\begin{array}{l} \kappa_{\nu \xi} \underline{u}_{\nu BStrt}^{B Strt} \times \left(\underline{u}_{\xi BStrt}^{B Strt} \times \underline{u}_{\nu BStrt}^{B Strt} \right) \\ + \kappa_{\sigma \xi} \underline{u}_{\nu BStrt}^{B Strt} \times \left(\underline{u}_{\xi BStrt}^{B Strt} \times \underline{u}_{\sigma BStrt}^{B Strt} \right) \end{array} \right] \end{array} \right\}_H \\ &= g \left(\underline{u}_{\nu BStrt}^{B Strt} \cdot \underline{u}_{Down}^{B Strt} \right) \left(\pm \pi \kappa_{Scal} \xi \underline{u}_{\nu BStrt}^{B Strt} \times \underline{u}_{\xi BStrt}^{B Strt} + 2 \kappa_{\nu \xi} \underline{u}_{\nu BStrt}^{B Strt} \times \underline{u}_{\xi BStrt}^{B Strt} \right) \end{aligned} \quad (107)$$

Substituting (104) and (107) into (95) then obtains:

$$\begin{aligned}
\Delta \hat{\underline{a}}_H^{BStrt} &= \Delta \hat{\underline{a}}_{H\phi}^{BStrt} + \Delta \hat{\underline{a}}_{HSF}^{BStrt} \\
\pm \pi g \kappa_{Scal\xi} &\left(\underline{u}_{vBStrt}^{BStrt} \cdot \underline{u}_{Dwn}^{BStrt} \right) \underline{u}_{vBStrt}^{BStrt} \times \underline{u}_{\xi BStrt}^{BStrt} - 2 \lambda_{\sigma} \underline{u}_{\sigma BStrt}^{BStrt} \\
&+ 2 g \left(\underline{u}_{Dwn}^{BStrt} \cdot \underline{u}_{vBStrt}^{BStrt} \right) \left(\lambda_{\xi v} + \kappa_{v\xi} \right) \underline{u}_{\xi BStrt}^{BStrt}
\end{aligned} \tag{108}$$

and with (43) and (8) or (14) for $\kappa_{Scal\xi}$:

$$\begin{aligned}
\Delta \hat{\underline{a}}_H^{BStrt} \pm \pi g &\left[\kappa_{\xi\xi} + \kappa_{\xi\xi\xi} \text{Sign}(\dot{\beta}_1) \right] \left(\underline{u}_{vBStrt}^{BStrt} \cdot \underline{u}_{Dwn}^{BStrt} \right) \underline{u}_{vBStrt}^{BStrt} \times \underline{u}_{\xi BStrt}^{BStrt} \\
&- 2 \lambda_{\sigma} \underline{u}_{\sigma BStrt}^{BStrt} + 2 g \left(\underline{u}_{Dwn}^{BStrt} \cdot \underline{u}_{vBStrt}^{BStrt} \right) \left(\lambda_{\xi v} + \kappa_{v\xi} \right) \underline{u}_{\xi BStrt}^{BStrt}
\end{aligned} \tag{109}$$

With (12) and (13) for *MARS* based *B* frame coordinates, (109) is equivalently:

$$\begin{aligned}
\Delta \hat{\underline{a}}_H^{BStrt} \pm \pi g &\left[\kappa_{\xi\xi} + \kappa_{\xi\xi\xi} \text{Sign}(\dot{\beta}_1) \right] \left(\underline{u}_{vBStrt}^{BStrt} \cdot \underline{u}_{Dwn}^{BStrt} \right) \underline{u}_{vBStrt}^{BStrt} \times \underline{u}_{\xi BStrt}^{BStrt} \\
&- 2 \lambda_{\sigma} \underline{u}_{\sigma BStrt}^{BStrt} + 2 g \left(\underline{u}_{Dwn}^{BStrt} \cdot \underline{u}_{vBStrt}^{BStrt} \right) \left(\mu_{\xi v} + \nu_{\xi v} / 2 \right) \underline{u}_{\xi BStrt}^{BStrt}
\end{aligned} \tag{110}$$

The $\underline{u}_{\xi BStrt}^{BStrt}$ component of $\Delta \hat{\underline{a}}_H^{BStrt}$ in (110) or (109) was used as the accelerometer-to-gyro misalignment measurement for rotation sequences 7 - 12 in Table 1. For example, for Sequence 7, the initial IMU *v* vertical axis is down along *y* (i.e., along $\underline{u}_{vBStrt}^{BStrt} = \underline{u}_{Dwn}^{BStrt} = \underline{u}_{yBStrt}^{BStrt}$) and the IMU ξ rotation axis is *x* (around $\underline{u}_{\xi BStrt}^{BStrt} = \underline{u}_{xBStrt}^{BStrt}$), thus using the traditional *x, y, z* right-hand rule, $\underline{u}_{vBStrt}^{BStrt} \times \underline{u}_{\xi BStrt}^{BStrt} = \underline{u}_{yBStrt}^{BStrt} \times \underline{u}_{xBStrt}^{BStrt} = -\underline{u}_{zBStrt}^{BStrt}$. From the form of (100) we select $\underline{u}_{\sigma BStrt}^{BStrt}$ for *x, y, z* right-hand compatibility, thus $\underline{u}_{xBStrt}^{BStrt} \times \underline{u}_{yBStrt}^{BStrt} = \underline{u}_{\xi BStrt}^{BStrt} \times \underline{u}_{vBStrt}^{BStrt} = \underline{u}_{zBStrt}^{BStrt} = \underline{u}_{\sigma BStrt}^{BStrt}$. Then, for Sequence 7 having positive $\dot{\beta}_1$ rotation rate around *x*, (110) becomes:

$$\Delta \hat{\underline{a}}_H^{BStrt} - \left[\pi g \left(\kappa_{xx} + \kappa_{xxx} \right) + 2 \lambda_z \right] \underline{u}_{zBStrt}^{BStrt} + 2 g \left(\mu_{xy} + \nu_{xy} / 2 \right) \underline{u}_{xBStrt}^{BStrt} \tag{111}$$

Eq. (111) matches Δa_{x7}^{BStrt} and Δa_{z7}^{BStrt} in Eq. (16) for the $\underline{u}_{xBStrt}^{BStrt}$ and $\underline{u}_{zBStrt}^{BStrt}$ components of $\Delta \hat{\underline{a}}_H^{BStrt}$. For confirmation, Part 3 derives the Δa_{x7}^{BStrt} and Δa_{z7}^{BStrt} Sequence 7 measurement formulas [4, Eq. (54)] directly from (7) with (5), obtaining the identical result.

6.3.1.2 Accelerometer Bias Error Determination

Eqs. (109) - (110) in Section 6.3.1.1 show that for the 180 degree single rotation sequence used for accelerometer misalignment determination (from the $\underline{u}_{\xi}^{BStrt}$ component of $\Delta \hat{\underline{a}}_H^{BStrt}$), accelerometer bias λ_σ also appears on the $\underline{u}_{\sigma}^{BStrt}$ component (but together with the $\pm \pi g \left[\kappa_{\xi\xi} + \kappa_{\xi\xi\xi} \text{Sign}(\dot{\beta}_1) \right]$ scale factor term). Thus, λ_σ can also be determined as part of the Section 6.3.1.1 misalignment test by subtracting $\pm \pi g \left[\kappa_{\xi\xi} + \kappa_{\xi\xi\xi} \text{Sign}(\dot{\beta}_1) \right]$ from the $\underline{u}_{\sigma}^{BStrt}$ component of $\Delta \hat{\underline{a}}_H^{BStrt}$. However, this method requires that the $\kappa_{\xi\xi}$ and $\kappa_{\xi\xi\xi}$ scale factor error coefficients be known from previously performed Section 6.2.1 gyro scale factor error determination tests. A problem with this approach (for some gyros) is the potential shift in gyro scale factor errors that could occur from the time of gyro scale factor measurement to the time of the accelerometer misalignment test. To eliminate this potential error source, this section discusses an alternative as an extension of the accelerometer misalignment determination test. The result will be the equivalent of (109) - (110), but with the gyro scale factor error replaced by gyro orthogonality error. Since gyro orthogonality is more stable than scale factor (for some gyros), the following test is recommended for accelerometer bias determination in general. Unfortunately, limitations of a two-axis rotation fixture only allow two of the accelerometer biases to be determined with this method (λ_x and λ_y for a Section 4.1 IMU mounting having IMU z along the inner rotation fixture axis). Thus, for the Table 1 sequence (based on a Section 4.2 type IMU mounting), the $\underline{u}_{z}^{BStrt}$ component of Eq. (111) would still be used for λ_z determination, as shown in Eqs. (16).

An alternative method for accelerometer bias determination adds a 180 degree rotation around the vertical preceding the 180 degree horizontal axis rotation discussed in the previous section. The added rotation reverses the polarity of the bias and misalignment effects along the horizontal rotation axis at the start of the second rotation. The bias polarity reversal holds during the second rotation along the rotation axis. In contrast, during the second rotation, the misalignment effect along the rotation axis again reverses polarity, returning to its value at the start of the rotation sequence. The difference between horizontal acceleration components before and after the rotation sequence (i.e., $\Delta \hat{\underline{a}}_H^{BStrt}$), thereby cancels the misalignment effect components along the second rotation axis and doubles the bias effect. The analytics are detailed next.

We define the first rotation to be around the IMU ν axis and the second around axis ξ . Because all rotations in the sequence are 180 degrees, the ν, ξ, σ axes following each rotation will remain parallel to ν, ξ, σ at the start of the rotation sequence. The first rotation is around the vertical (IMU axis ν), reversing the direction of the IMU ξ, σ axes so that following rotation 1,

$$\begin{aligned} \underline{u}_{\xi 1End}^{B Strt} = \underline{u}_{\xi B 2Strt}^{B Strt} = -\underline{u}_{\xi B Strt}^{B Strt} \quad \underline{u}_{\sigma B 1End}^{B Strt} = \underline{u}_{\sigma B 2Strt}^{B Strt} = -\underline{u}_{\sigma B Strt}^{B Strt} \\ \underline{u}_{\nu B 1End}^{B Strt} = \underline{u}_{\nu B 2Strt}^{B Strt} = \underline{u}_{\nu B Strt}^{B Strt} \end{aligned} \quad (112)$$

The second rotation is about the IMU ξ axis, reversing the direction of the IMU ν, σ axes. Thus, following rotation 2,

$$\begin{aligned} \underline{u}_{\nu B 2End}^{B Strt} = -\underline{u}_{\nu B 2Strt}^{B Strt} = -\underline{u}_{\nu B Strt}^{B Strt} \quad \underline{u}_{\sigma B 2End}^{B Strt} = -\underline{u}_{\sigma B 2Strt}^{B Strt} = \underline{u}_{\sigma B Strt}^{B Strt} \\ \underline{u}_{\xi B 2End}^{B Strt} = \underline{u}_{\xi B 2Strt}^{B Strt} = -\underline{u}_{\xi B Strt}^{B Strt} \end{aligned} \quad (113)$$

Since rotation 2 is the last in the sequence, $\underline{u}_{\sigma B End}^{B Strt} = \underline{u}_{\sigma B 2End}^{B Strt}$, $\underline{u}_{\xi B End}^{B Strt} = \underline{u}_{\xi B 2End}^{B Strt}$, $\underline{u}_{\nu B End}^{B Strt} = \underline{u}_{\nu B 2End}^{B Strt}$ and the (113) results are equivalently:

$$\underline{u}_{\nu B End}^{B Strt} = -\underline{u}_{\nu B Strt}^{B Strt} \quad \underline{u}_{\xi B End}^{B Strt} = -\underline{u}_{\xi B Strt}^{B Strt} \quad \underline{u}_{\sigma B End}^{B Strt} = \underline{u}_{\sigma B Strt}^{B Strt} \quad (114)$$

Substituting (114) into (103) then obtains for $\Delta \hat{\underline{a}}_{H SF}^{B Strt}$:

$$\Delta \hat{\underline{a}}_{H SF}^{B Strt} = 2 g \lambda_{\sigma \nu} \left(\underline{u}_{Down}^{B Strt} \cdot \underline{u}_{\nu B Strt}^{B Strt} \right) \underline{u}_{\sigma B Strt}^{B Strt} - 2 \lambda_{\xi} \underline{u}_{\xi B Strt}^{B Strt} \quad (115)$$

The $\Delta \hat{\underline{a}}_{H SF}^{B Strt}$ accelerometer error driven component from (115) combines in (95) with gyro error driven component $\Delta \hat{\underline{a}}_{H \phi}^{B Strt}$ from (96) to form the $\Delta \hat{\underline{a}}_H^{B Strt}$ horizontal differential measurement. For the first rotation around IMU axis ν in (112), we set rotation axis μ in (96) to $\mu = \nu$, and arbitrarily assign ζ, η in (96) to, respectively, ξ, σ . For the second rotation around the IMU ξ axis in (113) we set rotation axis μ in (96) to $\mu = \xi$, and arbitrarily assign ζ, η in (96), respectively, to ν, σ . Thus, for rotations 1 and 2,

$$\begin{aligned} \mu, \underline{u}_{\mu B 1Strt}^{B Strt} = \nu, \underline{u}_{\nu B 1Strt}^{B Strt} \quad \zeta, \underline{u}_{\zeta B 1Strt}^{B Strt} = \xi, \underline{u}_{\xi B 1Strt}^{B Strt} \quad \eta, \underline{u}_{\eta B 1Strt}^{B Strt} = \sigma, \underline{u}_{\sigma B 1Strt}^{B Strt} \\ \mu, \underline{u}_{\mu B 2Strt}^{B Strt} = \xi, \underline{u}_{\xi B 2Strt}^{B Strt} \quad \zeta, \underline{u}_{\zeta B 2Strt}^{B Strt} = \nu, \underline{u}_{\nu B 2Strt}^{B Strt} \quad \eta, \underline{u}_{\eta B 2Strt}^{B Strt} = \sigma, \underline{u}_{\sigma B 2Strt}^{B Strt} \end{aligned} \quad (116)$$

Equating $\underline{u}_{\nu B 1Strt}^{B Strt}$, $\underline{u}_{\xi B 1Strt}^{B Strt}$, $\underline{u}_{\sigma B 1Strt}^{B Strt} = \underline{u}_{\nu B Strt}^{B Strt}$, $\underline{u}_{\xi B Strt}^{B Strt}$, $\underline{u}_{\sigma B Strt}^{B Strt}$ by definition, (116) with (112) becomes:

$$\begin{aligned}
\mu, \underline{u}_{\mu B_{1Strt}}^{BStrt} = \nu, \underline{u}_{\nu B_{1Strt}}^{BStrt} \quad \zeta, \underline{u}_{\zeta B_{1Strt}}^{BStrt} = \xi, \underline{u}_{\xi B_{1Strt}}^{BStrt} \quad \eta, \underline{u}_{\eta B_{1Strt}}^{BStrt} = \sigma, \underline{u}_{\sigma B_{1Strt}}^{BStrt} \\
\mu, \underline{u}_{\mu B_{2Strt}}^{BStrt} = \xi, -\underline{u}_{\xi B_{2Strt}}^{BStrt} \quad \zeta, \underline{u}_{\zeta B_{2Strt}}^{BStrt} = \nu, \underline{u}_{\nu B_{2Strt}}^{BStrt} \quad \eta, \underline{u}_{\eta B_{2Strt}}^{BStrt} = \sigma, -\underline{u}_{\sigma B_{2Strt}}^{BStrt}
\end{aligned} \quad (117)$$

Substituting (117) in (96) then obtains for $\Delta\phi_{\underline{1}}^{BStrt}$ and $\Delta\phi_{\underline{2}}^{BStrt}$:

$$\begin{aligned}
\Delta\phi_{\underline{1}}^{BStrt} &= \pm\pi \kappa_{Scal\nu} \underline{u}_{\nu B_{1Strt}}^{BStrt} + 2 \left(\kappa_{\xi\nu} \underline{u}_{\nu B_{1Strt}}^{BStrt} \times \underline{u}_{\xi B_{1Strt}}^{BStrt} + \kappa_{\sigma\nu} \underline{u}_{\nu B_{1Strt}}^{BStrt} \times \underline{u}_{\sigma B_{1Strt}}^{BStrt} \right) \\
\Delta\phi_{\underline{2}}^{BStrt} &= - \left(\pm\pi \kappa_{Scal\xi} \underline{u}_{\xi B_{2Strt}}^{BStrt} \right) + 2 \left(-\kappa_{\nu\xi} \underline{u}_{\xi B_{2Strt}}^{BStrt} \times \underline{u}_{\nu B_{2Strt}}^{BStrt} + \kappa_{\sigma\xi} \underline{u}_{\xi B_{2Strt}}^{BStrt} \times \underline{u}_{\sigma B_{2Strt}}^{BStrt} \right)
\end{aligned} \quad (118)$$

Summing $\Delta\phi_{\underline{1}}^{BStrt}$ and $\Delta\phi_{\underline{2}}^{BStrt}$ from (118) in (96) then finds for $\phi_{\underline{End}}^{BStrt}$:

$$\begin{aligned}
\phi_{\underline{End}}^{BStrt} &= \Delta\phi_{\underline{1}}^{BStrt} + \Delta\phi_{\underline{2}}^{BStrt} = \pm\pi \kappa_{Scal\nu} \underline{u}_{\nu B_{1Strt}}^{BStrt} - \left(\pm\pi \kappa_{Scal\xi} \underline{u}_{\xi B_{2Strt}}^{BStrt} \right) \\
&+ 2 \left(\kappa_{\xi\nu} + \kappa_{\nu\xi} \right) \underline{u}_{\nu B_{1Strt}}^{BStrt} \times \underline{u}_{\xi B_{1Strt}}^{BStrt} + 2 \kappa_{\sigma\nu} \underline{u}_{\nu B_{1Strt}}^{BStrt} \times \underline{u}_{\sigma B_{1Strt}}^{BStrt} + 2 \kappa_{\sigma\xi} \underline{u}_{\xi B_{2Strt}}^{BStrt} \times \underline{u}_{\sigma B_{2Strt}}^{BStrt}
\end{aligned} \quad (119)$$

The impact of $\phi_{\underline{End}}^{BStrt}$ from (119) on the (95) $\Delta\hat{a}_H^{BStrt}$ measurement is determined by

$\Delta\hat{a}_{H\phi}^{BStrt} = g \underline{u}_{Dwn}^{BStrt} \times \phi_{\underline{End}}^{BStrt}$ in (96) which adds to $\Delta\hat{a}_{HSF}^{BStrt}$ in (95) to form $\Delta\hat{a}_H^{BStrt}$. Because $\underline{u}_{Dwn}^{BStrt}$ and $\underline{u}_{\nu B_{1Strt}}^{BStrt}$ are parallel, $\underline{u}_{Dwn}^{BStrt} = \left(\underline{u}_{Dwn}^{BStrt} \cdot \underline{u}_{\nu B_{1Strt}}^{BStrt} \right) \underline{u}_{\nu B_{1Strt}}^{BStrt}$, hence $\Delta\hat{a}_{H\phi}^{BStrt}$ in (96) becomes with (119):

$$\begin{aligned}
\Delta\hat{a}_{H\phi}^{BStrt} &= g \underline{u}_{Dwn}^{BStrt} \times \phi_{\underline{End}}^{BStrt} = g \left(\underline{u}_{Dwn}^{BStrt} \cdot \underline{u}_{\nu B_{1Strt}}^{BStrt} \right) \underline{u}_{\nu B_{1Strt}}^{BStrt} \times \phi_{\underline{End}}^{BStrt} \\
&= -g \left(\pm\pi \kappa_{Scal\xi} \right) \left(\underline{u}_{Dwn}^{BStrt} \cdot \underline{u}_{\nu B_{1Strt}}^{BStrt} \right) \underline{u}_{\nu B_{1Strt}}^{BStrt} \times \underline{u}_{\xi B_{2Strt}}^{BStrt} \\
&- 2g \left(\underline{u}_{Dwn}^{BStrt} \cdot \underline{u}_{\nu B_{1Strt}}^{BStrt} \right) \left[\left(\kappa_{\xi\nu} + \kappa_{\nu\xi} \right) \underline{u}_{\xi B_{1Strt}}^{BStrt} + \kappa_{\sigma\nu} \underline{u}_{\sigma B_{1Strt}}^{BStrt} \right]
\end{aligned} \quad (120)$$

Finally, we combine (120) for $\Delta\hat{a}_{H\phi}^{BStrt}$ with (115) for $\Delta\hat{a}_{HSF}^{BStrt}$ to form $\Delta\hat{a}_H^{BStrt}$ in (95) for the sequence horizontal measurement:

$$\begin{aligned}
\Delta \hat{\underline{a}}_H^{B Strt} &= \Delta \hat{\underline{a}}_{H \phi}^{B Strt} + \Delta \hat{\underline{a}}_{H SF}^{B Strt} \\
&= -g \left(\underline{u}_{Dwn}^{B Strt} \cdot \underline{u}_{\nu B Strt}^{B Strt} \right) \left[\pm \pi \kappa_{Scal \xi} \underline{u}_{\nu B Strt}^{B Strt} \times \underline{u}_{\xi B Strt}^{B Strt} - 2(\lambda_{\sigma \nu} - \kappa_{\sigma \nu}) \underline{u}_{\sigma B Strt}^{B Strt} \right] \\
&\quad - 2 \left(\underline{u}_{Dwn}^{B Strt} \cdot \underline{u}_{\nu B Strt}^{B Strt} \right) \left[\lambda_{\xi} + g(\kappa_{\xi \nu} + \kappa_{\nu \xi}) \right] \underline{u}_{\xi B Strt}^{B Strt}
\end{aligned} \quad (121)$$

Using the (11) - (12) gyro orthogonality error formulas and (13) for *MARS B* frame coordinates, (121) becomes equivalently:

$$\begin{aligned}
\Delta \hat{\underline{a}}_H^{B Strt} &= -g \left(\underline{u}_{Dwn}^{B Strt} \cdot \underline{u}_{\nu B Strt}^{B Strt} \right) \left[\pm \pi \kappa_{Scal \xi} \underline{u}_{\nu B Strt}^{B Strt} \times \underline{u}_{\xi B Strt}^{B Strt} - (2 \mu_{\sigma \nu} - \nu_{\sigma \nu}) \underline{u}_{\sigma B Strt}^{B Strt} \right] \\
&\quad - 2 \left(\underline{u}_{Dwn}^{B Strt} \cdot \underline{u}_{\nu B Strt}^{B Strt} \right) (\lambda_{\xi} + g \nu_{\nu \xi}) \underline{u}_{\xi B Strt}^{B Strt}
\end{aligned} \quad (122)$$

For Sequence 13 in Table 1, the initial IMU ν vertical axis is downward along z (along $\underline{u}_{\nu B Strt}^{B Strt} = \underline{u}_{Dwn}^{B Strt} = \underline{u}_{z B Strt}^{B Strt}$) and the IMU ξ rotation axis is y (around $\underline{u}_{\xi B Strt}^{B Strt} = \underline{u}_{y B Strt}^{B Strt}$), thus, using the traditional x, y, z right-hand rule, $\underline{u}_{\nu B Strt}^{B Strt} \times \underline{u}_{\xi B Strt}^{B Strt} = \underline{u}_{z B Strt}^{B Strt} \times \underline{u}_{y B Strt}^{B Strt} = -\underline{u}_{x B Strt}^{B Strt}$.

From the form of (100) we select $\underline{u}_{\sigma B Strt}^{B Strt}$ for x, y, z right-hand compatibility, thus,

$\underline{u}_{y B Strt}^{B Strt} \times \underline{u}_{z B Strt}^{B Strt} = \underline{u}_{\xi B Strt}^{B Strt} \times \underline{u}_{\nu B Strt}^{B Strt} = \underline{u}_{x B Strt}^{B Strt} = \underline{u}_{\sigma B Strt}^{B Strt}$. Then, for Sequence 13 having positive $\dot{\beta}_1$ rotation rate around x , (122) with (98) becomes with (43) and (8) or (14) for $\kappa_{Scal \xi}$:

$$\Delta \hat{\underline{a}}_H^{B Strt} = g \left[\pi (\kappa_{yy} + \kappa_{yyy}) + (2\mu_{xz} - \nu_{xz}) \right] \underline{u}_{x B Strt}^{B Strt} - 2(\lambda_y + g \nu_{yz}) \underline{u}_{y B Strt}^{B Strt} \quad (123)$$

Eq. (123) matches the Part 3 result [4, Eq. (63)] for Sequence 13 in Table 1.

The component of (122) along $\underline{u}_{\xi B Strt}^{B Strt}$ is used as the differential acceleration measurement in determining the $\lambda_{\xi} + g \nu_{\nu \xi}$ accelerometer-to-gyro misalignment:

$$\underline{u}_{\xi B Strt}^{B Strt} \cdot \Delta \hat{\underline{a}}_H^{B Strt} = -2(\lambda_{\xi} + g \nu_{\nu \xi}) \quad (124)$$

Eq. (124) was used to form the $\Delta a_{y13}^{B Strt} = -2(\lambda_y + g \nu_{yz})$ and $\Delta a_{x14}^{B Strt} = -2(\lambda_x + g \nu_{zx})$ measurement components in Eqs. (16) for rotation sequences 13 and 14 with $\underline{u}_{\xi B Strt}^{B Strt}$ defined to be along the outer rotation fixture axis and $\nu = z$ downward at rotation sequence start.

6.3.2 Sequences To Determine Accelerometer Scale Factor Errors

In contrast with the previous sections, accelerometer scale factor errors are determined from either the start or end of the rotation sequence vertical downward acceleration measurements in (7) with (6), using (9) or (15) for the $\lambda_{LinScal}$ and λ_{Asym} error components. For the 14 rotation sequences in Table 1, there are multiple choices of which vertical measurements to use. As a minimum, the choice should include a measurements for each IMU axis being up and down so that the components of $\lambda_{LinScal}$ and λ_{Asym} can be discriminated (e.g., Sequences 7 - 9 in Table 1).

Using (6) for $\hat{\delta}_{SF\ Strt}^{B\ Strt}$ and $\hat{\delta}_{SF\ End}^{B\ End}$, the vertical components in (7) become

$$\begin{aligned}\hat{a}_{Strt\ Down}^{B\ Strt} &\approx \underline{u}_{Dwn}^{B\ Strt} \cdot \left[-g \left(\lambda_{LinScal} + \lambda_{Mis} + \lambda_{Asym} A_{SF\ Sign}^{B\ Strt} \right) \underline{u}_{Dwn}^{B\ Strt} + \underline{\lambda}_{Bias} \right] \\ \hat{a}_{End\ Down}^{B\ Strt} &\approx \underline{u}_{Dwn}^{B\ End} \cdot \left[-g \left(\lambda_{LinScal} + \lambda_{Mis} + \lambda_{Asym} A_{SF\ Sign}^{B\ End} \right) \underline{u}_{Dwn}^{B\ End} + \underline{\lambda}_{Bias} \right]\end{aligned}\quad (125)$$

Because the IMU orientation at the start of a rotation sequence will have one of its axes parallel to $\underline{u}_{Dwn}^{B\ Strt}$, (9) or (15) show that $\lambda_{Mis} \underline{u}_{Dwn}^{B\ Strt}$ will have no component along $\underline{u}_{Dwn}^{B\ Strt}$ and $\left(\lambda_{LinScal} + \lambda_{Asym} A_{SF\ Sign}^{B\ Strt} \right) \underline{u}_{Dwn}^{B\ Strt}$ will be along $\underline{u}_{Dwn}^{B\ Strt}$. Similarly, because the IMU orientation at the end of a rotation sequence will have one of its axes parallel to $\underline{u}_{Dwn}^{B\ End}$, (9) or (15) show $\lambda_{Mis} \underline{u}_{Dwn}^{B\ End}$ will have no component along $\underline{u}_{Dwn}^{B\ End}$ and $\left(\lambda_{LinScal} + \lambda_{Asym} A_{SF\ Sign}^{B\ Strt} \right) \underline{u}_{Dwn}^{B\ End}$ is along $\underline{u}_{Dwn}^{B\ End}$. Thus, with (9) or (15) for the $\lambda_{LinScal}$ and λ_{Asym} components, (125) reduces to:

$$\begin{aligned}\hat{a}_{Strt\ Down}^{B\ Strt} &= -g \left(\lambda_{kk} - \lambda_{kkk} \underline{u}_{Dwn}^{B\ Strt} \cdot \underline{u}_{kB\ Strt}^{B\ Strt} \right) + \underline{u}_{Dwn}^{B\ Strt} \cdot \underline{\lambda}_{Bias} \\ \hat{a}_{End\ Down}^{B\ Strt} &= -g \left(\lambda_{ll} - \lambda_{lll} \underline{u}_{Dwn}^{B\ End} \cdot \underline{u}_{lB\ End}^{B\ End} \right) + \underline{u}_{Dwn}^{B\ End} \cdot \underline{\lambda}_{Bias}\end{aligned}\quad (126)$$

where

k = IMU axis parallel to $\underline{u}_{Dwn}^{B\ Strt}$ at the start of a rotation sequence.

$\underline{u}_{kB\ Strt}^{B\ Strt}$ = Unit vector along IMU axis k at the start of a rotation sequence.

λ_{kk} and λ_{kkk} = Elements in the (9) or (15) $\lambda_{LinScal}$ and λ_{Asym} matrices corresponding to IMU axis k .

l = IMU axis parallel to $\underline{u}_{Dwn}^{B\ End}$ at the end of a rotation sequence.

$\underline{u}_{lB_{End}}^{B_{End}}$ = Unit vector along IMU axis l at the end of a rotation sequence.

λ_{ll} and λ_{lll} = Elements in the (9) or (15) $\lambda_{LinScal}$ and λ_{Asym} matrices corresponding to IMU axis l .

As an example, consider Sequence 7 for which IMU axis k is y , downward at the start of the sequence, and IMU axis l is y , upward at the end of the sequence. Thus,

$\underline{u}_{kB_{Strt}}^{B_{Strt}} = \underline{u}_{yB_{Strt}}^{B_{Strt}} = \underline{u}_{Dwn}^{B_{Strt}}$ and $\underline{u}_{lB_{End}}^{B_{End}} = \underline{u}_{yB_{End}}^{B_{End}} = -\underline{u}_{Dwn}^{B_{Strt}}$. Then (126) becomes

$$\begin{aligned} \hat{a}_{Strt\ Down}^{B_{Strt}} &= -g \left(\lambda_{yy} - \lambda_{yyy} \underline{u}_{Dwn}^{B_{Strt}} \cdot \underline{u}_{yB_{Strt}}^{B_{Strt}} \right) + \underline{u}_{Dwn}^{B_{Strt}} \cdot \underline{\lambda}_{Bias} \\ &= -g \left(\lambda_{yy} - \lambda_{yyy} \underline{u}_{yB_{Strt}}^{B_{Strt}} \cdot \underline{u}_{yB_{Strt}}^{B_{Strt}} \right) + \underline{u}_{yB_{Strt}}^{B_{Strt}} \cdot \underline{\lambda}_{Bias} = -g \left(\lambda_{yy} - \lambda_{yyy} \right) + \lambda_y \end{aligned} \quad (127)$$

$$\begin{aligned} \hat{a}_{End\ Down}^{B_{Strt}} &= -g \left(\lambda_{yy} - \lambda_{yyy} \underline{u}_{Dwn}^{B_{End}} \cdot \underline{u}_{yB_{End}}^{B_{End}} \right) + \underline{u}_{Dwn}^{B_{End}} \cdot \underline{\lambda}_{Bias} \\ &= -g \left(\lambda_{yy} + \lambda_{yyy} \underline{u}_{yB_{End}}^{B_{End}} \cdot \underline{u}_{yB_{End}}^{B_{End}} \right) - \underline{u}_{yB_{End}}^{B_{End}} \cdot \underline{\lambda}_{Bias} = -g \left(\lambda_{yy} + \lambda_{yyy} \right) - \lambda_y \end{aligned}$$

which was used for $a_{Down7}^{B_{Strt}}$ and $a_{Down7}^{B_{End}}$ in (16). Part 3 [4, Eqs. (55)] confirms the same results based directly on using numerical values for the matrix and vector parameters.

REFERENCES

- [1] Savage, P. G., "Calibration Procedures For Laser Gyro Strapdown Inertial Navigation Systems", 9th Annual Electro-Optics / Laser Conference and Exhibition, Anaheim, California, October 25-27, 1977.
- [2] Savage, P. G., *Strapdown Analytics*, Strapdown Associates, Inc., Maple Plain, Minnesota, 2000, or *Strapdown Analytics - Second Edition*, Strapdown Associates, Inc., Maple Plain, Minnesota, 2007.
- [3] Savage, P.G., "Improved Strapdown Inertial System Calibration Procedures, Part 2, Analytical Derivations", WBN-14020-2, Strapdown Associates, Inc., October 20, 2017 (Updated November 10, 2017), free access available at www.strapdownassociates.com.
- [4] Savage, P.G., "Improved Strapdown Inertial System Calibration Procedures, Part 3, Numerical Examples", WBN-14020-3, Strapdown Associates, Inc., November 10, 2017, will be free access available at www.strapdownassociates.com.